

Prepared in cooperation with the California Department of Fish and Wildlife and Pheasants Forever

Monitoring Breeding and Survival of Ring-Necked Pheasant (*Phasianus colchicus*) in the Sacramento Valley, Sacramento-San Joaquin River Delta, and Klamath Basin, Northern California—Five-Year Summary, 2013–17



Open-File Report 2019–1062

Cover:

Background: Photograph showing Sutter Buttes at Gray Lodge Wildlife Area, northern California. Photograph by Rebecca Buer, U.S. Geological Survey, 2015.

Inset: Photograph showing female ring-necked pheasant (*Phasianus colchicus*) with transmitter. Photograph by Matt Meshriy, California Department of Fish and Wildlife, 2014.

Monitoring Breeding and Survival of Ring-Necked Pheasant (*Phasianus colchicus*) in the Sacramento Valley, Sacramento-San Joaquin River Delta, and Klamath Basin, Northern California—Five-Year Summary, 2013–17

By Ian A. Dwight, Peter S. Coates, Jessica H. Vogt, Joseph L. Atkinson, Joseph P. Fleskes, Daniel P. Connelly, Matt G. Meshriy, Scott C. Gardner, Simone T. Stoute, and Maurice E. Pitesky

Prepared in cooperation with the California Department of Fish and Wildlife and Pheasants Forever

Open-File Report 2019–1062

U.S. Department of the Interior
DAVID BERNHARDT, Secretary

U.S. Geological Survey
James F. Reilly II, Director

U.S. Geological Survey, Reston, Virginia: 2019

For more information on the USGS—the Federal source for science about the Earth, its natural and living resources, natural hazards, and the environment—visit <https://www.usgs.gov/> or call 1–888–ASK–USGS.

For an overview of USGS information products, including maps, imagery, and publications, visit <https://store.usgs.gov>.

Any use of trade, firm, or product names is for descriptive purposes only and does not imply endorsement by the U.S. Government.

Although this information product, for the most part, is in the public domain, it also may contain copyrighted materials as noted in the text. Permission to reproduce copyrighted items must be secured from the copyright owner.

Suggested citation:

Dwight, I.A., Coates, P.S., Vogt, J.H., Atkinson, J.L., Fleskes, J.P., Connelly, D.P., Meshriy, M.C., Gardner, S.C., Stoute, S.T., and Pitesky M.E., 2019, Monitoring breeding and survival of ring-necked pheasant (*Phasianus colchicus*) in the Sacramento Valley, Sacramento-San Joaquin River Delta, and Klamath Basin, northern California—Five-year summary, 2013–17: U.S. Geological Survey Open-File Report 2019–1062, 90 p., <https://doi.org/10.3133/ofr20191062>.

ISSN 2331-1258 (online)

Contents

1.0 Abstract	1
2.0 Background	2
3.0 Study Area	3
4.0 Methods	4
4.1 Capturing and Handling Pheasant	4
4.2 Monitoring Pheasant Populations	5
4.2.1 Radio and Global Positioning System Telemetry.....	5
4.2.2 Utilization Distributions	5
4.3 Invertebrate Sampling	6
4.4 Pheasant Disease	6
4.5 Pheasant Crowing Counts	7
4.6 Estimating Adult Survival, Nest Survival, and Brood Survival	8
4.7 Nest-Site Vegetation	9
4.8 Brood-Rearing Vegetation	11
4.9 Avian Predator Monitoring.....	11
5.0 Preliminary Results	11
5.1 Pheasant Space Use	12
5.2 Invertebrate Sampling	13
5.3 Disease	14
5.4 Crowing Counts	14
5.5 Pheasant Survival	16
5.6 Nest-Site Habitat Selection	18
5.7 Nest Survival	19
5.8 Brood-Rearing Habitat Selection	21
5.9 Brood Survival	22
5.10 Raven and Raptor Surveys	24
6.0 Interpretations	24
6.1 Sacramento-San Joaquin River Delta Region	24
6.2 Sacramento Valley Region	25
6.3 Klamath Basin Region	27
7.0 Acknowledgments	28
8.0 References Cited	28

Figures

[Figures located at back of report]

Figure 1. Map showing study regions and study sites for ring-necked pheasant (<i>Phasianus colchicus</i>) data collection, Sacramento-San Joaquin River Delta, Sacramento Valley, and Klamath Basin, northern California, 2013–17	32
Figure 2. Graph showing number of locations by year of Very High Frequency-marked ring-necked pheasant (<i>Phasianus colchicus</i>), Sacramento-San Joaquin River Delta, Sacramento Valley, and Klamath Basin, northern California, 2014–17	33
Figure 3. Graph showing number of locations by year of Global Positioning System-marked ring-necked pheasant (<i>Phasianus colchicus</i>), Sacramento-San Joaquin River Delta, Sacramento Valley, and Klamath Basin, northern California, 2014–16	34
Figure 4. Map showing general, nest, brood, and mortality telemetry locations of Very High Frequency-marked ring-necked pheasant (<i>Phasianus colchicus</i>), Gray Lodge Wildlife Area, Gridley, northern California, 2014–17	35
Figure 5. Map showing general, nest, brood, and mortality telemetry locations of Very High Frequency-marked ring-necked pheasant (<i>Phasianus colchicus</i>), Mandeville Island Duck Club, San Joaquin County, northern California, 2014–16 and 2017	36
Figure 6. Map showing general, nest, brood, and mortality telemetry locations of Very High Frequency-marked ring-necked pheasant (<i>Phasianus colchicus</i>), Roosevelt Ranch Duck Club, Zamora, northern California, 2014–17	37
Figure 7. Map showing general, nest, brood, and mortality telemetry locations of Very High Frequency-marked ring-necked pheasant (<i>Phasianus colchicus</i>), Yolo Bypass Wildlife Area, Davis, northern California, 2014–16	38
Figure 8. Map showing general, nest, brood, and mortality telemetry locations of Very High Frequency-marked ring-necked pheasant (<i>Phasianus colchicus</i>), Little Dry Creek Unit of Upper Butte Basin Wildlife Area, Gridley, northern California, 2016–17	39
Figure 9. Map showing general, nest, brood, and mortality telemetry locations of Very High Frequency-marked ring-necked pheasant (<i>Phasianus colchicus</i>), Lower Klamath National Wildlife Refuge, Dorris, northern California, 2016–17	40
Figure 10. Map showing cumulative utilization distribution of Very High Frequency-marked ring-necked pheasant (<i>Phasianus colchicus</i>), Gray Lodge Wildlife Area, northern California, spring and summer (March–September) 2014–17	41
Figure 11. Map showing cumulative utilization distribution of Very High Frequency-marked ring-necked pheasant (<i>Phasianus colchicus</i>), Mandeville Island Duck Club, northern California, spring and summer (March–September) 2014–16 and 2017	42
Figure 12. Map showing cumulative utilization distribution of Very High Frequency-marked ring-necked pheasant (<i>Phasianus colchicus</i>), Roosevelt Ranch Duck Club, northern California, spring and summer (March–September) 2014–17	43
Figure 13. Map showing cumulative utilization distribution of Very High Frequency-marked ring-necked pheasant (<i>Phasianus colchicus</i>), Yolo Bypass Wildlife Area, northern California, spring and summer (March–September) 2014–16	44

Figure 14. Map showing cumulative utilization distribution of Very High Frequency-marked ring-necked pheasant (<i>Phasianus colchicus</i>), Little Dry Creek Unit of Upper Butte Basin Wildlife Area, northern California, spring and summer (March–September) 2016–17	45
Figure 15. Map showing cumulative utilization distribution of Very High Frequency-marked ring-necked pheasant (<i>Phasianus colchicus</i>), Lower Klamath National Wildlife Refuge, northern California, spring and summer (March–September) 2016–17	46
Figure 16. Map showing cumulative utilization distribution of Global Positioning System-marked ring-necked pheasant, Roosevelt Ranch Duck Club, northern California, winter, spring, and summer (January–September) 2014–15	47
Figure 17. Map showing cumulative utilization distribution of Global Positioning System-marked ring-necked pheasant, Yolo Bypass Wildlife Area, northern California, spring and summer (March–September) 2015	48
Figure 18. Map showing cumulative utilization distribution of Global Positioning System-marked ring-necked pheasant, Lower Klamath National Wildlife Refuge, northern California, spring (March–May) 2016	49
Figure 19. Graphs showing mean ring-necked pheasant (<i>Phasianus colchicus</i>) rooster crow counts per station for 4-minute intervals for Gray Lodge Wildlife Area, Mandeville Island Duck Club, Roosevelt Ranch Duck Club, Yolo Bypass Wildlife Area, Little Dry Creek Unit of Upper Butte Basin Wildlife Area, and Lower Klamath National Wildlife Refuge, northern California, 2013–17	50
Figure 20. Graphs showing index of mean ring-necked pheasant (<i>Phasianus colchicus</i>) rooster crow counts per station for 4-minute intervals for Gray Lodge Wildlife Area, Mandeville Island Duck Club, Roosevelt Ranch Duck Club, Yolo Bypass Wildlife Area, Little Dry Creek Unit of Upper Butte Basin Wildlife Area, and Lower Klamath National Wildlife Refuge, northern California, 2013–17	51
Figure 21. Graph showing cumulative annual adult survival probabilities (in percent) for ring-necked pheasant (<i>Phasianus colchicus</i>) averaged across all field sites in the Sacramento-San Joaquin River Delta, Sacramento Valley, and Klamath Basin, northern California, 2013–17	52
Figure 22. Graphs showing cumulative annual adult survival probabilities for ring-necked pheasant (<i>Phasianus colchicus</i>) at Gray Lodge Wildlife Area, Mandeville Island Duck Club, Roosevelt Ranch Duck Club, Yolo Bypass Wildlife Area, Little Dry Creek Unit of Upper Butte Basin Wildlife Area, and Lower Klamath National Wildlife Refuge, northern California 2013–17	53
Figure 23. Graphs showing probabilities of selection for variables within the top global model significant to selection for ring-necked pheasant (<i>Phasianus colchicus</i>) nests in the Sacramento-San Joaquin River Delta and Sacramento Valley, northern California, 2014–17	54
Figure 24. Graphs showing multiplicative interactions of significant variables relative to selection within the top global model for ring-necked pheasant (<i>Phasianus colchicus</i>) nests in the Sacramento-San Joaquin River Delta and Sacramento Valley, northern California, 2014–17	55
Figure 25. Graph showing cumulative nest survival probabilities for ring-necked pheasant (<i>Phasianus colchicus</i>) in the Sacramento-San River Delta, Sacramento Valley, and Klamath Basin, northern California, over the 37-day laying and incubation period, 2014–17	56
Figure 26. Graphs showing cumulative nest survival probabilities for ring-necked pheasant (<i>Phasianus colchicus</i>) at Gray Lodge Wildlife Area, Mandeville Island Duck Club, Roosevelt Ranch Duck Club, Yolo Bypass Wildlife Area, Little Dry Creek Unit of Upper Butte Basin Wildlife Area, and Lower Klamath National Wildlife Refuge, northern California, over the 37-day laying and incubation period, 2014–17	57
Figure 27. Map showing successful and unsuccessful nest and brood telemetry locations of Very High Frequency-marked ring-necked pheasant (<i>Phasianus colchicus</i>) at Gray Lodge Wildlife Area, northern California, 2014–16	58

Figure 28. Map showing successful and unsuccessful nest and brood telemetry locations of Very High Frequency-marked ring-necked pheasant (<i>Phasianus colchicus</i>) at Mandeville Island Duck Club, northern California, 2014 and 2016–17	59
Figure 29. Map showing successful and unsuccessful nest and brood telemetry locations of Very High Frequency-marked ring-necked pheasant (<i>Phasianus colchicus</i>) at Roosevelt Ranch Duck Club, northern California, 2014–17	60
Figure 30. Map showing successful and unsuccessful nest and brood telemetry locations of Very High Frequency-marked ring-necked pheasant (<i>Phasianus colchicus</i>) at Yolo Bypass Wildlife Area, northern California, 2014–16	61
Figure 31. Map showing successful and unsuccessful nest and brood telemetry locations of Very High Frequency-marked ring-necked pheasant (<i>Phasianus colchicus</i>) at Little Dry Creek Unit of Upper Butte Basin Wildlife Area, northern California, 2016–17	62
Figure 32. Map showing successful and unsuccessful nest and brood telemetry locations of Very High Frequency-marked ring-necked pheasant (<i>Phasianus colchicus</i>) at Lower Klamath National Wildlife Refuge, northern California, 2016–17	63
Figure 33. Graphs showing cumulative nest survival probabilities for ring-necked pheasant (<i>Phasianus colchicus</i>) nests with increasing perennial grass cover at the 0.03-hectare [ha] scale, increasing perennial grass height at the 0.2-ha scale, ratio of selection (ROS) for perennial grass cover at the 0.03-ha scale, and ROS for perennial grass height at the 0.2-ha scale in the Sacramento-San Joaquin River Delta and Sacramento Valley, northern California, 2014–17	64
Figure 34. Graphs showing mean percentages of vertical cover and mean Robel pole height from ring-necked pheasant (<i>Phasianus colchicus</i>) brood locations and at random locations (dependent and independent), averaged across all study sites in the Sacramento-San Joaquin River Delta, Sacramento Valley, and Klamath Basin, northern California, 2014–17	65
Figure 35. Graphs showing mean percentages of perennial forb cover and annual forb cover from ring-necked pheasant (<i>Phasianus colchicus</i>) brood locations and at random locations averaged across all study sites in the Sacramento-San Joaquin River Delta, Sacramento Valley, and Klamath Basin, northern California, 2014–17	66
Figure 36. Graphs showing mean percentages of residual cover and litter cover from ring-necked pheasant (<i>Phasianus colchicus</i>) brood locations and at random locations averaged across all study sites in the Sacramento-San Joaquin River Delta, Sacramento Valley, and Klamath Basin, northern California, 2014–17	67
Figure 37. Graph showing mean percentages of bare ground from ring-necked pheasant (<i>Phasianus colchicus</i>) brood locations and at random locations averaged across all study sites in the Sacramento-San Joaquin River Delta, Sacramento Valley, and Klamath Basin, northern California, 2014–17	68
Figure 38. Graphs showing mean perennial and mean annual grass heights from ring-necked pheasant (<i>Phasianus colchicus</i>) brood locations and at random locations averaged across all study sites in the Sacramento-San Joaquin River Delta, Sacramento Valley, and Klamath Basin, northern California, 2014–17	69
Figure 39. Graphs showing mean perennial and annual forb heights from ring-necked pheasant (<i>Phasianus colchicus</i>) brood locations and at random locations averaged across all study sites in the Sacramento-San Joaquin River Delta, Sacramento Valley, and Klamath Basin, northern California, 2014–17	70
Figure 40. Graph showing mean residual cover height from ring-necked pheasant (<i>Phasianus colchicus</i>) brood locations and at random locations averaged across all study sites in the Sacramento-San Joaquin River Delta, Sacramento Valley, and Klamath Basin, northern California, 2014–17	71

Figure 41. Graph showing cumulative mean survival probabilities over the 50-day brood-rearing period for ring-necked pheasant (<i>Phasianus colchicus</i>) in the Sacramento-San Joaquin River Delta, Sacramento Valley, and Klamath Basin, northern California, 2014–17	72
Figure 42. Graphs showing cumulative mean survival probabilities for the 50-day brood-rearing phase across age of brood for ring-necked pheasant (<i>Phasianus colchicus</i>) broods at Gray Lodge Wildlife Area, Mandeville Island Duck Club, Roosevelt Ranch Duck Club, Yolo Bypass Wildlife Area, Little Dry Creek Unit of Upper Butte Basin Wildlife Area, and Lower Klamath National Wildlife Refuge, northern California, 2014–17	73

Tables

[Tables located at back of report]

Table 1. Number and gender of ring-necked pheasant (<i>Phasianus colchicus</i>) outfitted with Very High Frequency (VHF) and Global Positioning System (GPS) transmitters during winter (December–February), spring (March–April), and autumn (September–November) trapping seasons, Sacramento-San Joaquin River Delta, Sacramento Valley, and Klamath Basin, northern California, 2013–17	74
Table 2. Biological classifications of invertebrate specimens collected ($n = 217,536$) using pitfall traps deployed in brood-rearing pheasant habitat in the Sacramento-San Joaquin River Delta and Sacramento Valley, northern California, 2013–14.	75
Table 3. Insecticides applied to study sites containing ring-necked pheasant (<i>Phasianus colchicus</i>) habitat in the Sacramento-San Joaquin River Delta and Sacramento Valley, northern California, 2013–14.....	76
Table 4. Number of successful (one or more chicks hatched) and failed ring-necked pheasant (<i>Phasianus colchicus</i>) nests in the Sacramento-San Joaquin River Delta, Sacramento Valley, and Klamath Basin, northern California, 2014–17	76
Table 5. Means plus or minus standard error of variables included in model analyses of habitat surveys used to evaluate nest site selection and microhabitat characteristics of nests used to evaluate nest survival, for ring-necked pheasant (<i>Phasianus colchicus</i>) nests in the Sacramento-San Joaquin River Delta and Sacramento Valley, northern California, 2014–17	77
Table 6. Nest-site selection, nest survival, and ratio of selection models for ring-necked pheasant (<i>Phasianus colchicus</i>) nests in the Sacramento-San Joaquin River Delta and Sacramento Valley, northern California, 2013–17	80
Table 7. Descriptions of models with one or more interactive terms used to evaluate nest-site selection for ring-necked pheasant (<i>Phasianus colchicus</i>) nests in the Sacramento-San Joaquin River Delta and Sacramento Valley, northern California, 2014–17	83
Table 8. Comparison of global models with combinations of interaction terms used to evaluate nest-site selection for ring-necked pheasant (<i>Phasianus colchicus</i>) nests in the Sacramento-San Joaquin River Delta and Sacramento Valley, northern California, 2014–17	85
Table 9. Model descriptions for parameters included in a global selection model for ring-necked pheasant (<i>Phasianus colchicus</i>) nests in the Sacramento-San Joaquin River Delta and Sacramento Valley, northern California, 2013–17.....	86
Table 10. Nest selection, survival, and ratio of selection models for ring-necked pheasant (<i>Phasianus colchicus</i>) nests across five field sites within the Sacramento-San Joaquin River Delta and Sacramento Valley, northern California, 2014–17	87

Table 11. Number of successful, failed, and censored ring-necked pheasant (<i>Phasianus colchicus</i>) broods in the Sacramento-San Joaquin River Delta, Sacramento Valley, and Klamath Basin, northern California, 2014–17	90
--	----

Conversion Factors

International System of Units to U.S. customary units

Multiply	By	To obtain
Length		
centimeter (cm)	0.3937	inch (in.)
decimeter (dm)	3.937	inch (in.)
meter (m)	3.281	foot (ft)
kilometer (km)	0.6214	mile (mi)
Area		
hectare (ha)	2.471	acre
square hectometer (hm ²)	2.471	acre
square kilometer (km ²)	0.3861	square mile (mi ²)
square kilometer (km ²)	247.1	acre
Mass		
gram (g)	0.03527	ounce, avoirdupois (oz)

Temperature in degrees Celsius (°C) may be converted to degrees Fahrenheit (°F) as °F = (1.8 × °C) + 32.

Datums

Vertical coordinate information is referenced to the North American Vertical Datum of 1988 (NAVD 88).

Horizontal coordinate information is referenced to the North American Datum of 1983 (NAD 83).

Elevation, as used in this report, refers to distance above the vertical datum.

Supplemental Information

Note to USGS users: Use of hectare (ha) as an alternative name for square hectometer (hm²) is restricted to the measurement of small land or water areas.

Abbreviations

AIC	Akaike's Information Criterion
CAHFS	California Animal Health and Food Safety
CDFW	California Department of Fish and Wildlife
CI	confidence interval
DR	Dependent Random
ELISA	enzyme-linked immunosorbent assay
GPS	Global Positioning System
HEV	hemorrhagic enteritis virus
IBD	infectious bursal disease
ILT	infectious laryngotracheitis
IR	Independent Random
LCL	Lower Confidence Limit
LL	log-likelihood
MSD	marble spleen disease
PCR	polymerase chain reaction
PM	<i>Pasteurella multocida</i>
PTT	Platform Transmitter Terminal
PV1	avian paramyxovirus type 1

ROS	ratio of selection
RSF	Resource Selection Function
SC	Standardized Coefficient
SE	standard error
TDW	total dry weight
UCL	Upper Confidence Limit
UD	Utilization Distribution
USGS	U.S. Geological Survey
VHF	Very High Frequency
<i>w</i>	model probability

.

Monitoring Breeding and Survival of Ring-Necked Pheasant (*Phasianus colchicus*) in the Sacramento Valley, Sacramento-San Joaquin River Delta, and Klamath Basin, Northern California—Five-Year Summary, 2013–17

By Ian A. Dwight¹, Peter S. Coates¹, Jessica H. Vogt¹, Joseph L. Atkinson¹, Joseph P. Fleskes¹, Daniel P. Connelly², Matt G. Meshriy³, Scott S. Gardner³, Simone T. Stoute⁴, and Maurice E. Pitesky⁴

1.0 Abstract

The U.S. Geological Survey Western Ecological Research Center, Pheasants Forever, Mandeville Island Duck Club, and the California Department of Fish and Wildlife collaborated in a reconnaissance study to monitor populations of ring-necked pheasant (*Phasianus colchicus*) using radio-telemetry in the Sacramento Valley, Sacramento-San Joaquin River Delta, and Klamath Basin of northern California. The purpose of this study was to provide agencies and private landowners with a framework of decision-support tools to help manage pheasant populations in California. During winter, spring, and autumn of 2013–17, we radio- or Global Positioning System-marked 227 female pheasant across six study sites. Data collection was focused on investigating nest-site and brood-rearing habitat selection, examining avian predator composition, and estimating population vital rates to improve our understanding of pheasant population dynamics and to identify factors that may contribute to decreases in pheasant populations in California. The cumulative annual adult survival probability across all sites during 2013–17 was 27.6 percent (95-percent confidence interval [CI], 21.9–33.6), and the cumulative nest and brood survival probabilities were 34.5 percent (95-percent CI, 27.0–42.2) and 54.2 percent (95-percent CI, 43.7–63.5), respectively. Evidence from microhabitat surveys completed at nest-sites, brood locations, and random locations suggested that marked female pheasant tended to select increasing vertical cover and residual vegetation cover and tended to avoid areas of increasing bare ground cover regardless of life-history stage. However, females at nest-sites selected increasing grass cover and height, whereas brood-rearing females tended to select increasing forb cover and height. Only perennial grass cover and perennial grass height were shown to have a positive influence on nest survival, which suggests that increasing perennial grass cover in areas occupied by pheasant may increase nest survival. Analysis of environmental factors linked to vital rate information are ongoing and will continue with investigations at increased spatial scales (that is, macro-habitat) to develop integrated population models that can

¹U.S. Geological Survey.

²Pheasants Forever.

³California Department of Fish and Wildlife.

⁴University of California at Davis.

incorporate abundance estimates from crow count data with vital rates from telemetry data. This report includes results from 5 years of data collection and should be interpreted with caution, as these findings are preliminary.

2.0 Background

Ring-necked pheasant (*Phasianus colchicus*; hereinafter, pheasant) were introduced to the western United States from eastern Asia in the late 1800s (Lever, 1987). Using birds from established populations in Oregon, the California State Board of Fish Commissioners released pheasant across California in 1889, and sizeable populations were established in areas of northern and central California by the early 1900s (Hart, 1990). State game farms also were established to supplement populations until sufficient numbers were reached and populations could support themselves (Hart, 1990). Subsequently, the first pheasant hunting season in California was opened in 1933 and pheasant became an economically important game bird as well as an annual hunting tradition. Populations peaked in abundance from the late 1930s to the mid-1960s (Dahlgren, 1988), but in the last 30 years, populations of pheasant in agricultural areas of California have greatly decreased (Coates and others, 2017).

Decreases in farmland bird populations across North America have been attributed to the removal of hedges adjacent to crop fields (Chamberlain and others, 2000; Benton and others, 2003), changes in crop types and the timing of crop harvest (Glemnitz and others, 2015), increases in pesticide application (Mineau and Whiteside, 2006), and higher susceptibility to predation resulting from habitat change (Evans, 2004). Pheasant populations similarly decreased in California based on Annual Game Take Surveys (California Department of Fish and Wildlife, 2014), statewide Christmas Bird Counts (National Audubon Society 2014), and statewide North American Breeding Bird Surveys (Sauer and others, 2014). This marked response of California pheasant populations to environmental changes in agricultural regions makes these charismatic game birds a potential biological indicator of the overall health and biodiversity of farmland habitats in California. Furthermore, the Sacramento Valley refuges and wildlife areas typically produced some of the highest numbers of harvested pheasant in California, and hunter-harvest in these areas has decreased substantially since the early 1990s (California Department of Fish and Wildlife, 2014).

Aspects of agricultural intensification including changes in crop type, timing and amount of cropland harvested, increases in pesticide application, and changes in abundance of avian competitors and predators may all be contributing factors to pheasant population decreases in the study area. Many of the rice fields in the Sacramento Valley are disked or flooded during the winter (Hill and others, 1999), and the consistent increase in rice cultivation since the 1980s has come at the expense of fallowed fields and grain crops such as barley and winter wheat (U.S. Department of Agriculture, 2014a) that provide potential cover for pheasant. In the Sacramento-San Joaquin River Delta, wetland habitat and cereal grain crop cultivation also has decreased (U.S. Department of Agriculture, 2014b), which is thought to decrease the amount of potential nesting and brood rearing habitat in the region. Other factors are thought to influence pheasant population dynamics. First, agro-chemical application in farmland habitats for crop protection and mosquito abatement for human health, particularly the use of organophosphates and neonicotinoids, has strong potential for both lethal and sub-lethal effects on individual pheasant (Mineau and Whiteside, 2006). These pesticides also reduce the abundance of non-target arthropod food resources essential for chicks (Messick and others, 1974), as the timing of agricultural spraying generally coincides with the critical growth period of pheasant chicks

(Messick and others, 1974). Second, the additive effects of habitat change resulting from agricultural intensification coupled with the increase in corvid and raptor abundance in recent decades (Sauer and others, 2014) has been shown to reduce pheasant numbers (Coates and others, 2017), mostly because these conditions can increase predation pressure (Evans, 2004). Third, pheasant populations in California have experienced recent changes in annual precipitation resulting in drought conditions. Drought is thought to limit resources for concealment and food that could lead to increased movements across the landscape and, in turn, a decrease in reproduction and (or) survival rates (Prochazka and others, 2016). Fourth, farmed pheasant augmentation is likely to have adverse impacts on wild pheasant by increasing predation pressure and potential for disease exposure (Dwight and others, 2017). Information on population vital rates (for example, individual, nest, and brood survival) for pheasant, as well as anthropogenic and environmental factors that influence these rates, is lacking in the Central Valley. Such information would substantially benefit our understanding of factors that influence local population trends and provide wildlife and land managers with scientifically sound findings to support decisions that benefit pheasant population growth.

Thus, the U.S. Geological Survey (USGS), Pheasants Forever, and the California Department of Fish and Wildlife (CDFW), as well as private landowners, developed a multi-agency collaborative reconnaissance study of pheasant populations in the Central Valley and Klamath Basin of California over 5 years from 2013 to 2017. The purpose of this study was to improve the understanding of potential causes for pheasant population decline in California, and inform entities working to improve conditions for pheasant and other farmland bird species. The goals of this study were fourfold. First, we sought to develop effective field methodology that would be conducive to an in-depth comprehensive population dynamics study. Second, we investigated potential limiting factors for pheasant populations, including information on the predator community, and how these factors influence demographic rates. Third, we obtained preliminary estimations of population vital rates across different life phases as a baseline for an integrated population model. Fourth, we obtained high-resolution movement data and identified factors that influence resource selection across different life phases. Our primary objective was to clearly identify factors contributing to decreases in pheasant populations in the Central Valley by monitoring seasonal movements, estimating vital rates, and measuring changes in habitat selection. This information will be used to develop decision-support tools to help guide pheasant management practices by land and wildlife managers and other land stewards, particularly the CDFW. This cumulative data summary represents all 5 years of field data collection and 4 years of vital rate information collection in this study.

3.0 Study Area

The study area encompassed three regions of northern California: (1) the Sacramento Valley, (2) the Sacramento-San Joaquin River Delta, and (3) that part of the Klamath Basin in California (fig. 1A). The total area of our sites spanned about 16,200 ha with elevations ranging from -6 m to 1,244 m in relation to the North American Vertical Datum of 1988. Average temperatures across all sites ranged from -7 to 35 °C, and average annual precipitation across all sites was 48.8 cm (Intellicast, 2018). Four of the study sites—Gray Lodge Wildlife Area (hereinafter, Gray Lodge), Little Dry Creek Unit of Upper Butte Basin Wildlife Area (hereinafter, Little Dry Creek), Roosevelt Ranch Duck Club (hereinafter, Roosevelt Ranch), and Yolo Bypass Wildlife Area (hereinafter, Yolo)—were in the Sacramento Valley region (fig. 1B). Gray Lodge is just north of the Sutter Buttes, about 11 km southwest of Gridley, California.

Little Dry Creek is in Butte County, California, and is about 16 km northwest of Gridley. Yolo is located between West Sacramento and Davis, California, adjacent to the Sacramento Deep Water Ship Channel. The Roosevelt Ranch Duck Club is a privately owned, waterfowl and pheasant hunting club near the town of Zamora, California. The Mandeville Island Duck Club (hereinafter, Mandeville Island), also privately owned and managed for waterfowl and pheasant hunting, is in the Sacramento-San Joaquin River Delta region and is about 24 km northwest of Stockton, California (fig. 1B). Lower Klamath National Wildlife Refuge (hereinafter, Lower Klamath) is in Siskiyou County, California, and Klamath County, Oregon, in the Klamath Basin region, and is about 17 km west of Tulelake, California (fig. 1B). All our marked birds at Lower Klamath were trapped and located in California. Pheasant occasionally left the study sites and entered nearby private property; we followed them if permission was granted.

The study sites were composed of upland, managed wetland-riparian, and open rangeland habitats that typically were encompassed by irrigated agriculture and row crops, including rice, orchards, and hayfields. Common herbaceous cover types in the wetland-riparian communities included tule (*Schoenoplectus acutus* var. *occidentalis*), broadleaf cattail (*Typha latifolia*), dotted smartweed (*Persicaria punctata*), barnyard grass (*Echinochloa crus-galli*), swamp picklegrass (*Crypsis schoenoides*), and sprangletop (*Leptochloa fusca* ssp. *fascicularis*). Major cover types in upland communities consisted of sweetclover (*Melilotus albus*), common sunflower (*Helianthus annuus*), Great Valley gumweed (*Grindelia camporum*), rough cocklebur (*Xanthium strumarium*), curly dock (*Rumex crispus*), and broadleaved pepperweed (*Lepidium latifolium*). Rangeland communities contained perennial grasses such as creeping wild rye (*Elymus triticoides*) and timothy-grass (*Phleum pratense*), and annual grasses such as Italian ryegrass (*Lolium perenne*) and wild oat (*Avena fatua*). All study sites contained upland, grassland, and wetland-riparian communities, but species composition varied among sites based on local management. Agricultural practices were similar across sites, but crops harvested varied among sites. Surrounding agricultural practices included the cultivation of rice, almonds, walnuts, wheat, alfalfa, tomatoes, sunflower, safflower, and corn.

4.0 Methods

4.1 Capturing and Handling Pheasant

We captured females at nocturnal roosting locations from November to April during 2013–17. We also captured pheasant in September 2015 to bolster sample sizes and increase our ability to track winter survival into 2016. During the pilot phase of the study (Mandeville Island; 2013–2014), we tested the efficacy of trapping pheasant using two different techniques: (1) a modified spotlighting technique originally developed for greater sage-grouse (*Centrocercus urophasianus*) (Giesen and others, 1982; Wakkinen and others, 1992), and (2) a bait-trapping technique, which was only implemented during winter 2013. Bait-trapping was abandoned after winter 2013 because it was considerably less effective than spotlighting. Pheasant were not captured at Mandeville Island in 2015 because pen-reared pheasant were not toe-clipped and could not be distinguished from wild pheasant; however, pheasant were again captured and monitored at Mandeville Island during the 2016 and 2017 field seasons. Pheasant capture and radio-marking procedures were permitted by the California Department of Fish and Wildlife (Scientific Collecting Permit Number SC-12940) and approved by the U.S. Geological Survey Western Ecological Research Center Animal Care and Use Committee.

An all-terrain vehicle and spotlight were used to locate roosting birds, and females were preferentially targeted for capture when flushed. Birds were captured with nets attached to 3-m extension handles and then outfitted with battery-powered, necklace-style Very High Frequency (VHF) transmitters (<3-percent body mass, 1–1.8 kg; Schroeder and others, 1999; Advanced Telemetry Systems, Isanti, Minnesota) equipped with a mortality sensor. A subsample of pheasant was outfitted with a Global Positioning System (GPS), Platform Transmitter Terminal (PTT; <3-percent body mass, GeoTrak Inc., Apex, North Carolina) and a VHF transmitter. The purpose of the GPS transmitter was to collect locations remotely and transmit (using PTT) to a central database using satellites. The purpose of the VHF attachment to the GPS was to relocate the pheasant in the field and retrieve GPS devices that no longer transmitted. The weights of transmitters with collaring materials were much less than the recommended values based on pheasant body mass to minimize post-release researcher-induced stress and mortality.

Captured pheasants were weighed and multiple morphometric measurements were taken including tarsus, culmen, and flattened wing chord lengths. Blood was extracted from the brachial vein for disease analyses. Pheasants were classified as juvenile (pre-breeding) or adult (≥ 1 breeding year) based on the length or presence of a bursa of Fabricius, which is measured by inserting a metal probe into a small opening dorsal to the cloaca (Linduska, 1943). The bursa of Fabricius is only present in juvenile birds less than 1 year old. However, the accuracy of measuring the bursa decreases after January (Woodburn and others, 2009), so some pheasants were excluded from this measurement. Birds were processed within 30 minutes of capture and released at their capture location to minimize stress and disorientation.

4.2 Monitoring Pheasant Populations

4.2.1 Radio and Global Positioning System Telemetry

We completed intensive on-the-ground monitoring of pheasant movements, survivorship, and reproduction following release of marked birds during 2014–17. We used a three-element Yagi antenna and portable receiver (Advanced Telemetry Systems Inc., Isanti, Minnesota) to track radio-marked females. We minimized location error by circling each bird at a radius of 10–20 m and then walked within 10 m of the bird's location. We then approximated the distance and recorded the azimuth from the observer's location (recorded using GPS) to estimate the location coordinates (Universal Transverse Mercator) of the pheasant. On the approach to obtaining the pheasant location, we sought to prevent the bird from flushing or running. However, occasionally birds flushed or ran, and in these instances, we recorded the point of departure. Throughout the nesting and brood-rearing seasons (March–August), we attempted to locate females at least twice per week. Location frequency was scaled down to one location per week for females with a brood to minimize disturbance and was reduced to one location per month during autumn (September–November) to monitor seasonal movements and survival rates. Marked birds at Lower Klamath were only located once per week in 2016 because of logistical difficulties but were monitored twice per week during the 2017 field season.

4.2.2 Utilization Distributions

We estimated utilization distributions (UDs; Kernohan and others, 2001), which interpolate animal space use across unknown areas based on the distribution and density of known location telemetry data (Worton, 1989). These UD provide useful tools for evaluating pheasant use of space because they allow for estimation of the total area used by individual birds,

while accounting for the imperfect monitoring effort that is common to radio-telemetry studies. To calculate UD_s, we used a kernel density estimator in Geospatial Modeling Environment version 0.7.4.0 (Beyer 2015) with a likelihood-based technique to estimate the most appropriate smoothing parameter (Horne and Garton, 2006). UD_s were calculated at the population level for spring through summer (March–August). We also calculated UD_s of individual pheasants outfitted with GPS transmitters. We defined the regional core use area as the 50-percent contour (isopleth) from the UD and the home-range as the 95-percent contour.

4.3 Invertebrate Sampling

We deployed invertebrate pitfall traps during the summers of 2013 and 2014. Traps were deployed at Gray Lodge and Mandeville Island from June 18 through August 20, 2013, and at Gray Lodge and Roosevelt Ranch from June 2 through September 29, 2014. Invertebrates collected from pitfall traps were classified by order, and dried and weighed. We predicted that invertebrate diversity and abundance within pheasant habitat may be affected by the spraying of mosquito larvicide and adulticide. Hence, if pesticides are reducing available arthropods for chicks, then brood survival may be lower in areas that are heavily sprayed.

4.4 Pheasant Disease

During 2014–17, we collected blood from male and female pheasants at all six field sites. We also collected blood from pen-reared pheasants raised on game breeding farms in California. Blood collection and analysis methodologies were based on Dwight and others (2017). Blood samples from wild pheasants were collected in winter and early spring (January–April) during transmitter deployment. Wild pheasants sampled at Yolo, Gray Lodge, and Mandeville Island spatially overlapped with pen-reared pheasants released at these sites. We used enzyme-linked immunosorbent assays (ELISAs) to test for titers specific to avian influenza, avian paramyxovirus type 1 (PV1), infectious bursal disease (IBD), infectious bronchitis virus, hemorrhagic enteritis virus (HEV), infectious laryngotracheitis (ILT), and *Pastuerella multocida* (PM), and we used microagglutination tests for *Salmonella enterica* serovar *Pullorum*. These ELISA tests have only been validated for domestic poultry and may have greater potential for false positives. Hence, titer results are suggestive of exposure to screened disease agents, and primarily are qualitative evidence for further investigation of diseases affecting wild and pen-reared pheasant. For this reason, we completed a follow-up investigation to go beyond disease exposure and test for the presence of disease in pen-reared pheasant. An important caveat is that marble spleen disease (MSD) virus of pheasant is genetically similar and serologically indistinguishable from HEV of turkeys (Saif and others, 2008), and both are in the same group of avian adenoviruses. In the follow up study, HEV diagnostic tests were used as a proxy for MSD virus detection in wild and pen-reared pheasant since MSD virus test kits are not commercially available and validated in pheasant. Hence, results that are positive for HEV are a strong indication of the presence of MSD virus. In collaboration with the University of California Davis School of Veterinary Medicine Cooperative Extension, we submitted live, apparently healthy, pen-reared pheasant to the California Animal Health and Food Safety (CAHFS) diagnostic laboratory for necropsies to be completed. Blood also was collected for ELISA testing on each bird submitted for necropsy to increase the evidence for or against a positive result.

4.5 Pheasant Crowing Counts

Pheasant (rooster) crowing counts were initiated at Mandeville Island and Gray Lodge during 2013, and all field sites were surveyed at some point during the study. Crowing counts are useful to estimate peaks in breeding activity and can be used as a relative annual index to monitor trends in breeding populations (Rice, 2003). We also were evaluating the utility of using these survey data coupled with demographic data to more reliably estimate population growth rates using an integrated population model. These counts typically are done in spring (March–May), as males establish territories (harems) prior to the nesting season. An observer completed the counts on pre-established routes just before sunrise and drove for at least 2 km between sampling stations to minimize duplication of crow counts. Individual rooster crows were counted for 2- or 4-minute intervals at each station along the route, and visual detections of males or females were recorded in the notes. Crow counts were averaged across all stations and days within a single site-season combination. Survey stations were equally spaced, but the distance between stations varied between sites. Seven stations were established at Mandeville Island, Yolo, and Roosevelt Ranch. Gray Lodge had 15 stations, with 8 stations on the west side and 7 stations on the east side of the wildlife area. Eleven stations were established at Little Dry Creek and 10 stations at Lower Klamath. Surveys were completed on days with minimal wind (<20 km per hour) and no precipitation to minimize detection interference from weather.

All crow counts in 2013 and 2014 were recorded at 4-minute intervals, but counts were reduced to 2-minute intervals in 2015 to decrease the probability of double-counting individual rooster crows. However, reducing counts to 2 minutes also increased the probability of not counting any roosters in areas where roosters were present, especially at sites with low population densities such as Gray Lodge. Counts were completed using both 2- and 4-minute intervals simultaneously in 2016 and 2017, such that 2-minute intervals are nested within 4-minute intervals.

We evaluated the efficacy of using 2- or 4-minute count intervals during the 2016 and 2017 field seasons by setting up an experimental design that tracked the frequency of crows by individual roosters. These experimental counts took place at randomly selected, pre-established crow count stations at all field sites, excluding Mandeville Island. Surveys were completed by two observers, began 45 minutes prior to sunrise, and ended 60 minutes after sunrise (105-minute survey period). The first observer recorded all male pheasant “background crows” heard during the survey. The second observer focused on 1–3 unique roosters and recorded each time that each individual crowed. In the instance that one individual stopped crowing or moved out of the area, the second observer would identify another individual to monitor. All observations (that is, individual crows) were recorded to the second.

These data will help us estimate an optimal interval length that minimizes the probability of double-counting roosters while avoiding counting no roosters when they actually are present. For purposes of comparing 2-minute to 4-minute intervals across all years of the study, we transformed 2-minute counts to 4-minute counts by calculating the ratio of 2- to 4-minute counts completed simultaneously in 2016 and 2017. Additionally, we developed an index that tracks changes in 4-minute counts for each site across all years. The index is based on the average count across all years for each site and is centered at 0, so negative values indicate years that counts were lower than the site average and positive values indicate years that counts were higher than the site average. We report annual crow count averages and index values with 95-percent confidence intervals (CIs) to help estimate significant differences in counts from year to year across each site.

4.6 Estimating Adult Survival, Nest Survival, and Brood Survival

We used the maximum likelihood estimation approach to estimate cumulative survival probabilities for adults, nests, and broods. Model parameters for all analyses were estimated in program R Version 3.4.1 (R Development Core Team, 2008) using package “Rmark” (Laake and Rexstad, 2007). We developed a monthly encounter history for adult pheasant using telemetry data that included the date of capture, last date known to be alive, and fate (confirmed mortality or censored). A censored bird is either still alive or its fate is unknown. We used these data to calculate cumulative annual survival probabilities. We derived cumulative adult survival probabilities across a 12-month period (annual) using the estimated coefficients. We report point estimates with a 95-percent CI.

We estimated cumulative nest survival probability over the 37-day egg laying and incubation phase using a modeling technique like that of adult survival. To minimize nest abandonment, nests were not verified visually until the nest was depredated or the eggs hatched. After females were detected in the same location on two consecutive observations, we assumed they were nesting. Each nest was then monitored two times or more per week until its fate was determined. A nest was considered successful if one or more eggs hatched, and nest fate was based on eggshell remains or observing one or more chicks in the nest bowl. Nests were considered unsuccessful when the entire clutch failed to hatch. Failed nests were scored as depredated or abandoned. We developed an encounter history of individual nests based on the dates each nest was detected and last checked, and its fate was determined.

We used R statistical software with the “Rmark” package (Laake and Rexstad, 2007) that implements MARK (White and Burnham, 1999) to estimate the effects of environmental factors on pheasant nest survival probability. Methods for describing vegetation at nest-sites and evaluating evidence of selection are described in subsequent sections. In this analysis, we first investigated variation in survival between years and study sites. Second, we investigated groups of models that included variables developed from vegetation components measured in habitat surveys. Finally, we compared models to identify factors that were significant. We evaluated model support using Akaike’s Information Criterion (AIC) (Akaike, 1973). We also included a second-order bias correction (c) described by Anderson (2008). Model uncertainty was evaluated by subtracting differences between AIC_c values (ΔAIC_c). We calculated model probabilities ($W_{\text{model } i}$) for the most explanatory model compared to other models within the group (Anderson, 2008). Change in AIC_c and AIC_c weights were used to evaluate individual model strength relative to an intercept-only model (Anderson 2008). Individual models were considered supported by factors when $\Delta AIC_c \geq 2$ relative to the intercept-only model. Nests were removed from the survival analysis if they were abandoned and we suspected abandonment to be researcher-induced (that is, pheasant did not return to nest following incidental flush). However, these nests were included in the habitat selection analysis to avoid losing data.

To further link selection behavior with respect to nest-site vegetation characteristics to nest survival probability, we evaluated selection ratios developed from variables identified as important for influencing nest-site selection. These selection ratios were calculated by taking the used point measurement and dividing it by the mean of the available points within a given population. The final selection ratio covariates included in subsequent modeling were also logarithmic (log) transformed. By incorporating the log selection ratios as covariates in a nest survival analysis, we could estimate whether pheasant selected for a particular factor or combination of factors translated into significant changes in survival probability for pheasant nests (Lockyer and others, 2015). We used the same modeling approach outlined in the survival

analysis using R statistical software with the “RMark” package (Laake and Rexstad, 2007) to evaluate nest survival relative to nest-site selection ratios. Models were considered supported by factors when the differences between Akaike’s Information Criterion second-order bias correction values were greater than or equal to 2 ($\Delta AIC_c \geq 2$) relative to the intercept-only model. Following the completion of a successful nest, we monitored brood-rearing pheasant once per week (every 7 days) for 50 or more days. During our observations, we took extra precautions on approaches to minimize disturbance to the brood, such as minimizing flushing or brood break-up. A brood was considered successful if at least one chick survived to 50 days post-hatch. During some surveys, we counted the number of surviving chicks in the brood. However, the accuracy of these counts is unreliable, as it often was challenging to detect chicks in dense cover. To confirm unsuccessful broods and prevent false negative counts, an additional search for chicks was done in subsequent days or weeks. On some occasions, confirming brood failure was difficult because females would run from the observer and flush without chicks. Hence, some females were monitored for more than 50 days to confirm brood fate. We reported preliminary findings by estimating cumulative brood survival probabilities using the same methods that were used to determine adult and nest survival. Our preliminary results include estimated survival probabilities for a 7-day interval and cumulative across the 50-day period.

4.7 Nest-Site Vegetation

We adapted the USGS monitoring protocol for greater sage-grouse to measure pheasant nest microhabitat in the field (U.S. Geological Survey, 2017). Following nest success or failure, we recorded understory cover at the nest bowl using a Jones coverboard (Jones, 1968) and Robel pole (Robel, 1970). The coverboard is divided into 25 squares (5×5 cm each) of alternating red and white colors, and is placed parallel (flat) and perpendicular (vertical) to the ground. When oriented perpendicularly, the board is rotated so that it faces three different directions, each of which is separated by 120 degrees. The number of squares that are unobstructed by vegetation (with >50-percent visibility) are then recorded by the observer at angles of 0 and 45 degrees. When laid flat, measurements are recorded from directly above the board (that is, 90 degrees). The proportion of visible squares provides a measure of visual obstruction. However, the coverboard tended to crush vegetation and may not be the most accurate way to measure visual obstruction in habitats dominated by herbaceous cover. Hence, visual obstruction also was measured using the Robel pole, which is a 1.5-m-tall pole marked with numbered bands that correspond to a height in decimeters from the ground. A 1-m-tall viewing pole is placed 2 m from the Robel pole and is used to read the numbered bands. The measurement is taken by recording the last band visible before the pole is completely covered by vegetation. We also measured vegetation composition cover at seven subplots (20×50 cm) along three transects located less than or equal to 25 m of each nest using the Daubenmire method (Daubenmire, 1959). Finally, we measured the height of vegetation within 0.5 m of all subplots for each cover type (for example, grass, forb, and shrub). Orientation of the first transect was randomly assigned and the remaining two transects were sequentially oriented at 120-degree intervals to the previous transect. Measurements were recorded at the nest bowl (0 m), and at 10- and 25-m distances from the nest along all three transect lines. These distances correspond to an overall spatial scale of 0, 0.03, and 0.2 ha, respectively.

We implemented a date-adjustment recommendation to prevent plant phenology from confounding differences between successful and failed nests (Gibson and others, 2016). Vegetative measurements recorded at nest failure or success may not be an accurate

representation of vegetative structure at the time of nest-site selection, as they do not account for plant growth throughout the season (Hausleitner and others, 2005). We adjusted cover and height measurements for some vegetation types by fitting linear mixed-effect models. We specified ordinal date as the only fixed effect and vegetation measurements at used sites as the response, and we also fit random intercepts of year and site for all models to account for spatiotemporal differences in our observations. Estimated growth rates were derived for each microhabitat variable measured using the slope coefficient of each model provided. We assessed support for growth rate changes for each microhabitat factor by evaluating 95-percent CIs of the slope coefficient, and we did not consider the growth rate to be different from 0 if the interval overlapped 0. Vegetation measurements were adjusted according to the estimated slope coefficient for factors with evidenced growth rates. Measurements were adjusted to a mean peak nesting date (greatest frequency of females incubating) of April 26 for factors that required date adjustment to account for phenology.

To examine nest-site microhabitat selection, we compared vegetation characteristics at nest sites to available habitat within each study site. To characterize available sites, we generated independent random points in a geographic information system and completed the same microhabitat measurements at those locations. The number of independent random locations surveyed was approximately equivalent to the number of nests surveyed at each site during each year of the study. The boundary of the study area was established using the borders of the study sites combined with a minimum convex polygon generated from all telemetry locations.

We used a design II approach (Manly and others, 2002) to evaluate habitat selection, in which habitat use was measured at the individual pheasant level but habitat availability was measured at the population level. Hence, we defined these resource units as being used or available. We then developed generalized linear mixed models and specified a binomial distribution (Zuur and others, 2009) to contrast used and available units. We included random effect terms for year and study site in all selection models to represent spatial clustering and temporal correlation. We also standardized the data across all used and available nest vegetation surveys such that variables had mean 0 and standard deviation 1. Coefficients were back-transformed when interpreting and visualizing the data.

Models were compared using a multi-step exploratory approach, and variables were based on *a priori* hypotheses (Burnham and Anderson, 2002). First, we examined the data for linear and quadratic effects to identify the most explanatory single-factor models for each microhabitat variable. In this process, each factor was evaluated at each of the microsite spatial scales (0, 0.03, and 0.2 ha). Evaluation of single-factor models at these spatial scales allowed us to identify the most explanatory factor at the most appropriate spatial scale within a group of related factors. The most explanatory models were extracted and compared to each other to develop global models that included all the significant fixed effects and their interactions. Models were considered significant if ΔAIC_c was ≥ 2 relative to an intercept-only model. We looked for correlation among significant variables and dropped those variables for which the correlation coefficient was greater than 0.65 ($R \geq 0.65$). Finally, we developed global models that included all fixed effects identified as significant in contributing to selection and tested several interactions with these effects based on *a priori* hypotheses. We selected models where ΔAIC_c was ≥ 2 relative to a base model that included all fixed effects but did not include any interactions.

4.8 Brood–Rearing Vegetation

We completed the same habitat measurements for brood locations (U.S. Geological Survey, 2017) that were completed at nests. However, visual obstruction was measured with both the coverboard and Robel pole at all subplots along the three 25-m transects rather than just at the nest bowl. To characterize habitat availability, we made the same habitat measurements at Dependent Random (DR) and Independent Random (IR) points. Surveys were completed during the day at used and random point locations. To accurately relocate a site where a brood was observed, the telemetry point was recorded by GPS and a description of the area was recorded.

The first three locations following nest success served as a site for brood-rearing habitat sampling. We considered these three locations to be within a critical period in which chicks had not yet gained the ability to fly and were close to the brooding female. The difficulty in getting accurate locations greatly increased once chicks gained the ability to fly and became more mobile. Furthermore, the brooding female tended to run away immediately as the observer approached, which decreased our certainty in assessing whether chicks were still with the female. We flushed or made visual confirmation of the brooding female once per week, but chicks did not always flush. Hence, we could determine with greater certainty that chicks were still with the female during the first three locations. Therefore, we stopped conducting habitat surveys after the third location to avoid sampling areas that may have been selected because of observer influence.

4.9 Avian Predator Monitoring

We followed USGS predator survey protocol for common raven (*Corvus corax*; hereinafter, ravens) and raptor surveys (U.S. Geological Survey, 2017) completed from mid-April to late August 2014–17. We completed visual surveys (using binoculars and unaided eyes) for each pheasant location (nest and brood) from a distance of about 50–100 m. Surveys were completed over a 10-minute period wherein all four directional quadrants around the survey point were scanned for an equal amount of time. For each avian predator detected, the time, bearing, and distance from the survey point when first detected (determined with a rangefinder) were recorded, and all birds were classified as to species. The same survey technique was carried out at random points (DR and IR) as well. We also recorded the raptor/raven behavior and subsidies such as livestock, buildings, or power lines. For the 2016 and 2017 field seasons, we completed the raptor and raven survey for the used nest site as soon as a nest was suspected rather than later, when the habitat survey took place.

5.0 Preliminary Results

Data for some populations were too sparse to reliably estimate vital rate parameters. For example, we marked a sample of pheasant at Lower Klamath during spring 2016 and 2017, but adult survival and nest survival were such that only 12 nests were monitored and only 3 nests hatched. Thus, we did not have sufficient data to reliably estimate brood survival at Lower Klamath, but we did report apparent survival. Lower Klamath also was excluded from the nest survival and selection analyses because of small sample sizes. We also were not able to relate pesticide or mosquito abatement chemical applications to changes in arthropod abundance or diversity. These chemicals are sprayed on an as-needed basis, and usually were sprayed over water and not over pheasant brood locations.

5.1 Pheasant Space Use

During 2013–17, we radio- or GPS-marked a total of 227 female pheasant and 7 male pheasant across the six study sites (table 1). Most pheasant were trapped during winter (December–February), but this varied by site; all pheasant at Lower Klamath and almost all pheasant at Mandeville Island were trapped during spring (March–April). We also trapped and banded 103 pheasant (33 male and 70 female) for disease analysis; 1 male and 64 females from that analysis are included in our numbers of radio- or GPS-marked individuals. We gathered a total of 4,782 VHF telemetry locations over the 2014, 2015, 2016, and 2017 field seasons (1,375, 981, 1,700, and 726, respectively; fig. 2). Additionally, we recorded 6,608 GPS locations in the 2014, 2015, and 2016 field seasons (2,549, 2,983, and 1,076, respectively; fig. 3).

During winter and spring (December–April) 2013–14, we captured and marked 60 females with VHF ($n = 58$) or GPS ($n = 2$) transmitters. Additionally, one female was captured and fitted with a VHF collar in November 2013 at Gray Lodge, and three males and two females were captured at Mandeville Island and fitted with VHF ($n = 3$) or GPS ($n = 2$) transmitters in April 2013. However, both female pheasant captured at Mandeville Island in April 2013 died within 1 week of being released and the female pheasant captured at Gray Lodge in November 2013 died within 1 month of being released. We monitored the remaining VHF- and GPS-marked female pheasant using ground telemetry in 2014, but because of VHF failures on both GPS units deployed at Roosevelt Ranch, we were unable to obtain ground locations for those two birds after July 2014.

In 2015, we captured and marked a total of 58 females with VHF ($n = 57$) or GPS ($n = 1$) transmitters during January–November (table 1). Additionally, one male was marked with a GPS transmitter at Yolo in March (table 1). We monitored a total of 76 VHF-marked pheasant using ground telemetry, which includes the surviving marked females from 2013 ($n = 7$) and 2014 ($n = 12$).

During winter and spring (January–April) 2016, we captured and marked 70 females with VHF ($n = 68$) or GPS ($n = 2$) transmitters (table 1). Additionally, during spring 2016, two males were captured and fitted with a GPS transmitter at Lower Klamath (table 1). We monitored a total of 100 VHF-marked pheasant using ground telemetry, which includes the surviving marked females captured in 2014 ($n = 1$) and 2015 ($n = 31$). None of the pheasant marked in 2013 and 2014 survived past December 2016. Additionally, the four GPS-marked pheasant at Lower Klamath were monitored remotely by satellite.

During winter and spring (January–April) 2017, we captured and marked 37 females with VHF transmitters (table 1). No GPS transmitters were deployed in 2017. We monitored a total of 60 VHF-marked pheasant using ground telemetry, which includes surviving marked females from 2015 ($n = 2$) and 2016 ($n = 13$).

We calculated spring (March–May) and summer (June–August) UD_s for VHF-marked pheasant during 2014–17. Using VHF locations during spring ($n = 1,339$) and summer ($n = 948$; figs. 4–9), the core area of pheasant activity (50-percent UD) was 177, 53, 109, 113, 30, and 252 ha at Gray Lodge, Mandeville Island, Roosevelt Ranch, Yolo, Little Dry Creek, and Lower Klamath, respectively. The population level home range (95-percent UD) encompassed 922, 259, 654, 535, 146, and 1,387 ha, respectively (figs. 10–15). There was an overall increase from 2014 to 2016 in both core area and home range of VHF-marked pheasant at Gray Lodge and Yolo. This likely was due to changes in the areas where pheasant were captured, not a result of greater utilization of area per bird. During summer, pheasant showed minimal movement away from nesting sites. Females with broods tended to move into neighboring areas with relatively more herbaceous cover dominated by forbs.

We also calculated UD_s for GPS-marked pheasant at Roosevelt Ranch ($n = 2$), Yolo ($n = 2$), and Lower Klamath ($n = 3$) during all months in which GPS transmitters were deployed at these sites. Using GPS locations acquired in 2014 ($n = 2,820$), 2015 ($n = 2,983$), and 2016 ($n = 1,076$) that were reduced to one location per day for each bird, the core area of pheasant activity (50-percent UD) was 10 ha for Roosevelt Ranch, 3 ha for Yolo, and 5 ha for Lower Klamath. The population level home range (95-percent UD) encompassed 47, 18, and 29 ha at Roosevelt Ranch, Yolo, and Lower Klamath, respectively (figs. 16–18). Two female and two male pheasant were outfitted with GPS transmitters at Lower Klamath in March 2016. One of the four transmitters immediately stopped sending locations after deployment, and the other three stopped sending locations after May 2016, which resulted in fewer locations than GPS-marked birds at Roosevelt Ranch and Yolo.

5.2 Invertebrate Sampling

A total of 478 (2013, $n = 314$; 2014, $n = 164$) pitfall trap samples were collected over the duration of the study, yielding a total of 217,545 invertebrate individuals that were classified to order (2013, $n = 175,833$; 2014, $n = 41,712$) with a total dry weight (TDW) of 670.3 g. At Gray Lodge, 308 (2013, $n = 262$; 2014, $n = 46$) samples were collected, yielding a total of 152,145 classified invertebrate individuals. At Mandeville Island, 52 samples were collected in 2013, which yielded 36,912 individual classified invertebrates. Finally, at Roosevelt Ranch, 118 samples were collected in 2014, yielding a total of 28,488 identified invertebrate individuals.

We detected the presence of 42 invertebrate orders across the three field sites that were sampled. Of the 42 orders we detected, at least 7 orders are important invertebrate food sources for pheasant chicks (Hill, 1985). Using arthropod remains from fecal samples collected at nocturnal roost sites, Hill (1985) determined that the diet of pheasant chicks was composed of arthropods from the orders Araneae (2.3 percent), Coleoptera (11.9 percent), Dermaptera (0.6 percent), Diptera (12.1 percent), Hemiptera (40.1 percent), Hymenoptera (21.2 percent), and Lepidoptera (11.6 percent). Most specimens (62.2 percent, standard error [SE] = 3.5) belonged to the order Collembola ($n = 135,288$; TDW not estimated; table 2), which are known to be consumed by pheasant chicks (Rusek, 1998). Additional invertebrate orders identified are described in table 2.

We also documented the application of five known insecticides and three unknown chemicals across three of our field sites (table 3). Both adulticide and larvicide chemicals were applied at all three field sites sampled (table 3). Additionally, most insecticides used at our study sites were applied aerially (table 3). Messick and others (1974) determined that aerial application of pesticides caused irregular distributions of chemicals on the ground, leading to an unknown

magnitude of exposure to target species and non-target species alike. Organophosphates, such as Trumpet[®] EC, target neurotransmitters and their associated enzymes, and have been shown to decrease the fitness of non-target invertebrates, as well as fish (Fulton and Key, 2001). The active ingredient in Trumpet[®] EC is naled (1,2-dibromo-2,2-dichloroethyl dimethyl phosphate). According to the US Environmental Protection Agency list of insecticides that are known to be moderately toxic to birds, naled was observed to be most toxic to pheasant (Davis and others, 2007). Vectobac[®] 12AS is a microbial larvicide that uses the bacteria *Bacillus thuringiensis israelensis* (*Bti*) to control mosquitoes and black flies. *Bti* has been shown to decrease overall breeding success in bird species that ingest invertebrates that have been exposed to the bacterial strain (Poulin and others, 2010).

5.3 Disease

We collected blood from captured pen-reared pheasant (that is, previously released) at Gray Lodge ($n = 6$) and Mandeville Island ($n = 3$), and sampled pen-reared pheasant at six game breeding farms ($n = 67$) in the Central Valley during 2014–17. ELISA results from the breeding farms showed positive serology against HEV ($n = 47$), ILT ($n = 9$), IBD ($n = 14$), PV1 ($n = 5$), and PM ($n = 6$). From pen-reared pheasant captured in the field, we observed positive serology against HEV ($n = 2$), ILT ($n = 3$), IBD ($n = 3$), PV1 ($n = 2$), and PM ($n = 6$). We tested wild pheasant captured at our six field sites in California ($n = 79$). Wild pheasant showed positive serology against HEV ($n = 23$), IBD ($n = 27$), PV1 ($n = 6$), and PM ($n = 24$). Although these data indicate exposure to pathogens in the past, they are not an estimate of pathogen prevalence in game bird farming systems. Additionally, the use of ELISA tests on a species in which the test has not been validated may increase the risk of false positives. Wild and pen-reared pheasant tested positive for titers specific to diseases that can be detected in other wild birds.

Pheasant necropsies from five game breeding farms were submitted to CAHFS during November and December 2017. Eight pheasant from each farm were submitted on five separate occasions. During gross pathology, we documented evidence of clinical symptoms of disease in three of five submissions. All eight birds from these three farms were observed to have splenic lesions associated with MSD; a viral disease which causes mottling and enlargement of the spleen in pheasant. Further investigation, using a polymerase chain reaction (PCR) technique, confirmed the presence of HEV viral amplicons within samples of spleen tissue. Results from all tissue samples taken from mottled or enlarged spleens were positive for HEV. We also detected indeterminate results for HEV by PCR in the fourth submission, but ELISA results were negative, and the spleens did not show signs of infection. Mild to moderate roundworm (*Heterakis* species) infections of the ceca also were observed in all five submissions in at least one bird. This finding suggests that MSD may be endemic on some pheasant breeding farms in the Central Valley. Although MSD virus occurs in natural environments, it is unclear whether wild pheasant are more likely to be exposed to the virus from wildlife or from released pen-reared birds. Further investigation of diseases detected in wild birds at pheasant release sites could clarify potential sources of contact contributing to pathogen exposure.

5.4 Crowing Counts

Pheasant (rooster) crowing counts were completed at Gray Lodge during 2013–17 (fig. 19A). For 4-minute counts, the mean in 2017 was 5 (95-percent CI, 1.9–8.2) with a high of 20. The mean 4-minute count was 5 (95-percent CI, 1.1–8.6) with a high of 25 in 2016, 7 (95-percent CI, 5.6–8.6) with a high of 35 in 2015, 10 (95-percent CI, 7.5–12.1) with a high of 40 in

2014, and 5 (95-percent CI, 4.1–6.8) with a high of 16 in 2013. The index values were greater than the site mean in 2014, and less than the site mean in 2013, 2015, 2016, and 2017 (fig. 20A). The average individual crowing frequency estimated from experimental counts completed at Gray Lodge was 1 call every 190 seconds (95-percent CI, 129–251).

Rooster crow counts were completed at Mandeville Island during all 5 years of the study (fig. 19B). During 2017, the mean rooster crows heard per station were 22 with a high of 50 for 2-minute intervals and 45 with a high of 101 for 4-minute intervals. Roosters often were seen crowing just off the road along the survey route. In 2016, the mean for 4-minute counts was 52 (95-percent CI, 43.0–61.1) with a high of 103. For purposes of comparison, we transformed 2-minute counts to 4-minute counts for 2015 data. The estimate for 2-minute counts transformed to 4-minute counts at Mandeville Island in 2015 was 75 (95 percent CI, 53.3–97.1). The mean for actual 4-minute counts was 86 (95-percent CI, 64.4–108.3) with a high of 172 in 2014, and 71 (95-percent CI, 57.0–85.9) with a high of 121 in 2013. The index values for crow counts at Mandeville Island indicate that counts were greater than the site mean in 2014 and less than the site mean in 2013, 2015, 2016, and 2017 (fig. 20B).

We completed crow counts at Roosevelt Ranch in 2014, 2015, 2016, and 2017, but only used 4-minute counts in 2014, 2016 and 2017 (fig. 19C). In 2017, the mean rooster crow count per station was 11 with a high of 26 for 2-minute intervals and 22 with a high of 41 for 4-minute intervals. For 4-minute counts in 2016, the mean was 18 (95-percent CI, 10.0–25.1) with a high of 76. The estimate for the transformed 4-minute count in 2015 was 19 (95-percent CI, 11.3–27.5), and the mean for the actual count in 2014 was 26 (95-percent CI, 18.9–33.5) with a high of 64. The index values were less than the site mean in 2015 and 2016, and greater than the site mean in 2014 (fig. 20C). The average individual crowing frequency estimated from experimental counts completed at Roosevelt Ranch was 1 call every 180 seconds (95 percent CI, 164–196).

We also completed crow counts at Yolo in 2014, 2015, and 2016, but only used 4-minute counts in 2014 and 2016 (fig. 19D). The mean for actual 4-minute counts in 2016 was 4 (95-percent CI, 3.5–5.1) with a high of 28. The estimate for transformed 4-minute counts at Yolo in 2015 was 20 (95-percent CI, 14.8–24.6), and the mean for actual 4-minute counts in 2014 was 16 (95-percent CI, 10.1–21.3) with a high of 43. The index values were greater than the site mean in 2015 and less than the site mean in 2014 and 2016 (fig. 20D). The average individual crowing frequency estimated from experimental counts completed at Yolo was 1 call every 215 seconds (95 percent CI, 188–241).

Crow counts also were completed at Little Dry Creek during all 5 years of the study (fig. 19E). However, confidence intervals are not reported because the counts at Little Dry Creek were completed by CDFW and individual counts per station were not known. The mean count per station in 2017 was 17 with a high of 74 for 4-minute intervals. For 4-minute counts in 2016, the mean was 24 with a high of 55. The mean count per station was 32 in 2015, 38 in 2014, and 34 in 2013 based on the total counts across 10 stations. The index values were less than the mean in 2016 and 2017 and greater than the mean in 2013, 2014, and 2015 (fig. 20E). The average individual crowing frequency estimated from experimental counts completed at Little Dry Creek was 1 call every 171 seconds (95-percent CI, 151–192).

We completed crow counts at Lower Klamath beginning in 2016 and continuing in 2017 (fig. 19F). In 2017, the mean crow count per station was 10 with a high of 13 for 2-minute intervals and 19 with a high of 27 for 4-minute intervals. For 4-minute counts in 2016, the mean was 32 (95-percent CI, 18.3–45.2) with a high of 62. The 2017 index value was negative, indicating a possible drop in the population from 2016 to 2017 (fig. 20F). The average individual crowing frequency estimated from experimental counts completed at Lower Klamath was 1 call every 190 seconds (95-percent CI, 172–209).

5.5 Pheasant Survival

The mean monthly survival probability for adult pheasant across all field sites during the study period was 89.8 percent (95-percent CI, 88.1–91.3; fig. 21) and the 12-month (annual) cumulative survival probability for adult pheasant was 27.6 percent (95-percent CI, 21.9–33.6; fig. 21). We recovered 147 telemetry-marked pheasant mortalities during the 2013 ($n = 1$), 2014 ($n = 26$), 2015 ($n = 32$), 2016 ($n = 50$), and 2017 ($n = 38$) field seasons. Twelve mortalities were recovered at Mandeville Island, 28 were recovered at Gray Lodge, 41 were recovered at Roosevelt Ranch, 22 were recovered at Yolo, 17 were recovered at Little Dry Creek, and 27 were recovered at Lower Klamath. Diagnostic remains of pheasant and transmitters were used to classify cause of mortality as mammalian ($n = 37$), avian ($n = 15$), and unknown predators ($n = 40$); and unknown causes ($n = 55$). Most of the remains were limited to pieces of bone and feathers, which suggests that many carcasses were scavenged by a mammal before being recovered. Under those circumstances, we classified the cause of mortality as unknown.

The mean monthly adult survival probability for Gray Lodge during 2013–17 was 89.2 percent (95 percent CI, 85.2–92.3; fig. 22A) and the annual cumulative adult survival probability was 25.5 percent (95-percent CI, 14.6–38.2; fig. 22A). One mortality was recovered at Gray Lodge in 2013, nine mortalities were recovered in 2014, eight mortalities were recovered in 2015, seven mortalities were recovered in 2016, and three mortalities were recovered in 2017. Mortality classifications included avian ($n = 3$), mammalian ($n = 7$), and unknown predators ($n = 7$); and unknown causes ($n = 11$). During the 2016 field season, one female was observed with body intact, but chest and legs picked clean, suggesting avian predation. Another female recovered in February 2015 was sighted in a large burrow on the side of a levee, which suggests that her remains were cached by a mammal.

We did not track radio-marked pheasant at Mandeville Island in 2015 because captured females in 2014 could not be distinguished from previously released pen-reared birds. The mean monthly adult survival probability for Mandeville Island during 2013–14 and 2016–17 was 89.1 percent (95-percent CI, 81.4–93.9; fig. 22B) and the annual cumulative adult survival probability was 25.2 percent (95-percent CI, 14.6–38.2; fig. 22B). Two mortalities were recovered at Mandeville Island in 2014, four mortalities were recovered in 2016, and six mortalities were recovered in 2017. Mortality classifications included avian ($n = 1$), mammalian ($n = 5$), and unknown predators ($n = 3$); and unknown causes ($n = 3$). One female was sighted during the 2016 field season at the bottom of a well that controls water flow to canals with no evidence of predation, which suggests that she likely drowned. The transmitter of another female located in 2017 was found near the nest site at which she had been incubating, but the nest site had been plowed by farming equipment, likely killing the incubating female at the same time.

The mean monthly adult survival probability for Roosevelt Ranch during 2013–17 was 92.0 percent (95-percent CI, 81.4–92.3; fig. 22C) and the annual cumulative adult survival probability was 36.9 percent (95-percent CI, 25.8 – 48.2; fig. 22C). Eleven mortalities were recovered at Roosevelt Ranch in 2014, 14 mortalities were recovered in 2015, 11 mortalities were recovered in 2016, and 5 mortalities were recovered in 2017. The suspected causes of death include depredation by avian ($n = 4$), mammalian ($n = 7$), and unknown predators ($n = 13$); and unknown causes ($n = 17$). In 2014, one female was recovered in a freshly cut alfalfa field, but only some shredded feathers and one crushed leg were located, so it is likely that she was run over by a harvester. Two mortalities also recovered in 2014 and one recovered in 2015 were recovered as intact carcasses with no evidence of predation, which indicates that they may have died from heat-stress, disease, or other related causes.

The mean monthly adult survival probability for Yolo during 2013–16 was 88.9 percent (95-percent CI, 84.1–92.4; fig. 22D) and the annual cumulative adult survival probability was 24.4 percent (95-percent CI, 12.5–38.8; fig. 22D). Four mortalities were recovered at Yolo in 2014, 8 mortalities were recovered in 2015, and 10 mortalities were recovered in 2016. The suspected causes of death include depredation by avian ($n = 1$), mammalian ($n = 9$), and unknown predators ($n = 5$); and unknown causes ($n = 7$). In May 2015, the remains of a female outfitted with a GPS transmitter were sighted in a field east of her nest location. Body and tail feathers were located near the nest and flight feathers on the carcass showed evidence of teeth marks, suggesting mammalian predation.

The mean monthly adult survival probability for Little Dry Creek during 2015–17 was 89.8 percent (95-percent CI, 83.9–93.7; fig. 22E) and the annual cumulative adult survival probability was 27.4 percent (95-percent CI, 12.2–45.6; fig. 22E). Two mortalities were recovered at Little Dry Creek in 2015, 10 mortalities were recovered in 2016, and 5 mortalities were recovered in 2017. Mortality classifications included avian ($n = 2$), mammalian ($n = 1$), and unknown predators ($n = 6$); and unknown causes ($n = 8$). In May 2016, the remains of a hen were located at the nest site. The head was decapitated, and the internal organs were removed, suggesting avian predation.

The mean monthly adult survival probability for Lower Klamath during 2016–17 was 84.4 percent (95-percent CI, 76.8–89.8; fig. 22F) and the annual cumulative adult survival probability was 13.1 percent (95-percent CI, 4.2–27.7; fig. 22F). Lower Klamath had the lowest adult survival rate of all six field sites. Additionally, 10 marked females were lost owing to transmitter failure or their moving out of the study area, or because they were taken by predators. Eight mortalities were recovered at Lower Klamath in 2016 and 19 mortalities were recovered in 2017. Mortality classifications included avian ($n = 4$), mammalian ($n = 8$), and unknown predators ($n = 6$); and unknown causes ($n = 9$). During the 2016 field season, feathers with teeth marks on them were located next to a small pile of mammalian scat, but no carcass was located, suggesting mammalian predation. We also located one transmitter in an eagle's nest, which suggests that some marked birds may have been lost because they were taken by a raptor. In 2017, a transmitter and some feathers were detected about 20 cm underground in a freshly disked field, suggesting that the female was killed by farming equipment. Most remains at Lower Klamath in 2017 showed evidence of teeth marks on either the transmitter or feather remains, suggesting mammalian predation.

5.6 Nest-Site Habitat Selection

A total of 191 nests were located across all six sites over the course of the study (table 4). A total of 163 used ($n = 55$, 2014; $n = 40$, 2015; $n = 38$, 2016; $n = 31$, 2017) and 162 IR locations were assessed for nest-site habitat characteristics. One hundred and thirty nests were first nesting attempts ($n = 40$, 2014; $n = 30$, 2015; $n = 37$, 2016; $n = 23$, 2017), 51 nests were second attempts ($n = 16$, 2014; $n = 11$, 2015; $n = 11$, 2016; $n = 13$, 2017), and 10 nests were third nest attempts ($n = 5$, 2014; $n = 2$, 2015; $n = 1$, 2016; $n = 2$, 2017). Many of the captured pheasant at Lower Klamath died before initiating nests; thus, we were only able to monitor and conduct habitat surveys at seven nest sites. These nests were excluded from selection and survival analyses, as we did not have sufficient data to reliably estimate selection and survival parameters at this site and this allowed for better inferences to be made within the context of the Sacramento Valley and San-Joaquin River Delta regions.

Sixty univariate models, each representing a single spatial scale for each variable, were evaluated (table 5). We found the strongest model support for vertical cover over both horizontal cover and Robel pole height. Furthermore, vertical cover with a second-order effect term included in the model was the strongest microhabitat component that distinguished used from random locations across all field sites (model probability [w] = 0.98; table 6) when compared to the other single-variable models.

We noted the greatest model support when we included second-order terms in the model for vertical cover and residual cover at the nest bowl, as well as residual cover height at the 0.2-ha scale (fig. 23). A mean of 53.2 percent (SE = 2.5 percent) vertical cover was recorded at the nest bowl and a mean of 31.7 percent (SE = 2.6 percent; table 5) was recorded at available sites. Mean residual cover at the nest was 41.4 percent (SE = 2.5 percent), whereas mean residual cover at available sites was 21.6 percent (SE = 2.3 percent; table 5). We noted little difference in model support between linear and quadratic effects of bare ground cover at the nest, perennial grass height at the 0.2-ha scale, and annual grass height at the 0.2-ha scale (table 6; fig. 24). Hence, the base global model included vertical cover, residual cover, and bare ground cover at the nest, as well as perennial grass height, residual vegetation height, and annual grass height at the 0.2-ha scale (table 7). The most supported global model (Global 21; table 8) included three interactions based on *a priori* hypotheses, including interactions of vertical cover with annual grass height, residual cover with bare ground cover, and residual vegetation height with bare ground cover (Global 21; table 7). The first two of these three interactions showed the greatest support from the data (that is, 95-percent CIs of the coefficient did not overlap 0; table 9), as indicated in figure 24. There also was evidence of selection for perennial grass cover at the 0.03-ha scale, but it was highly correlated with perennial grass height ($R > 0.65$) and was not included in the global model.

We also investigated selection at each field site across sampling years and reported similar support for microhabitat characteristics that were significant for selection across all sites (table 10). We noted model support for selection of increasing vertical cover at all sites except Gray Lodge (table 10). We also reported evidence of female pheasant avoiding bare ground cover at all sites except Gray Lodge and Yolo. Additionally, residual cover was shown to be selected for at Gray Lodge, Roosevelt Ranch, and Yolo (table 10). Hence, pheasant tended to select similar habitat characteristics across study sites and across years. This could be partly due to the propensity of female pheasant to select certain types of cover for nesting as well as the availability of similar cover types at these study sites.

5.7 Nest Survival

Nest initiation rate across all females and all years of the study was 92.9 percent (SE = 6.0). In 2014, we located 61 nests, of which 35 were successful and 26 failed. In 2015, we located 43 nests, of which 27 were successful and 16 failed. In 2016, we located 49 nests, of which 21 were successful and 28 failed. In 2017, we located 38 nests, of which 15 were successful and 23 failed. Multiple re-nesting attempts were observed across all years and all sites. The cumulative nest survival probability across all sites for 2014–17 for the 37-day egg-laying and incubation phase was 34.5 percent (95-percent CI, 27.0–42.2; fig. 25).

The cumulative nest survival probability for Gray Lodge across all 4 years of the study was 33.7 percent (95-percent CI, 20.2–47.7; fig. 26A). We detected a total of 49 nests during the 2014–17 field seasons; 24 of these were successful and 25 failed (fig. 27). No females were monitored at Gray Lodge beyond April 6, 2017, because of transmitter failure and mortality; hence, no nests were monitored at this site in 2017. In 2016, we detected 17 nests, of which 6 were successful and 11 failed. In 2015, we located 18 nests, of which 9 were successful and 9 failed. Of the nine failed nests, eight nests were depredated (of which five appeared to be the result of mammalian depredation); one nest showed evidence of avian depredation; and one nest in a seasonal wetland was flooded before the eggs could hatch. In 2014, we located 14 nests, of which 9 were successful and 5 failed. Of the five failed nests in 2014, two nests showed evidence of mammalian depredation, one nest was destroyed by farming equipment, one nest failed due to unknown causes, and one nest bowl was observed to be empty (from which the eggs may have been removed by a predator).

The cumulative nest survival probability for Mandeville Island was 11.9 percent (95-percent CI, 2.6–29.3; fig. 26B). We discovered a total of 19 nests in the 2014 and 2016–17 field seasons; 7 nests were successful, and 12 nests failed (fig. 28). During the 2017 field season, we located 11 nests; 2 nests were successful and 9 nests failed. One hen was killed by farming equipment while incubating. Most failed nests in 2017 showed evidence of depredation by avian and mammalian predators. In 2014, we located four nests; one of these was successful and three failed. At least one failed nest showed evidence of an avian depredation, as the eggs were mostly intact with small holes in the sides and yolk residue still present in the shells. Nests were not monitored at Mandeville Island during the 2015 field season. In 2016, we located four nests; two nests were successful, and two nests failed.

At Roosevelt Ranch, the cumulative nest survival probability was 33.6 percent (95-percent CI, 20.8–46.9; fig. 26C). We located 61 nests during the 2014–17 field seasons; of these, 32 nests were successful, and 29 nests failed (fig. 29). In 2014, 29 nests were located, of which 16 were successful and 13 failed. Of the 13 failed nests, 4 nests were depredated (of which 1 nest appeared to be avian depredation; 1 nest appeared to be mammalian depredation; and 1 nest bowl was observed to be empty, from which the eggs may have been removed by a predator). One nest was destroyed by farming equipment, one nest failed because of female mortality, and seven nests were abandoned. Three nests were abandoned after field crews attempted to install cameras at the nest. The remaining abandoned nests occurred after females were determined to be on a nest by field technicians and were determined to not have returned during the subsequent visit. In 2015, 14 nests were located, of which 10 were successful and 4 failed. Of the four failed nests, one nest was depredated by an avian predator, the contents of two nest bowls were observed to be empty, and one nest was abandoned. Ravens were observed in all areas in which nest bowls were observed to be empty in 2014 and 2015. Furthermore, all nests that failed in 2015 at Roosevelt were in areas in which ravens were observed on a regular basis. In 2016, we detected

nine nests; two nests were successful and seven nests failed. Most failed nests showed evidence of depredation by either mammalian or avian predators. In 2017, we detected nine nests; four were successful and five failed. One individual made three nest attempts within the same field in 2017, and all three nests showed evidence of depredation by avian predators.

The cumulative nest survival probability for Yolo was 42.9 percent (95-percent CI, 22.6–61.9; fig. 26D). We detected 33 nests during the 2014–17 field seasons; 20 nests were successful, and 13 nests failed (fig. 30). In 2014, we located 14 nests, of which 7 were successful and 7 failed. Of the seven failed nests, four nests were depredated, of which two nests showed evidence of depredation by an avian predator. Furthermore, one of the two nests depredated by an avian predator may have failed because of female mortality, as her remains were located within 10 m of the nest on the same day the nest was determined to be depredated. Additionally, one nest was destroyed by mowing equipment and two nests were abandoned. The abandoned nests were not included in the survival analysis to keep data consistent across sampling years. In 2015, we located 11 nests, of which 8 were successful and 3 failed. Of the three failed nests, one appeared to be depredated by a mammalian predator and two failed because of female mortality. Yolo had the highest nest survival probability in 2015 and the lowest number of nest attempts per bird, mostly because females did not initiate another nest unless their brood failed early in the season. In 2016, we located eight nests, five of which were successful; the three remaining nests failed. No females were monitored at Yolo in 2017; hence, no nests were monitored during this season.

At Little Dry Creek, the cumulative nest survival probability was 66.1 percent (95-percent CI, 33.4–85.7; fig. 26E). We detected a total of 17 nests during the 2016–17 field seasons; of these, 12 nests were successful, and 5 nests failed (fig. 31). In 2016, we located six nests; five nests were successful, and one nest failed. The lone failure had nearly finished the incubation period before the female was killed at the nest; some eggs were pipped when the mortality was recovered. In 2017, we located 11 nests, of which 7 were successful and 4 failed.

The cumulative nest survival probability for Lower Klamath was 17.3 percent (95-percent CI, 1.0–52.3, fig. 26F). We located 12 nests during the 2016–17 field seasons; 3 nests were successful and 9 nests failed (fig. 32). In 2016, we located three nests; one was successful and two failed. In 2017, we located seven nests; two were successful and five failed. The small amount of data for Lower Klamath means that few conclusions should be drawn from the cumulative nest survival probability for this site.

Using factors identified as important for influencing nest-site selection (see section, “5.7 Nest Survival”), we also investigated selection relative to nest survival probabilities. Because of small sample sizes for nests assessed for habitat selection at Lower Klamath ($n = 7$), we excluded Lower Klamath from all nest site selection and survival analyses, as we did not have sufficient data to reliably estimate selection and survival parameters at this site. We did not find support for effects of interannual variation or variation across sites relative to the intercept-only model. Therefore, we did not include site or year as an additive fixed effect in the subsequent modeling steps. The most explanatory microhabitat feature predicting nest survival across all study sites was perennial grass cover at the 0.03-ha spatial scale ($w = 0.35$; table 6). Nest survival increased by 1.4 percent (95-percent CI, 0.2–2.8) for every 1 percent increase in perennial grass cover within the 0.03-ha radius of the nest (fig. 33A). Perennial grass cover at the nest bowl was the only other model significantly better than the intercept-only model (table 6), but it was removed from the table because it was highly correlated with perennial grass at the 0.03-ha spatial scale. For comparative purposes, we also showed the effects of perennial grass height at the 0.2-ha spatial scale (fig. 33B), mostly because this covariate was stronger in explaining selection.

We reported variability among the effects of specific habitat characteristics that explain nest survival among individual field sites using restricted data for each site. Vertical cover at Yolo, perennial forb cover at Roosevelt Ranch, and annual grass height at Little Dry Creek were most supported by the data ($\Delta AIC_c \geq 2$) in explaining nest survival (table 10). Because year was determined to be a significant predictor of survival at Roosevelt Ranch, we retained this variable as a fixed effect at this site, and the models with additional vegetation covariates were compared to a year-only model.

We investigated ratios of selection to clarify links between individual pheasant choice of microhabitats to their survival outcome. We noted strong model support for perennial grass cover at the 0.03-ha scale (table 6; fig. 33C) and perennial grass height at the 0.2-ha scale (table 6; fig. 33D) based on ratios of selection relative to an intercept-only model ($w_{\text{models 1 and 2}} = 0.32$ and 0.29 , respectively; table 6). We did not find support for other factors, although vertical cover, bare ground, and residual cover were determined to be significant relative to the intercept-only model in the nest selection analysis. Single-factor ratio of selection models also was analyzed at the site level, but we did not find model support for any of the tested effects relative to pheasant nest survival at individual field sites (table 10).

5.8 Brood-Rearing Habitat Selection

Preliminary results indicate that brood-rearing pheasant used a significantly greater percentage of vertical cover compared to DR and IR locations and that mean Robel pole height was significantly greater at brood locations in comparison to DR and IR locations (fig. 34). Mean percentage of perennial forb cover was significantly greater at used locations compared to DR and IR locations at all spatial scales, and mean annual forb cover was significantly higher at used locations compared to DR and IR locations at the 10- and 25-m spatial scale (fig. 35). Mean percentages of residual cover and litter were significantly higher at used and DR locations compared to IR locations at all spatial scales (fig. 36). Conversely, mean bare ground cover was significantly lower at used and DR locations compared to IR locations, suggesting that bare ground was avoided at brood locations (fig. 37). Mean heights for perennial and annual grasses were significantly higher at brood locations and DR locations in comparison to IR locations across all spatial scales (fig. 38). Similarly, mean heights for perennial and annual forbs were significantly higher at used locations compared to DR and IR locations across all spatial scales (fig. 39). Mean residual height also was significantly higher at used and DR locations in comparison to IR locations at all spatial scales (fig. 40). These results suggest that greater vegetative height and density likely were selected for by pheasant to provide adequate concealment for chicks. However, most brood surveys were completed later in the season, so taller mean forb heights could be the result of forbs growing as the season progresses and not the product of selection.

5.9 Brood Survival

We monitored 98 broods across the six field sites during 2014–17, of which 45 were successful (≥ 1 chick survived to 50 days post-hatch), 48 failed, and 5 were considered censored (fate could not be determined due to transmitter failure) (table 11). The 7-day interval brood survival probability was 98.8 percent (95-percent CI, 98.4–99.1), and the cumulative mean survival probability for the 50-day brood rearing period across all study sites was 54.2 percent (95-percent CI, 43.7–63.5; fig. 41). Overall, brood success was slightly higher compared to nest success, and success varied little between sites. Many of the unsuccessful broods were not confirmed as failed until at least 50 days post-hatch because of the difficulty in observing chicks. Females with broods tended to run away from the observer and leave their brood behind or would flush a short distance before returning to their chicks. Hence, we had to assume that a brood was still present until no chicks were observed for at least 2 weeks. We also had difficulty counting chicks until they were capable of flight and could be flushed, so chicks were rarely seen before 20 days of age. Occasionally, we could hear chicks calling after the female had moved away or flushed. Brood-rearing females generally used areas close to the nest and tended to move out of areas that lacked dense herbaceous forb cover. However, during summer, broods sometimes were observed in fields and seasonal wetlands with moist soil that consisted primarily of annual watergrass. Therefore, females may be selecting areas with contiguous herbaceous cover and areas with moist soil during the brood-rearing phase to provide cover from predators and adequate foraging opportunities for their chicks.

We monitored 24 broods at Gray Lodge during 2014–16, of which 8 were successful, 15 failed, and 1 was censored due to transmitter failure (table 11). The cumulative survival probability for 2014–16 was 43.1 percent (95-percent CI, 23.3–61.5; fig. 42A). In 2014, we monitored nine broods, of which five were successful and four failed. In 2015, we tracked nine broods, of which two were successful, six failed, and one was censored. One female in 2015 that was not detected on a nest was later located with a brood. In 2016, we followed six broods; only one was successful and five failed. No nests were monitored at Gray Lodge in 2017; hence, no broods were tracked during this year. Most successful broods at Gray Lodge in 2014 and 2015 used areas close to the nest. This suggests that brood-rearing females that moved farther away from the nest had more difficulty finding areas with adequate foraging opportunities. Females that nested in seasonal wetlands subsequently moved out of the wetlands and into adjacent fields with more contiguous cover. Females with broods also were present in large stands of blackberry (*Rubus armeniacus*; *Rubus ursinus*) along the edges of fields, as well as in fields with moist soil that consisted primarily of barnyard grass.

We tracked seven broods at Mandeville Island during 2014 and 2016–17, of which three were successful and four failed (table 11). The cumulative mean survival probability was 47.7 percent (95-percent CI, 13.9–75.9; fig. 42B). Broods were concentrated on the northern part of the island along the eastern levee. All brood locations in 2014 were within 350 m of the nest. Females with broods often were in areas of dense cover within seasonal wetlands, along drainage canals, and in crop fields. No broods were tracked at Mandeville Island in 2015, so results should be interpreted with caution until larger sample sizes are obtained. In 2016, we followed two broods; one was successful and one failed. All brood locations for the first 2 weeks were within about 150 m of their respective nest sites; thereafter, the females began to move away from the area. In 2017, we tracked two broods belonging to the same female; the first attempt failed, and the second attempt was successful.

We monitored 32 broods at Roosevelt Ranch during 2014–17, of which 11 were successful, 18 failed, and 3 were censored due to transmitter failure (table 11). The cumulative survival probability for 2014–17 was 51.7 percent (95-percent CI, 32.7–67.7; fig. 42C). In 2014, we tracked 16 broods, of which 6 were successful, 9 failed, and 1 was censored. In 2015, we tracked 10 broods, of which 4 were successful, 5 failed, and 1 was censored. During 2014 and 2015, females that nested in the large creeping wild rye field on the west end of the property tended to move into the fallowed rice fields to the south after their nests hatched. Additionally, brood-rearing females that nested in the large upland area on the southeastern corner of the property and that nested in the fields south of the permanent ponds often were in the corn, wheat, tomato, sunflower, and alfalfa fields bordering the southern and eastern edges of the property. In 2016, we tracked two broods, which both failed. During the 2017 season, we tracked four broods, of which one was successful, two failed, and one was censored due to transmitter failure. The successful brood spent the entire time outside the study area and we were not able to determine the brood fate until the female came back onto the property and flushed with three chicks at 51 days post-hatch. Females with broods generally stayed within about 200 m of the nest site for the first 2 weeks post-hatch; however, one individual in 2017 was recorded about 980 m from her nest site at 3 days post-hatch, before moving back within 200 m by 10 days post-hatch.

A total of 20 broods were monitored at Yolo during 2014–16, of which 14 were successful and 6 failed (table 11). The cumulative survival probability for 2014–16 was 66.9 percent (95-percent CI, 43.1–82.6; fig. 42D). No birds were monitored at Yolo in 2017; hence, no broods were tracked during this year. In 2014, we tracked seven broods, all of which were successful. Eight broods were tracked in 2015, of which four were successful and four failed. In 2016, we tracked five broods; three were successful and two failed. Brood-rearing females in the Parker and Twin Lakes units often were located along inundated canals and sloughs near their nesting locations. They used various herbaceous forbs for cover, including wild mustard (*Brassica campestris*), blessed milkthistle (*Silybum marianum*), common sunflower, and sweetclover.

Of the 12 total broods that were monitored at Little Dry Creek during 2016–17, 7 were successful and 5 failed (table 11). The cumulative brood survival probability for Little Dry Creek during 2016–17 was 55.8 percent (95-percent CI, 24.6–78.5; fig. 42E). In 2016, we monitored five broods, of which four were successful and one failed. In 2017, we monitored seven broods, of which three were successful and four failed. Broods at Little Dry Creek tended to stay within 200 m of their nest, often closer, during the first few weeks of brood-rearing, before moving about 200–400 m from the areas in which they nested in the final weeks of brood-rearing.

Three total broods were monitored at Lower Klamath in 2016 and 2017, two were successful and one was censored due to transmitter failure (table 11), giving a cumulative brood survival probability of 100.0 percent (95-percent CI; 100.0–100.0; fig. 42F). In 2016, the brood-rearing female was detected more than 2 km from her nest site by 16 days post-hatch and was recorded about 1,500 m from the nest site when her brood was ultimately confirmed as successful. The brood in 2017, however, stayed within about 200 m of the nest site during the first 3 weeks of brood-rearing, and was recorded less than 500 m from the nest site when the brood was confirmed as successful. We strongly advise against drawing conclusions from the cumulative brood survival probability figures for Lower Klamath because of their reliance on only two broods.

5.10 Raven and Raptor Surveys

We completed 1,407 raptor and raven surveys during March–September of 2014–2017 across all six field sites following USGS survey protocols (see section, “4.9 Avian Predator Monitoring”). Raptors and (or) ravens were detected in 1,308 surveys (93.0 percent), whereas no birds were detected in 99 surveys. We observed a total of 6,345 raptor and 291 raven detections throughout the study period and across all sites. Raptor species included turkey vulture (*Cathartes aura*; $n = 5,378$), red-tailed hawk (*Buteo jamaicensis*; $n = 485$), Swainson’s hawk (*Buteo swainsoni*; $n = 199$), northern harrier (*Circus cyaneus*; $n = 92$), white-tailed kite (*Elanus leucurus*; $n = 31$), American kestrel (*Falco sparverius*; $n = 9$), burrowing owl (*Athene cunicularia*; $n = 4$), Cooper’s hawk (*Accipiter cooperii*; $n = 4$), red-shouldered hawk (*Buteo lineatus*; $n = 4$), bald eagle (*Haliaeetus leucocephalus*; $n = 3$), great horned owl (*Bubo virginianus*; $n = 3$), osprey (*Pandion haliaetus*; $n = 2$), ferruginous hawk (*Buteo regalis*; $n = 2$), and unidentified raptors ($n = 125$). Barn owl (*Tyto alba*), golden eagle (*Aquila chrysaetos*), peregrine falcon (*Falco peregrinus*), and prairie falcon (*Falco mexicanus*) were only sighted once during the 5-year survey period. Other avian species detected included American crow (*Corvus brachyrhynchos*; $n = 118$) and unidentified bird species ($n = 706$).

Over the course of the study, evidence from nest remains suggests that of the 29 suspected avian depredations, at least 5 likely were the result of raven depredation. We classified these failures as suspected raven depredations because (1) ravens were regularly observed in these areas; and (2) nest bowls were found empty, and ravens are known to remove eggs from the nest before consuming them (Coates and others, 2008). One nest at Gray Lodge in 2014, one nest at Mandeville Island in 2017, and three nests at Roosevelt Ranch in 2015 ($n = 2$) and 2016 ($n = 1$) were suspected to be depredated by ravens. Of the 291 ravens detected across all field sites during raptor-raven surveys, most (64.9 percent; $n = 189$) were at Roosevelt Ranch. Yolo had the second highest proportion of raven detections (14.1 percent; $n = 41$), followed by Lower Klamath (8.3 percent; $n = 24$), Gray Lodge (8.6 percent; $n = 25$), and Mandeville Island (3.8 percent; $n = 11$). Only one raven was detected by raptor-raven surveys at Little Dry Creek over the duration of the study.

6.0 Interpretations

We focused interpretation of vital rate estimates from populations grouped by region. Mandeville Island and Lower Klamath are both in geographically distinct regions of California and populations at these sites are subject to different conditions in comparison to the four Sacramento Valley study sites. Therefore, Mandeville Island is the only site that we considered a part of the Sacramento-San Joaquin River Delta Region and Lower Klamath is the only site that we included in the Klamath Basin Region.

6.1 Sacramento-San Joaquin River Delta Region

Thousands of pen-reared pheasant are released each year on Mandeville Island, which makes this population somewhat unique with respect to the proportion of pen-reared to naturalized pheasant on the island. Adult survival and brood survival estimates were like those in Sacramento Valley study sites. However, the estimated nest survival rate at Mandeville Island was substantially lower than at study sites elsewhere. For example, we determined that only 2 of 11 monitored nests hatched during 2017, and nearly twice as many nests failed as succeeded over the duration of the study (table 4). We also captured and collected blood from three previously

released pen-reared pheasants and four naturalized pheasants that had hatched on the island. We detected that the pen-reared and naturalized pheasants were positive for titers specific to different pathogens, which suggests that disease exposure did not overlap between these two groups. However, small sample sizes preclude our ability to test for differences in pathogen exposure at the site level.

Mandeville Island is intensively farmed, which results in inconsistent concealment cover through time. Fields often are mowed or plowed when not being cultivated for crops, and the division of fields into small irrigated units likely increases edge effects. Farming practices that facilitate the availability of consistent nesting cover likely would increase nest survival and, thus, would benefit pheasant population growth rates on Mandeville Island. Specifically, retaining cover in areas adjacent to fields that are plowed, mowed, or cultivated for crops would not only provide additional nesting cover but also would increase available refugia when pheasants are escaping predators or farming equipment. Furthermore, the most nests are detected during the months of April, May, and June. Hence, adjustment in timing strategies of farming practices, such as mowing and disking during these critical months for reproduction, likely would provide enough time for pheasant to complete incubation and reduce the number of nests destroyed by farm equipment. Six total nests failed as the result of being plowed by farming equipment across all study sites and years. Two of the six nests destroyed by farm equipment were at Mandeville Island, one of which also resulted in the female being killed on the nest. Disking often kills complete broods, and can kill or injure incubating females (Rodgers, 1983). Basore and others (1986) reported that low nest densities for agriculturally associated bird species were more linked with tilled cropland when compared to other land-use practices. Implementing no-tillage practices allows sufficient time for completion of the nest incubation in birds that nest in row crops (Best, 1986). Examining alternate agricultural practices, such as no-till or delayed tillage, could increase productivity by allowing ample time for pheasant to complete the nesting and brood-rearing cycles without suffering direct losses due to farming practices, as well as providing adequate cover for concealment from predators.

6.2 Sacramento Valley Region

Four of the six study sites—Gray Lodge, Roosevelt Ranch, Yolo, and Little Dry Creek—were grouped within the Sacramento Valley region. These sites represent some of the largest and most productive historical pheasant populations in the Central Valley. Annual adult survival estimates at these sites ranged from 24.4 to 36.9 percent (SE 2.9), and nest and brood survival estimates ranged from 33.6 to 66.1 percent (SE 7.7) and 43.1 to 66.9 percent (SE 4.9), respectively. We noted little variation in adult survival estimates across these four sites, but nest and brood survival estimates were less consistent. Nest survival was highest at Little Dry Creek (66.1 percent; 95-percent CI, 33.4–85.7; fig. 26E), and brood survival was highest at Yolo (66.9 percent; 95-percent CI, 43.1–82.6; fig. 42D). Environmental factors contributing to higher nest and brood survival may be most influential at larger spatial scales. The areas surrounding each of these study sites is intensively farmed, and the abundance of cover is dependent on the time of year. During autumn and winter (August–February), crop fields often are disked or flooded to prepare for the following planting season. Additionally, seasonal wetlands are flooded during this time of year, which further reduces cover available to pheasant in the study area.

Gray Lodge is adjacent to nut orchards, rice, and seasonal wetlands belonging to surrounding hunting clubs. Seasonal wetlands also are a predominant land-cover type within Gray Lodge. Hence, pheasants at Gray Lodge often used emergent vegetation in seasonal wetlands as cover from predators. Four of the 23 failed nests at Gray Lodge were subject to flooding during summer irrigation of wetlands and 2 were destroyed by farming equipment, which suggests that predation is still a greater threat to nest survival at Gray Lodge. The cumulative nest survival probability for Gray Lodge was 33.7 percent (95-percent CI, 20.2–47.7; fig. 26A), which was similar the cumulative nest survival probability at Roosevelt Ranch (33.6 percent; 95-percent CI, 20.8–46.9; fig. 26C). Gray Lodge had its highest nest success rate in 2014, in which 9 of 13 nests hatched, but nest survival decreased each subsequent year. This decrease in nest survival coincided with the height of the drought in the Central Valley and increases in predation on nest of marked birds may be due to larger-scale factors. Further investigation of the effects of drought likely would benefit our understanding of environmental factors influencing pheasant population dynamics at Gray Lodge.

Like the other three study sites in this region, Roosevelt Ranch is surrounded by agriculture, but the crop types differ from those grown near Gray Lodge and Little Dry Creek. Gray Lodge and Roosevelt Ranch had almost identical nest survival probabilities, but the brood survival probability across all years of the study at Roosevelt Ranch was almost 10 percent higher. Roosevelt also had the highest annual adult survival probability of all six sites. Additionally, Roosevelt Ranch was the smallest of the study sites and marked female pheasant frequently moved on and off property to adjacent crop fields, especially when rearing broods. Crops commonly grown in the area include alfalfa, winter wheat, sunflower, tomato, and safflower. Rice is grown to the west and north of Roosevelt, and nut orchards also are common in the area. A major difference between Roosevelt Ranch and Gray Lodge is the distribution of grassland and upland habitat relative to seasonal wetland habitat. Fields dominated by grasses and forbs are connected and are placed in between crop fields to the south and a few large wetlands to the north.

We primarily monitored marked pheasant south of the auto tour loop at Yolo, specifically in the Parker and Twin Lakes units. These units were composed of grassland fields mixed with seasonal wetland-upland complexes. Pheasant monitored in these areas tended to stay within the unit boundaries, except for an occasional female that flew over the slough running along the eastern border to the levee adjacent to the Sacramento Deep Water Ship Channel. Additionally, marked birds were only monitored at Yolo during 2014–16 because of an extensive flood event in 2017 that precluded trapping during winter and spring. We were unable to find marked birds from the 2016 season, which suggests that our remaining marked females left the area or that radio-transmitters ceased functioning.

We began monitoring marked pheasant at Little Dry Creek in 2016. Hence, we only have 2 years of vital rate information, which may increase the difficulty in estimating factors related to pheasant population dynamics at this site. Agricultural practices and other environmental conditions at Little Dry Creek are like those at Gray Lodge, which makes differences between these sites important to examine. Like Gray Lodge, Little Dry Creek is surrounded by orchards, rice agriculture, and private hunting clubs. The mean crowing counts at Little Dry Creek were higher than at Gray Lodge (fig. 19), although counts at Little Dry Creek have decreased each year. Adult, nest, and brood survival estimates at Little Dry Creek also were higher than estimates at Gray Lodge, but confidence intervals were wider because of smaller sample sizes. Nest and brood survival estimates for Little Dry Creek were 66.1 percent (95-percent CI, 33.4–

85.7; fig. 26E) and 55.8 percent (95-percent CI, 24.6–78.5; fig. 42E), respectively, and were higher compared to almost all other sites in the study. The nest survival data from Little Dry Creek indicated that annual grass height was positively linked to nest survival (table 10), but other factors that may have been influential were not noted to be significant given the small sample size of nests at this site. Marked females at Little Dry Creek nested mostly in mixed grassland units in closed zone areas and moved into more forb-dominated areas during the brood-rearing phase. Furthermore, the UD of marked females at Little Dry Creek indicated that they rarely moved farther than 1 km from their capture location. A key difference that distinguished Gray Lodge from Little Dry Creek is that females often nested in wetlands with emergent vegetation at Gray Lodge, whereas females at Little Dry Creek did not. Both sites have a large part of the wildlife area allocated to seasonal wetlands for wintering waterfowl. However, seasonal wetlands are dominant throughout Gray Lodge with upland and grassland units interspersed to a lesser extent, whereas Little Dry Creek has seasonal wetlands and grassland units grouped together such that multiple units of similar habitat are adjacent to each other. Therefore, providing larger areas of mixed grassland habitat or a greater number of management units close together that are dominated by grasses (especially perennial grasses that retain concealment structure throughout the breeding season) may increase the nest survival rates of pheasant populations in areas that have high proportions of seasonal wetland compared to grassland habitat units.

6.3 Klamath Basin Region

The Lower Klamath National Wildlife Refuge is one of six refuges in the Klamath Basin National Wildlife Refuge Complex. Lower Klamath is about 300 km north of the next closest study site, and the climate in the region is cooler than the Central Valley. Agriculture in the region is dominated by cereal grains, potatoes, and other crops adapted to muck soils and shorter growing seasons. These crops may provide more consistent cover than many of the crops grown in the Sacramento Valley during critical times of year when pheasant are rearing broods or when cover is less abundant. Although adult and nest survival estimates for Lower Klamath were some of the lowest across all six study sites, pheasant abundance at Lower Klamath is high. A major difference between Klamath and the other sites is the size of the field site. Lower Klamath is much larger than the other sites, individual fields are larger, and a higher proportion of fields are used for agriculture or left fallow. The large population size at Lower Klamath may increase compensatory mortality and reduce mortality that is additive within the population. More information on pheasant vital rates at Lower Klamath would substantially benefit our understanding of population dynamics at this site.

7.0 Acknowledgments

We thank M. Meshriy, B. Burkholder, J. Stoddard, A. Atkinson, D. Van Baren, T. Hermansen, and L. Cockrell of the California Department of Fish and Wildlife for their expertise and logistical support. We also thank J. Beckstrand and S. Freitas of the U.S. Fish and Wildlife for facilitating access to resources and logistical support. We thank the Mandeville Island Duck Club for providing funding and access to their lands. We also thank Roosevelt Ranch Duck Club for providing access to their private lands. We appreciate the expertise of M. Cadena of the University of California Davis School of Veterinary Medicine in preparing samples and helping run laboratory assays for disease analysis. We also thank B. Brussee for assistance with completing statistical analyses. Finally, we are extremely grateful to G. Riggs, R. Shin, S. Haynes, and R. Buer of the U.S. Geological Survey for their diligence in collecting data in the field and compiling data for analyses.

8.0 References Cited

- Akaike, H., 1973, Information theory as an extension of the maximum likelihood principle, *in* Petrov, B.N., and Caaki, F., eds., *Second International Symposium on Information Theory: Budapest, Hungary, Akademiai Kiado*, p. 267–281.
- Anderson, D.R., 2008, *Model based inferences in the life sciences—A primer on evidence*: New York, Springer Science, 184 p.
- Basore, N.S., Best, L.B., and Wooley, J.B. Jr., 1986, Bird nesting in Iowa no-tillage and tilled cropland: *The Journal of Wildlife Management*, v. 50, p. 19–28.
- Benton, T.G., Vickery, J.A., and Wilson, J.D., 2003, Farmland biodiversity—Is habitat heterogeneity the key?: *Trends in Ecology and Evolution*, v. 18, p. 182–188.
- Best, L.B., 1986, Conservation tillage—Ecological traps for nesting birds?: *Wildlife Society Bulletin*, v. 14, p. 308–317.
- Burnham, K.P., and Anderson, D.R., 2002, *Model selection and multimodel inference—A practical information-theoretic approach* (2d ed.): New York, Springer.
- Beyer, H.L., 2015, *Geospatial modelling environment* (Version 0.7.4.0): Spatial Ecology LLC, <http://www.spatial ecology.com/gme>.
- California Department of Fish and Wildlife, 2014, *Game take hunter survey reports*: California Department of Fish and Wildlife web page, accessed July 13, 2015, at, <https://www.dfg.ca.gov/wildlife/hunting/uplandgame/reports/surveys.html>.
- Chamberlain, D.E., Fuller, R.J., Bunce, R.G.H., Duckworth, J.C., and Shrubb, M., 2000, Changes in the abundance of farmland birds in relation to the timing of agricultural intensification in England and Wales: *Journal of Applied Ecology*, v. 37, p. 771–788.
- Coates, P.S., Brussee, B.E., Howe, K.B., Fleskes, J.P., Dwight, I.A., Connelly, D.P., Meshriy, M.G., and Gardner, S.C., 2017, Long-term and widespread changes in agricultural practices influence ring-necked pheasant abundance in California: *Ecology and Evolution*, v. 7, no. 8, p. 2546–2559.
- Coates, P.S., Connelly, J.W., and Delehanty, D.J., 2008, Predators of greater sage-grouse nests identified by video monitoring: *Journal of Field Ornithology*, v. 79, no. 4, p. 421–428.
- Dahlgren, R.B., 1988, Distribution and abundance of the ring-necked pheasant in North America: *Proceedings of the Midwest Fish and Wildlife Conference*, v. 49, p. 29–43.
- Daubenmire, R.F., 1959, A canopy-coverage method of vegetation analysis: *Northwest Science*, v. 33, p. 224–227.

- Davis, R.S., Peterson, R.K.D., and Macedo, P.A., 2007, An ecological risk assessment for insecticides used in adult mosquito management: Integrated Environmental Assessment and Management, v. 3, p. 373–382.
- Dwight, I.A., Coates, P.S., Stoute, S.T., Senties-Cue, C.G., Gharpure, R.V., and Pitesky, M.E., 2017, Serologic surveillance of wild and pen-reared ring-necked pheasants (*Phasianus colchicus*) as a method of understanding disease reservoirs: Journal of Wildlife Diseases, v. 54, p. 414–418.
- Evans, K.L., 2004, The potential for interactions between predation and habitat change to cause population declines of farmland birds: Ibis, v. 146, p. 1–13.
- Fulton, M.H., and Key, P.B., 2001, Acetylcholinesterase inhibition in estuarine fish and invertebrates as an indicator of organophosphorus insecticide exposure and effects: Environmental Toxicology and Chemistry, v. 20, p. 37–45.
- Gibson, D., Bloomberg, E.J., and Sedinger, J.S., 2016, Evaluating vegetation effects on animal demographics—The role of plant phenology and sampling bias: Ecology and Evolution, v. 6, p. 3621–3631.
- Giesen, K.M., Schoenberg, T.J., and Braun, C.E., 1982, Methods for trapping sage grouse in Colorado: Wildlife Society Bulletin, v. 10, no. 3, p. 224–231.
- Glemnitz, M., Zander, P., and Stachow, U., 2015, Regionalizing land use impacts on farmland birds: Environmental Monitoring and Assessment, v. 187, p. 1–21.
- Hart, C.M., 1990, Management plan for the ring-necked pheasant in California: Sacramento, California Department of Fish and Game, Wildlife Management Branch, 111 p.
- Hausleitner, D., Reese, K., and Appa, A., 2005, Timing of vegetation sampling at greater sage-grouse nests: Rangeland Ecology and Management, v. 58, p. 553–556.
- Hill, D.A., 1985, The feeding ecology and survival of pheasant chicks on arable farmland: Journal of Applied Ecology, v. 22, p. 645–654.
- Hill, J.E., Brandon, D.M., and Brouder, S.M., 1999, Agronomic implications of alternative straw management practices—Winter flooding and straw management—Implications for rice production 1994–1996: Davis, University of California, Agronomy Progress Report No. 264, 116 p.
- Horne, J. S., and Garton, E.O., 2006, Likelihood cross-validation versus least squares cross-validation for choosing the smoothing parameter in kernel home-range analysis: Journal of Wildlife Management, v. 70, no. 3, p. 641–648.
- Intellicast, 2018, Climate data: Intellicast web page, accessed April 12, 2018, at <http://www.intellicast.com/Local/History.aspx?location=USCA1260>.
- Jones, R.E., 1968, A board to measure cover used by prairie grouse: Journal of Wildlife Management, v. 32, p. 28–31.
- Kernohan, B.J., Gitzen, R.A., and Millspaugh, J.J., 2001, Analysis of animal space use and movements, chap 5 of Millspaugh, J.J., and Marzluff, J.M., eds., Radiotracking and animal populations: San Diego, Academic Press, p. 126–166.
- Laake, J., and Rexstad, E., 2007, RMark—An alternative approach to building linear models in MARK, appendix C of Cooch, E., and White, G., eds., Program MARK—A gentle introduction: Fort Collins, Colorado State University, p. C-1–C-115.
- Lever, C., 1987, Naturalized birds of the world: Harlow, United Kingdom, Longman Scientific and Technical, 615 p.
- Linduska, J.P., 1943, A gross study of the bursa of Fabricius and cock spurs as age indicators in the ring-necked pheasant: The Auk, v. 60, p. 426–437.

- Lockyer, Z.B., Coates, P.S., Casazza, M.L., Espinosa, S. and Delehanty, D.J., 2015, Nest-site selection and reproductive success of greater sage-grouse in a fire-affected habitat of northwestern Nevada: *The Journal of Wildlife Management*, v. 79, no. 5, p.785-797.
- Manly, F.J., McDonald, L.L., Thomas, D.L., McDonald, T.L., and Erickson, W.P., 2002, *Resource selection by animals—Statistical design and analysis for field studies*: London, Chapman and Hall, 240 p.
- Messick, J.P., Bizeau, E.G., Benson, W.W. and Mullins, W.H., 1974, Aerial pesticide applications and ring-necked pheasants: *The Journal of Wildlife Management*, p. 679–685.
- Mineau, P., and Whiteside, M., 2006, Lethal risk to birds from insecticide use in the United States—A spatial and temporal analysis: *Environmental Toxicology and Chemistry*, v. 25, p. 1214–1222.
- National Audubon Society, 2014, The Christmas bird count historical results: National Audubon Society web page, accessed November 1, 2015, at <http://www.christmasbirdcount.org>.
- Poulin, B., Lefebvre, G., and Paz, L., 2010, Red flag for green spray—Adverse trophic effects of *Bti* on breeding birds: *Journal of Applied Ecology*, v. 47, p. 884–889.
- Prochazka, B.G., Coates, P.S., Ricca, M.A., Casazza, M.L., Gustafson, K.B., and Hull, J.M., 2016, Encounters with pinyon-juniper influence riskier movements in greater sage-grouse across the Great Basin: *Rangeland Ecology and Management*, v. 70, p. 39–49.
- R Development Core Team, 2008, *R—A language and environment for statistical computing*: Vienna, Austria, R Foundation for Statistical Computing, ISBN 3-900051-07-0, <https://www.R-project.org>.
- Rice, C.G., 2003, Utility of pheasant call counts and brood counts for monitoring population density and predicting harvest: *Western North American Naturalist*, v. 63, p. 178–188.
- Robel, R.J., Briggs, J.N., Dayton, A.D., and Hulbert, L.C., 1970, Relationships between visual obstruction measurements and weight of grassland vegetation: *Journal of Range Management*, v. 23, no. 4, p. 295–297.
- Rodgers, R.D., 1983, Reducing wildlife losses to tillage in fallow fields: *Wildlife Society Bulletin*, v. 11, p. 31–38.
- Rusek, J., 1998, Biodiversity of Collembola and their functional role in the ecosystem: *Biodiversity and Conservation*, v. 7, p. 1207–1219.
- Saif, Y.M., Fadly, A.M., Glisson, J.R., McDougald, L.R., Lisa, K. N., and David, E.S., 2008. *Diseases of Poultry* 12th Edition.
- Sauer, J.R., Hines, J.E., Fallon, J.E., Pardieck, K.L., Ziolkowski, D.J., Jr., and Link, W.A., 2014, *The North American breeding bird survey—Results and analysis, 1966–2012* (Version 02.19.2014): Laurel, Maryland, U.S. Geological Survey Patuxent Wildlife Research Center.
- Schroeder, M.A., Young, J.R., and Braun, C.E., 1999, Greater sage-grouse (*Centrocercus urophasianus*), in Poole, A., ed., *The birds of North America online*, no. 425: Ithaca, New York, Cornell Laboratory of Ornithology, accessed April 18, 2018, at <http://bna.birds.cornell.edu/bna/species/425>.
- U.S. Department of Agriculture, 2014a, Census of agriculture: U.S. Department of Agriculture web page, accessed July 14, 2015, at <http://www.agcensus.usda.gov/Publications/index.php>.
- U.S. Department of Agriculture, 2014b, Crop acreage data: U.S. Department of Agriculture web page, accessed July 14, 2015, at <http://www.fsa.usda.gov/FSA/webapp?area=newsroom&subject=landing&topic=foi-er-fri-cad>.

- U.S. Geological Survey, 2017, Greater sage-grouse project, Nevada—General information and protocols for field operations and monitoring (2015 ed.): U.S., Geological Survey, Western Ecological Research Center, Dixon, California, 83 p.
- Wakkinen, W.L., Reese, K.P., Connelly, J.W. and Fischer, R.A., 1992, An improved spotlighting technique for capturing sage grouse: Wildlife Society Bulletin, v. 20, p. 425–426.
- White, G.C., and Burnham, K.P., 1999, Program MARK—Survival estimation from populations of marked animals: Bird Study, v. 46, p. 120–138.
- Woodburn, M.I.A., Carroll, J.P., Robertson, P.A., and Hoodless, A.N., 2009, Age determination of pheasants (*Phasianus Colchicus*) using discriminant analysis: National Quail Symposium Proceedings, v. 6, article 53, p. 505–516.
- Worton, B.J., 1989, Kernel methods for estimating the utilization distribution in home-range studies: Ecology, v. 70, p. 164–168.
- Zuur, A.F., Leno, E.N., Valker, N.J., Saveliev, A.A., and Smith, G.M., 2009, Mixed effects models and extensions in ecology with R—Statistics for biology and health: New York, Springer, 574 p.

Figures

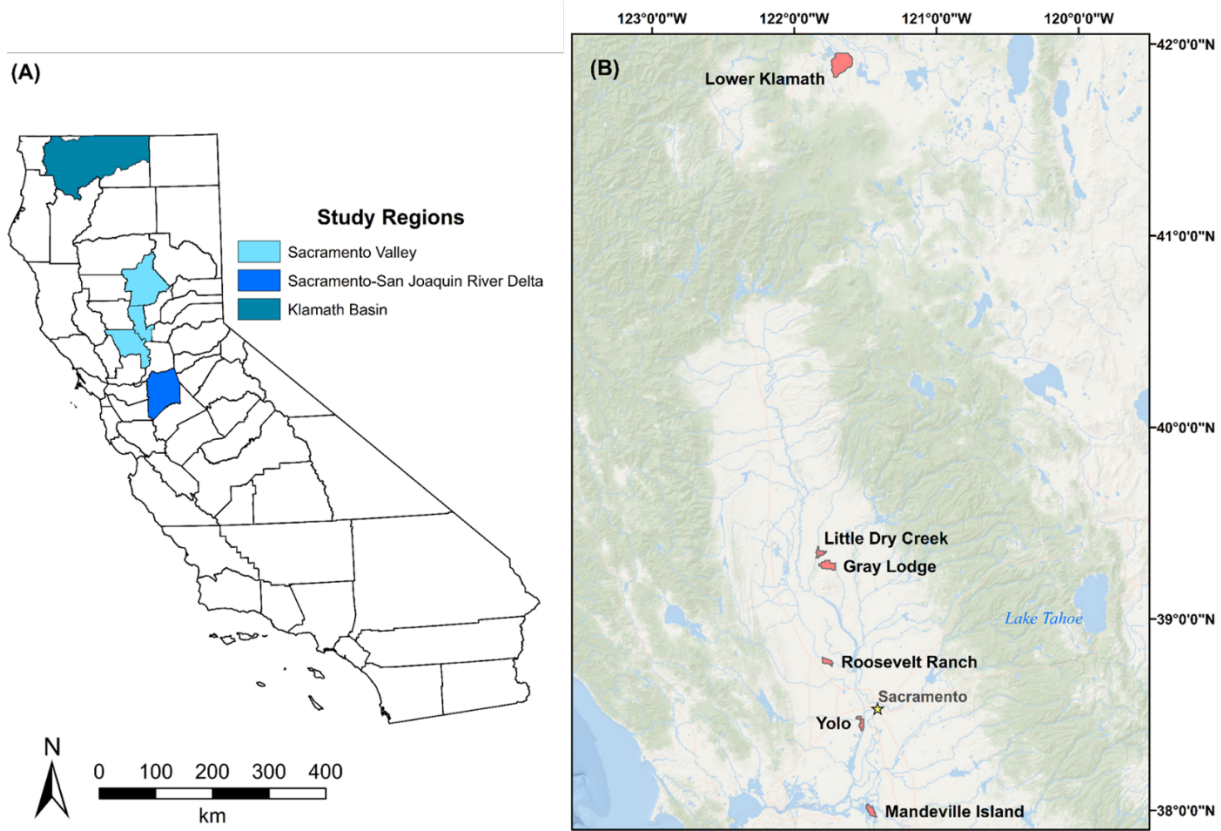


Figure 1. Map showing (A) study regions and (B) study sites for ring-necked pheasant (*Phasianus colchicus*) data collection, Sacramento-San Joaquin River Delta, Sacramento Valley, and Klamath Basin, northern California, 2013–17.

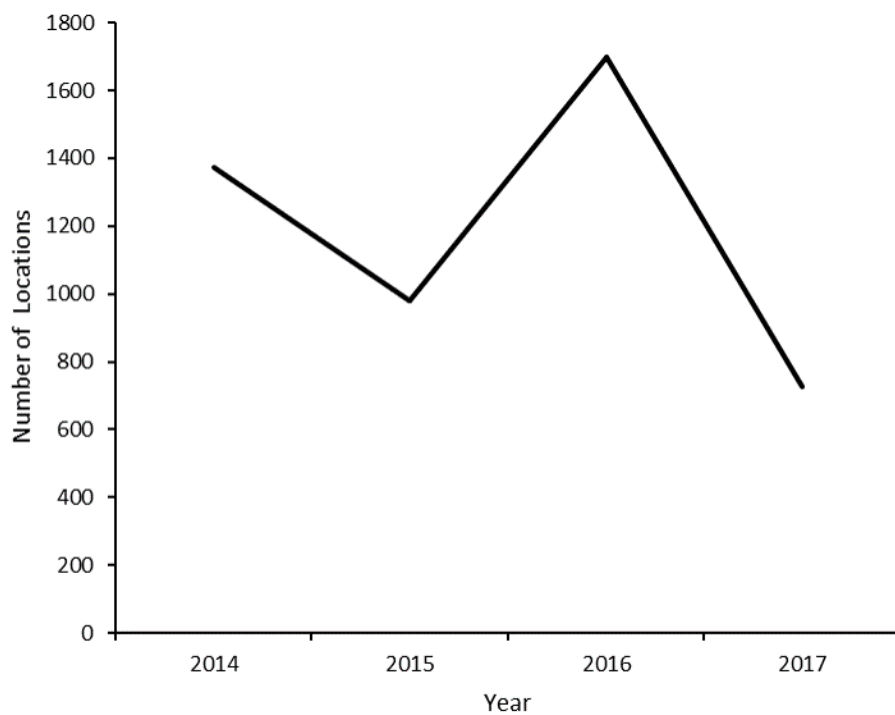


Figure 2. Graph showing number of locations by year of Very High Frequency-marked ($n = 53$, 2014; $n = 72$, 2015; $n = 106$, 2016; $n = 60$, 2017) ring-necked pheasant (*Phasianus colchicus*), Sacramento-San Joaquin River Delta, Sacramento Valley, and Klamath Basin, northern California, 2014–17.

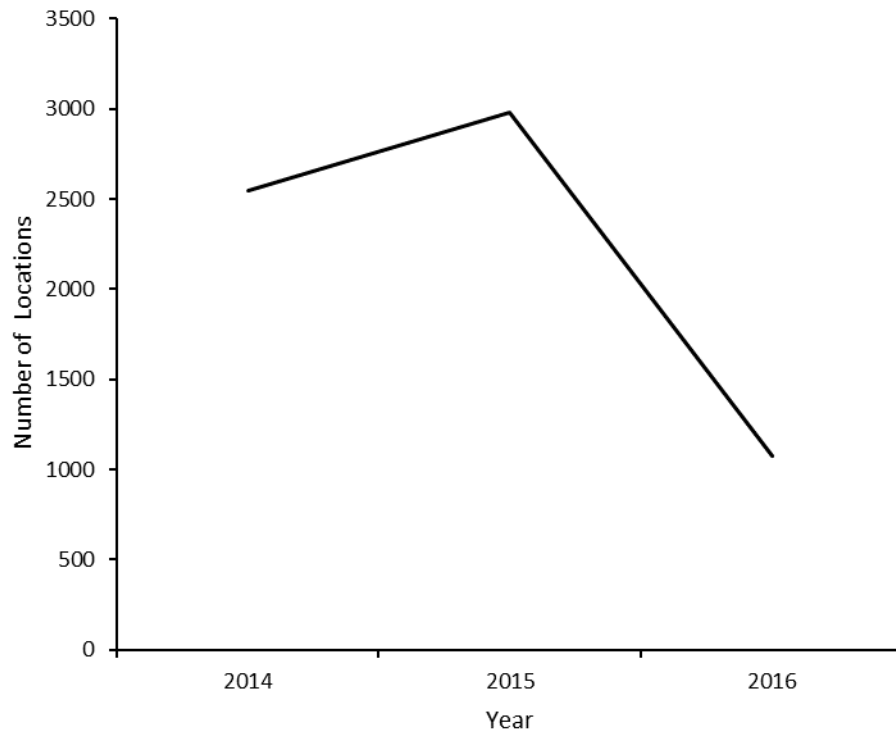


Figure 3. Graph showing number of locations by year of Global Positioning System-marked ($n = 2$, 2014; $n = 2$, 2015; $n = 3$, 2016) ring-necked pheasant (*Phasianus colchicus*), Sacramento-San Joaquin River Delta, Sacramento Valley, and Klamath Basin, northern California, 2014–16.

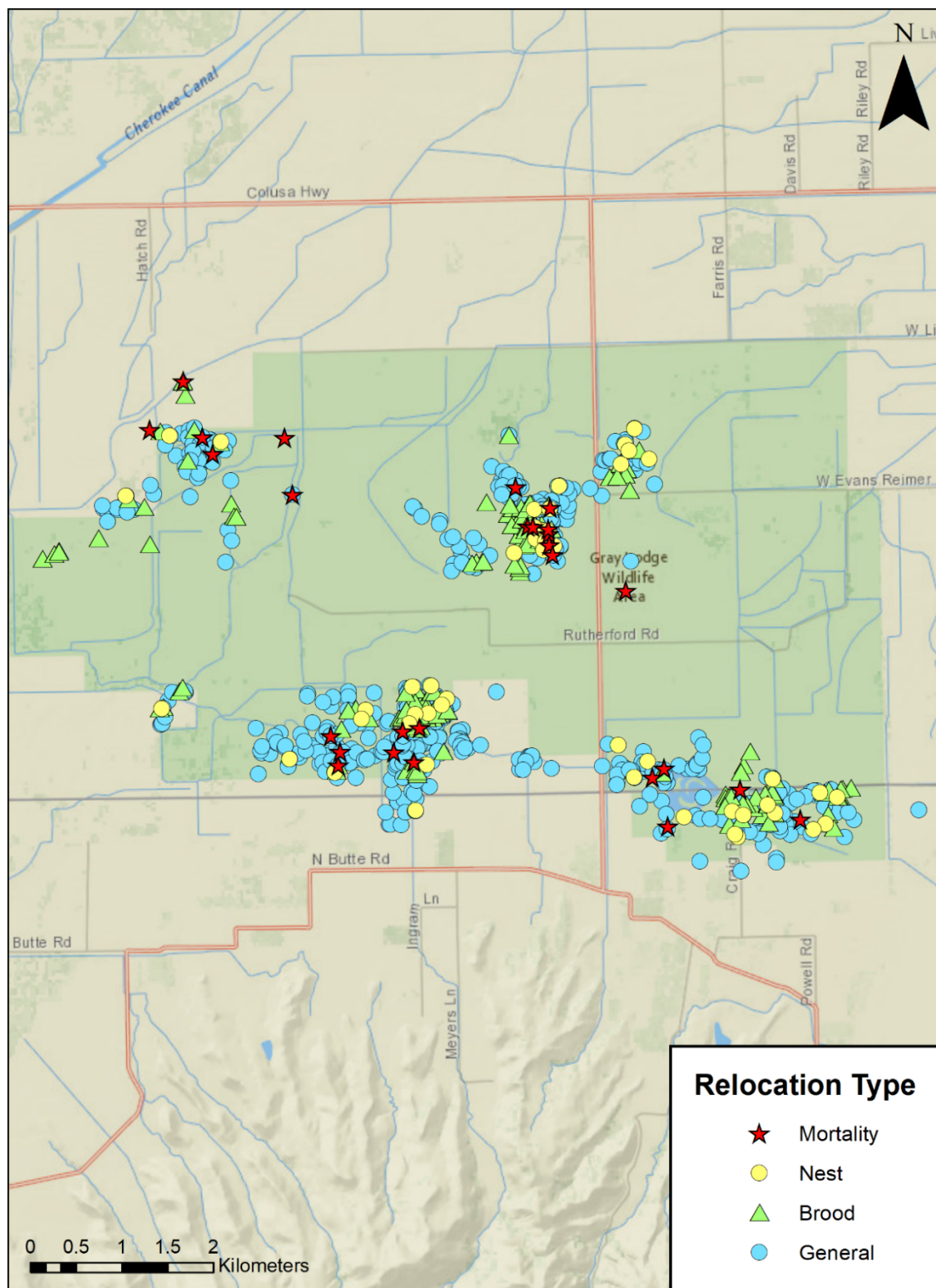


Figure 4. Map showing general, nest, brood, and mortality telemetry locations of Very High Frequency-marked ring-necked pheasant (*Phasianus colchicus*), Gray Lodge Wildlife Area, Gridley, northern California, 2014–17.

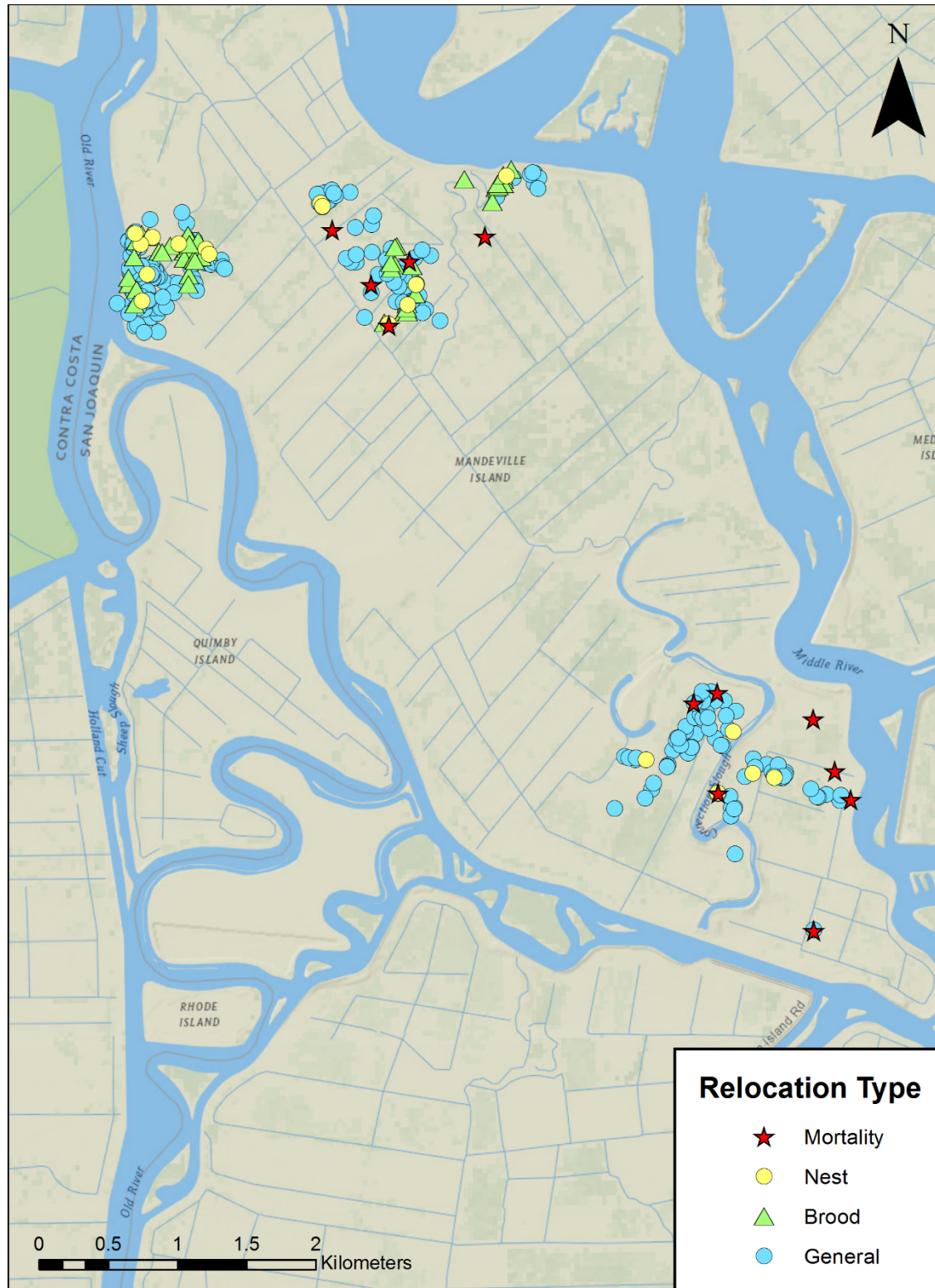


Figure 5. Map showing general, nest, brood, and mortality telemetry locations of Very High Frequency-marked ring-necked pheasant (*Phasianus colchicus*), Mandeville Island Duck Club, San Joaquin County, northern California, 2014–16 and 2017.

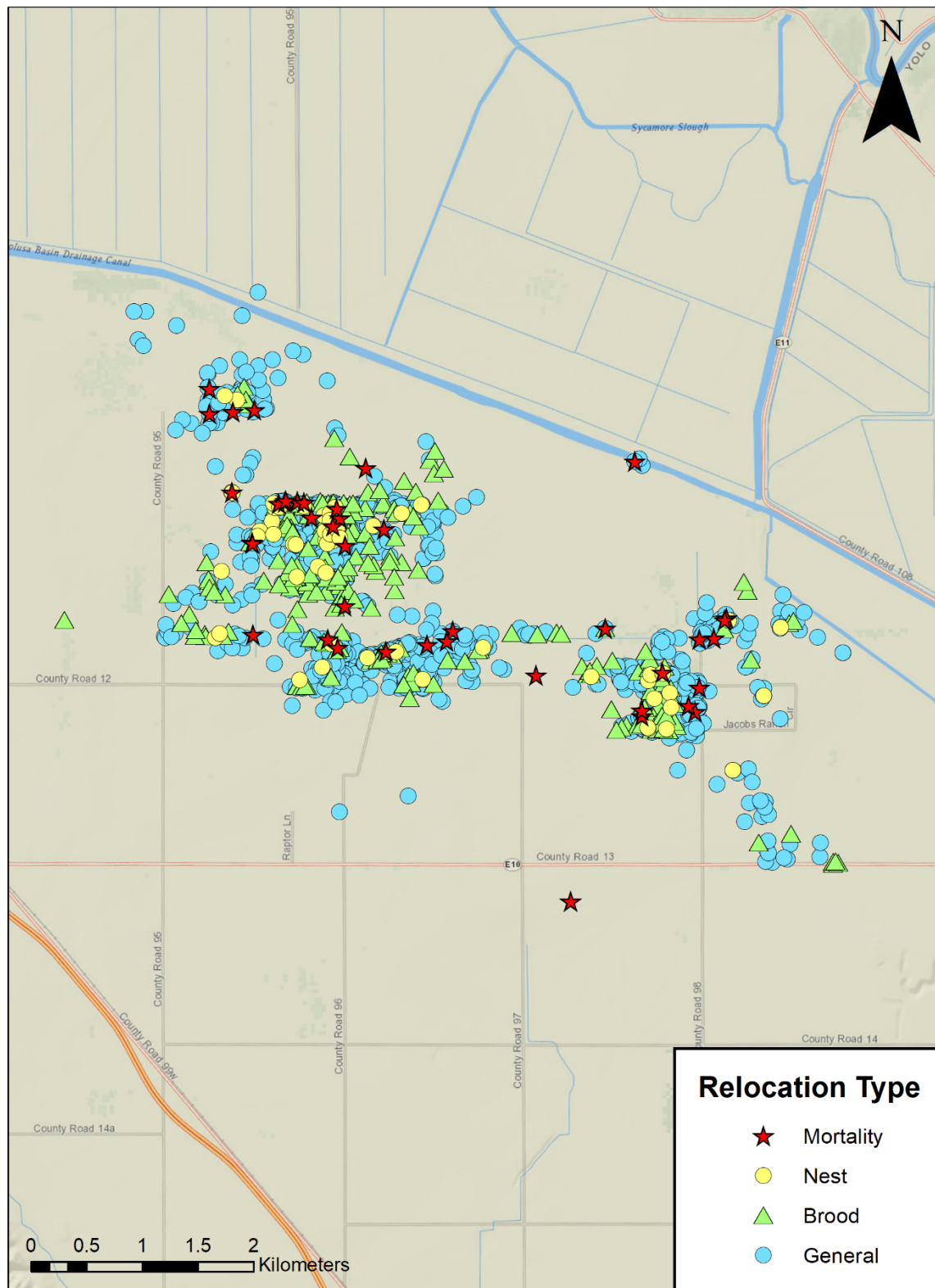


Figure 6. Map showing general, nest, brood, and mortality telemetry locations of Very High Frequency-marked ring-necked pheasant (*Phasianus colchicus*), Roosevelt Ranch Duck Club, Zamora, northern California, 2014–17.

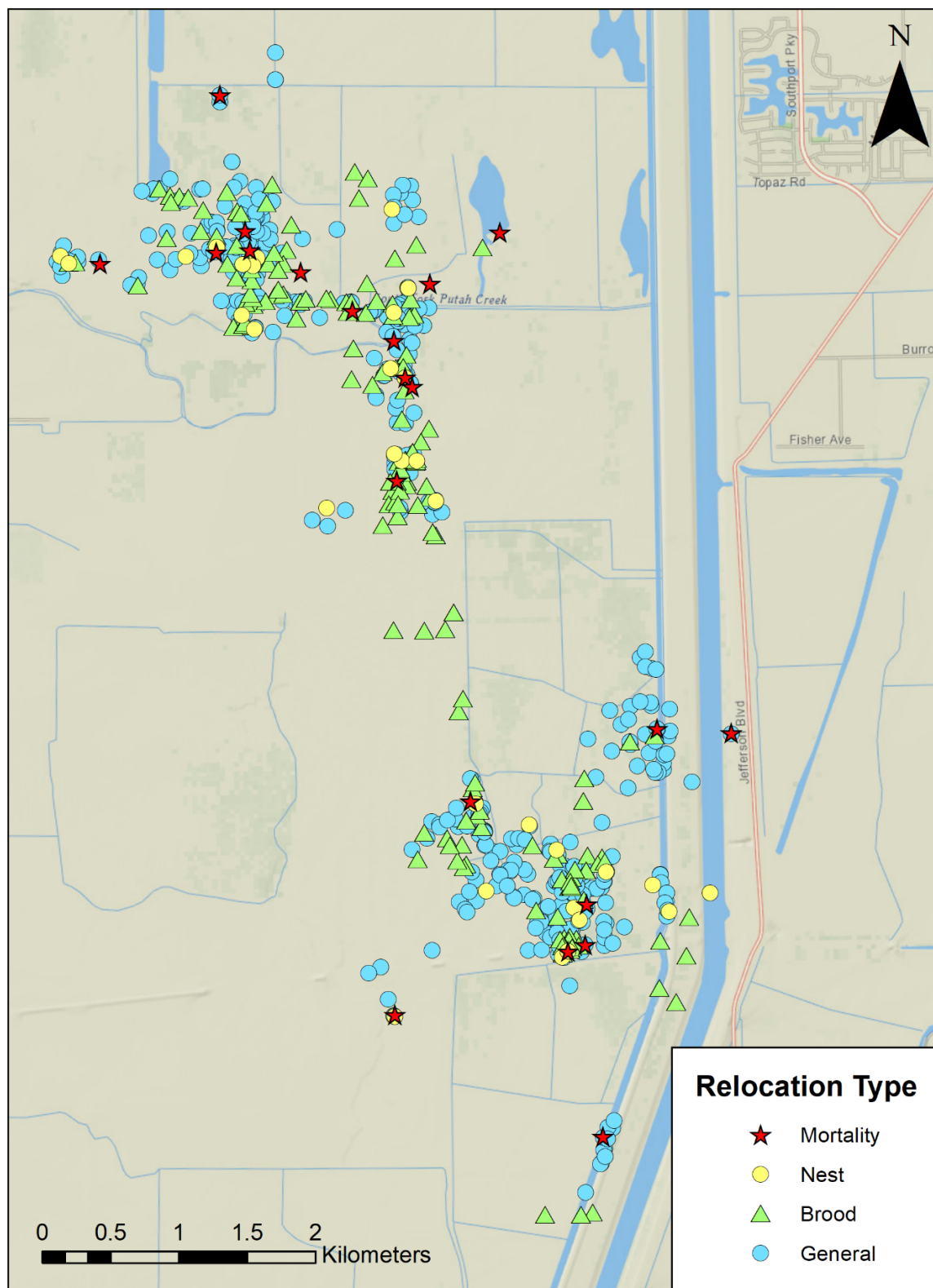


Figure 7. Map showing general, nest, brood, and mortality telemetry locations of Very High Frequency-marked ring-necked pheasant (*Phasianus colchicus*), Yolo Bypass Wildlife Area, Davis, northern California, 2014–16.

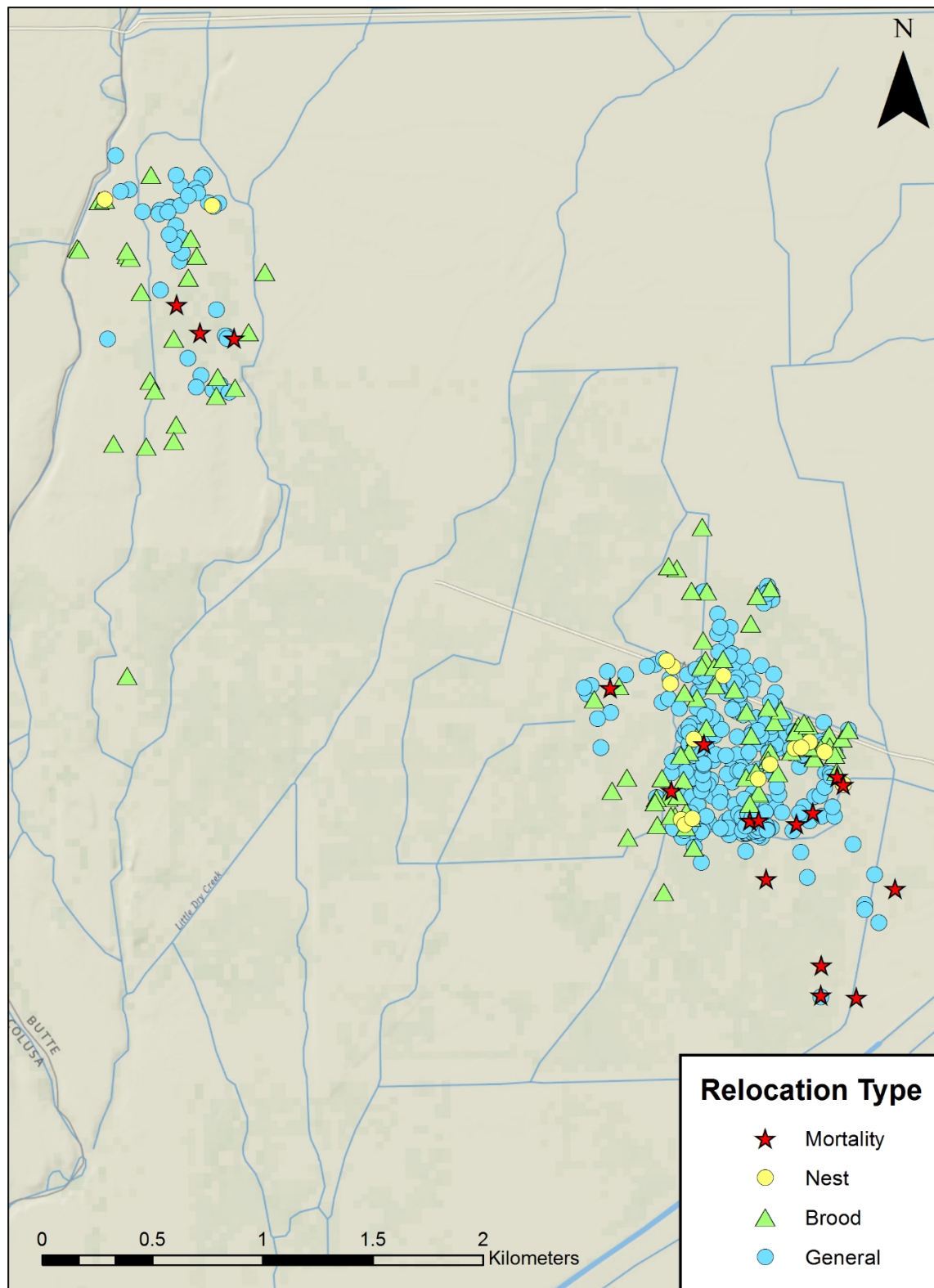


Figure 8. Map showing general, nest, brood, and mortality telemetry locations of Very High Frequency-marked ring-necked pheasant (*Phasianus colchicus*), Little Dry Creek Unit of Upper Butte Basin Wildlife Area, Gridley, northern California, 2016–17.

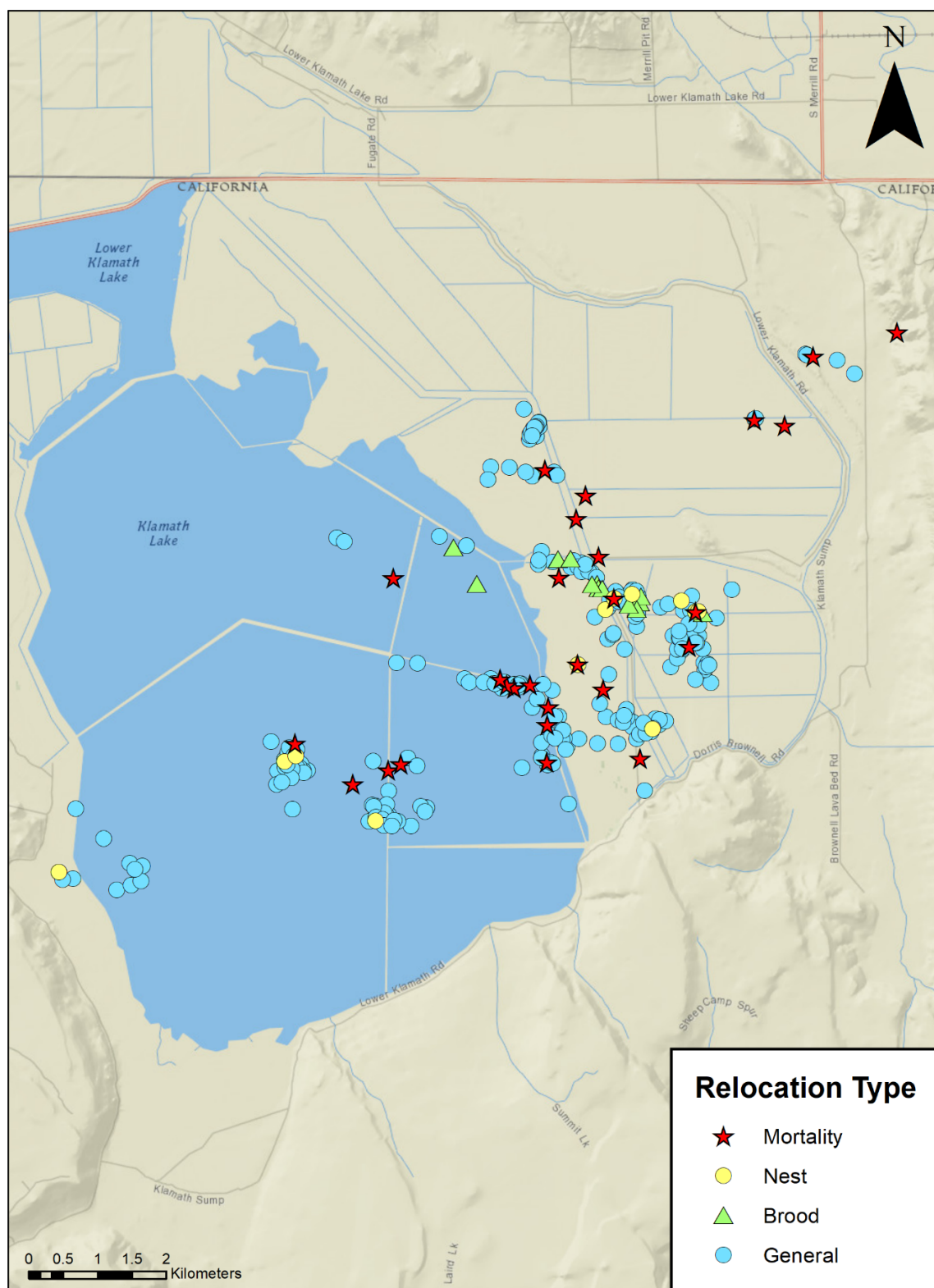


Figure 9. Map showing general, nest, brood, and mortality telemetry locations of Very High Frequency-marked ring-necked pheasant (*Phasianus colchicus*), Lower Klamath National Wildlife Refuge, Dorris, northern California, 2016–17.

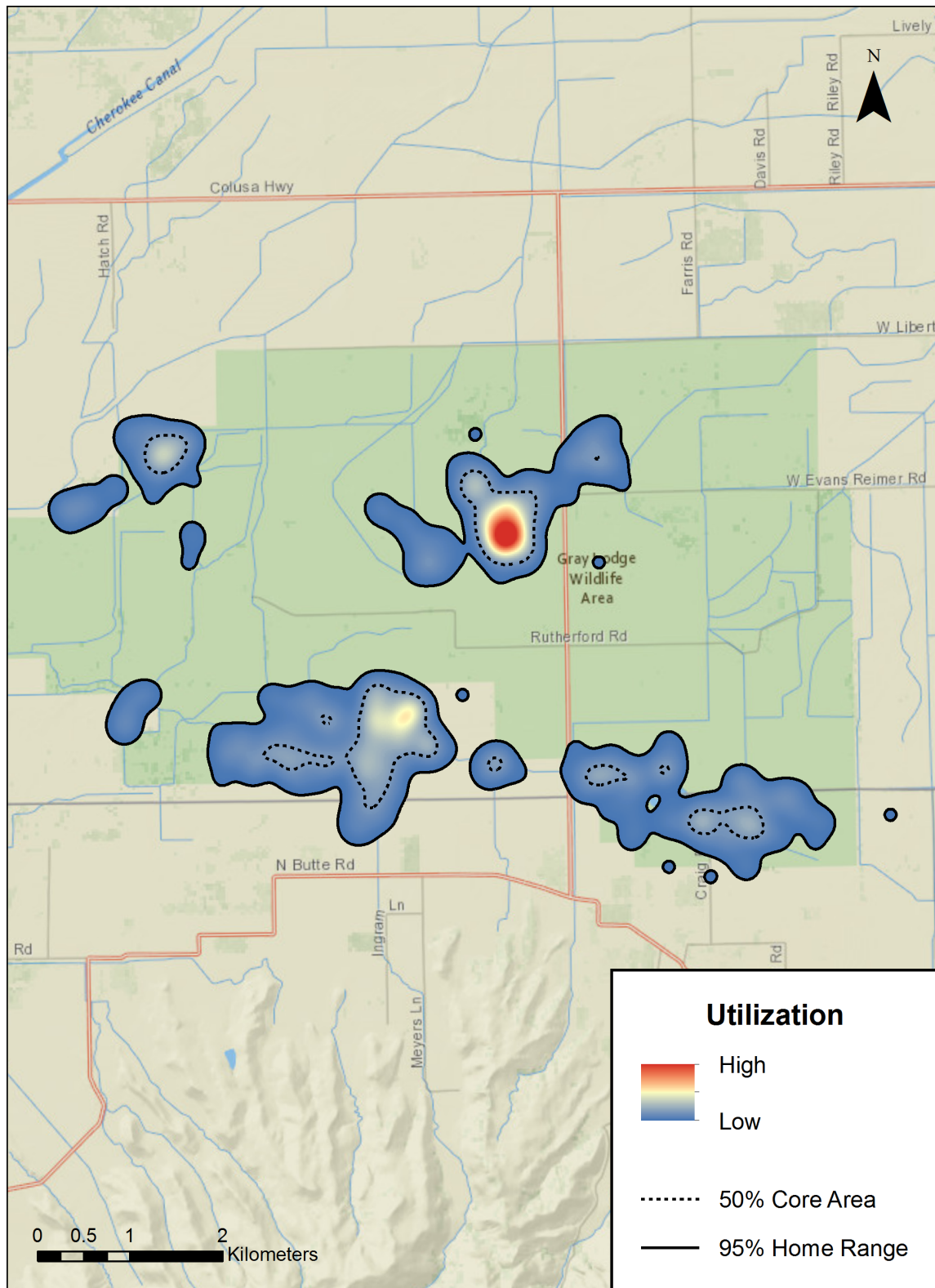


Figure 10. Map showing cumulative utilization distribution of Very High Frequency-marked ring-necked pheasant (*Phasianus colchicus*), Gray Lodge Wildlife Area, northern California, spring and summer (March–September) 2014–17. Utilization distribution was approximated by using kernel density estimators.

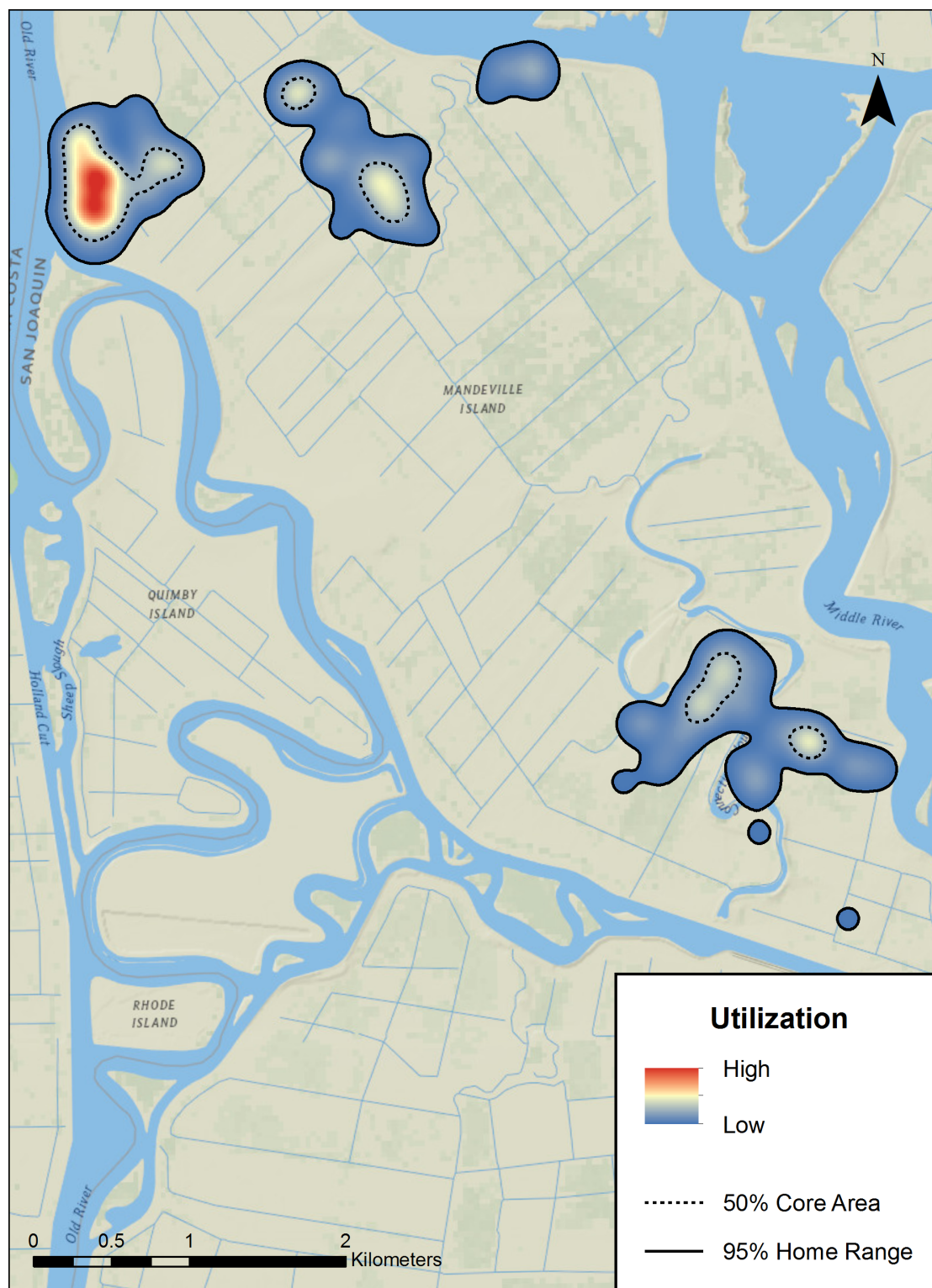


Figure 11. Map showing cumulative utilization distribution of Very High Frequency-marked ring-necked pheasant (*Phasianus colchicus*), Mandeville Island Duck Club, northern California, spring and summer (March–September) 2014–16 and 2017. Utilization distribution was approximated by using kernel density estimators.

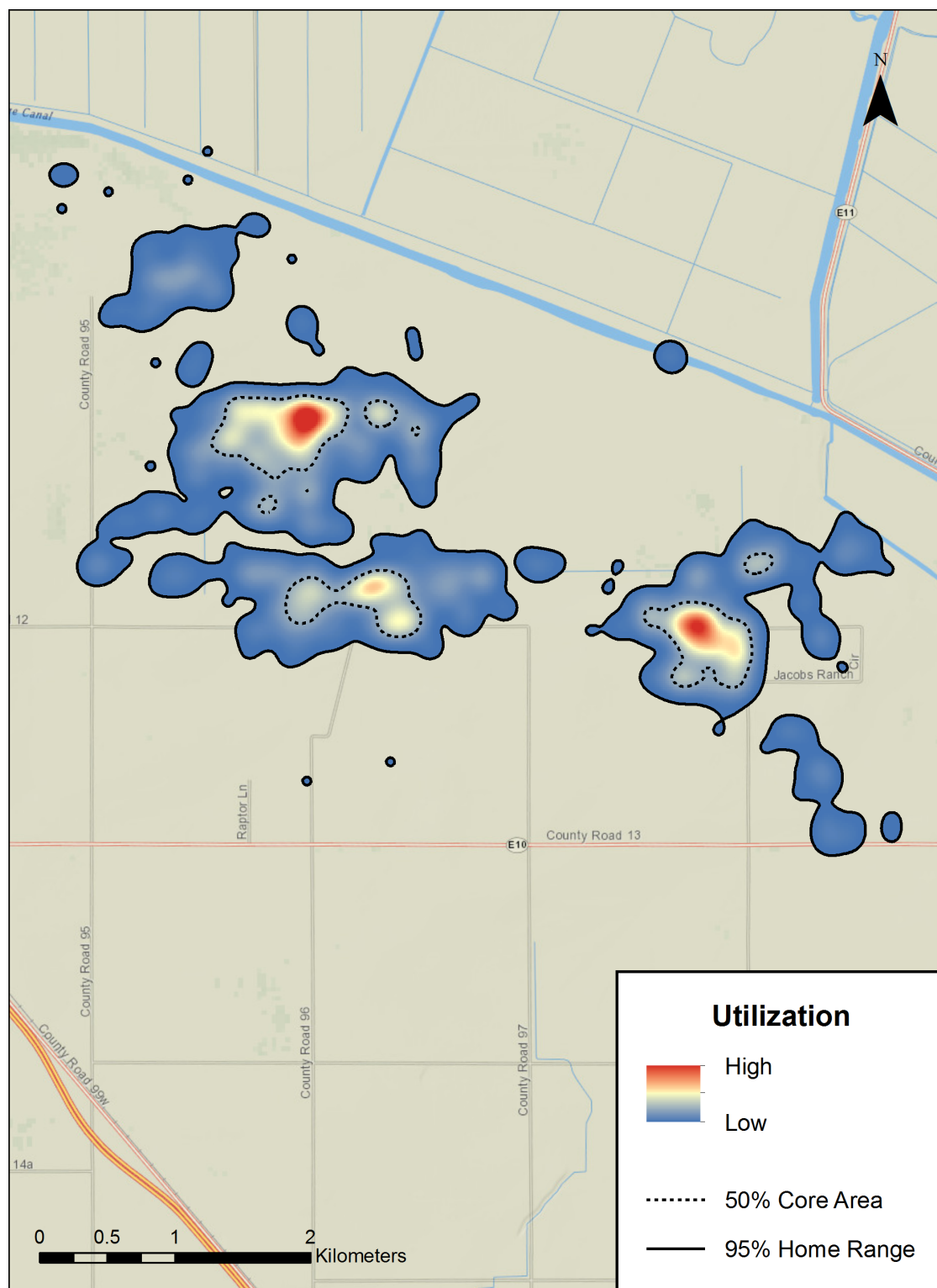


Figure 12. Map showing cumulative utilization distribution of Very High Frequency-marked ring-necked pheasant (*Phasianus colchicus*), Roosevelt Ranch Duck Club, northern California, spring and summer (March–September) 2014–17. Utilization distribution was approximated by using kernel density estimators.

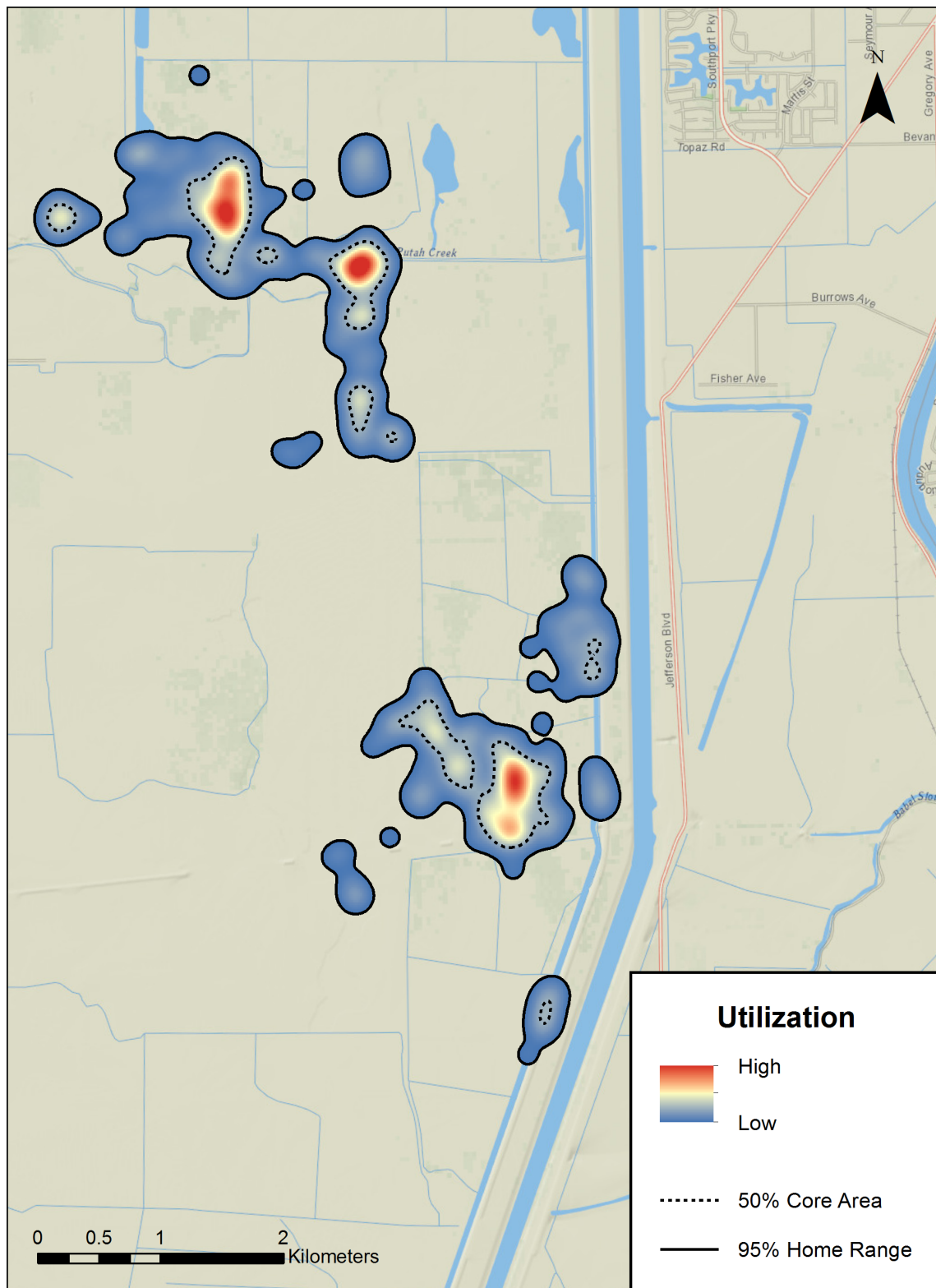


Figure 13. Map showing cumulative utilization distribution of Very High Frequency-marked ring-necked pheasant (*Phasianus colchicus*), Yolo Bypass Wildlife Area, northern California, spring and summer (March–September) 2014–16. Utilization distribution was approximated by using kernel density estimators.

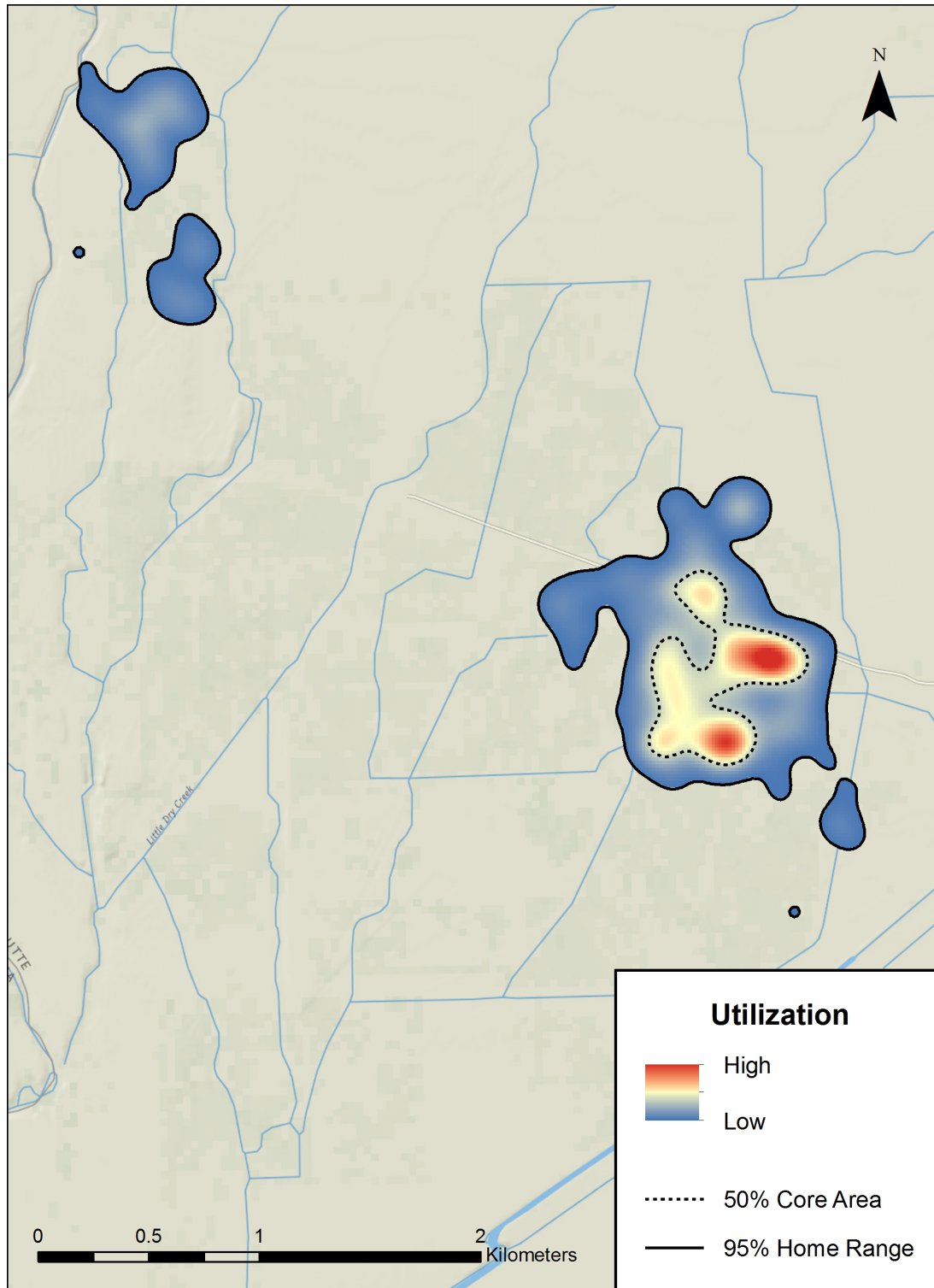


Figure 14. Map showing cumulative utilization distribution of Very High Frequency-marked ring-necked pheasant (*Phasianus colchicus*), Little Dry Creek Unit of Upper Butte Basin Wildlife Area, northern California, spring and summer (March–September) 2016–17. Utilization distribution was approximated by using kernel density estimators.

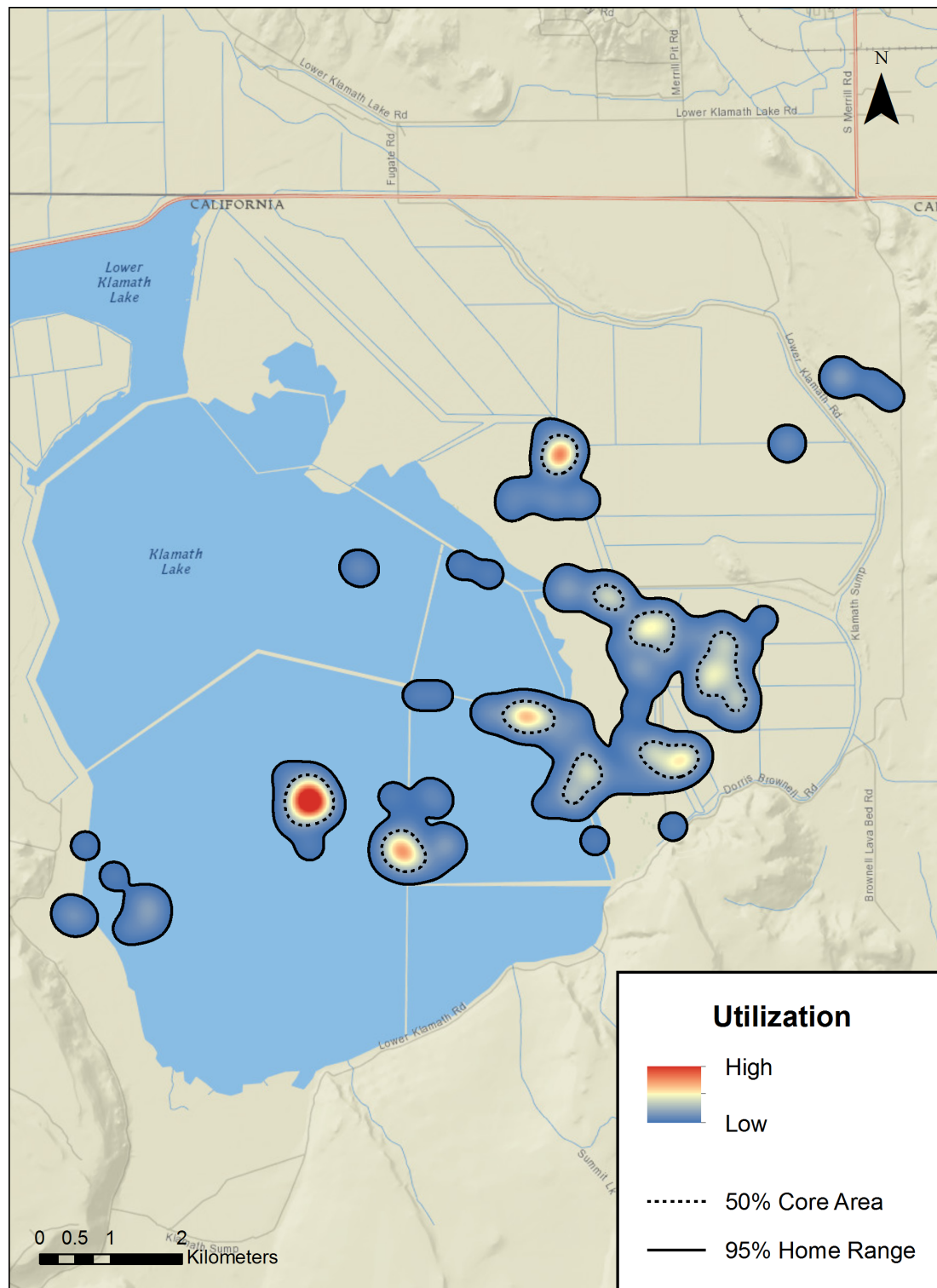


Figure 15. Map showing cumulative utilization distribution of Very High Frequency-marked ring-necked pheasant (*Phasianus colchicus*), Lower Klamath National Wildlife Refuge, northern California, spring and summer (March–September) 2016–17. Utilization distribution was approximated by using kernel density estimators.

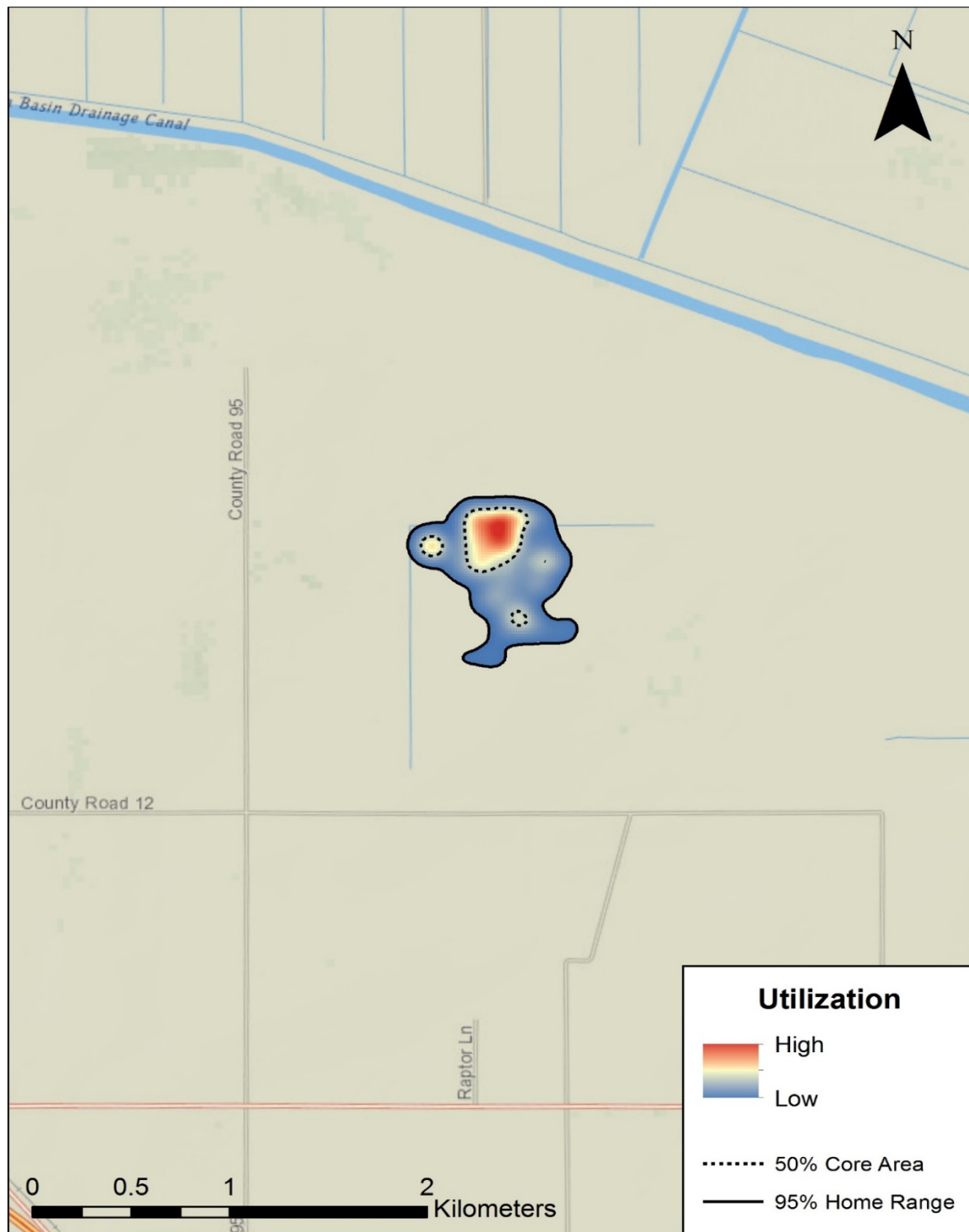


Figure 16. Map showing cumulative utilization distribution of Global Positioning System-marked ring-necked pheasant ($n = 2$, *Phasianus colchicus*), Roosevelt Ranch Duck Club, northern California, winter, spring, and summer (January–September) 2014–15. Utilization distribution was approximated by using kernel density estimators.

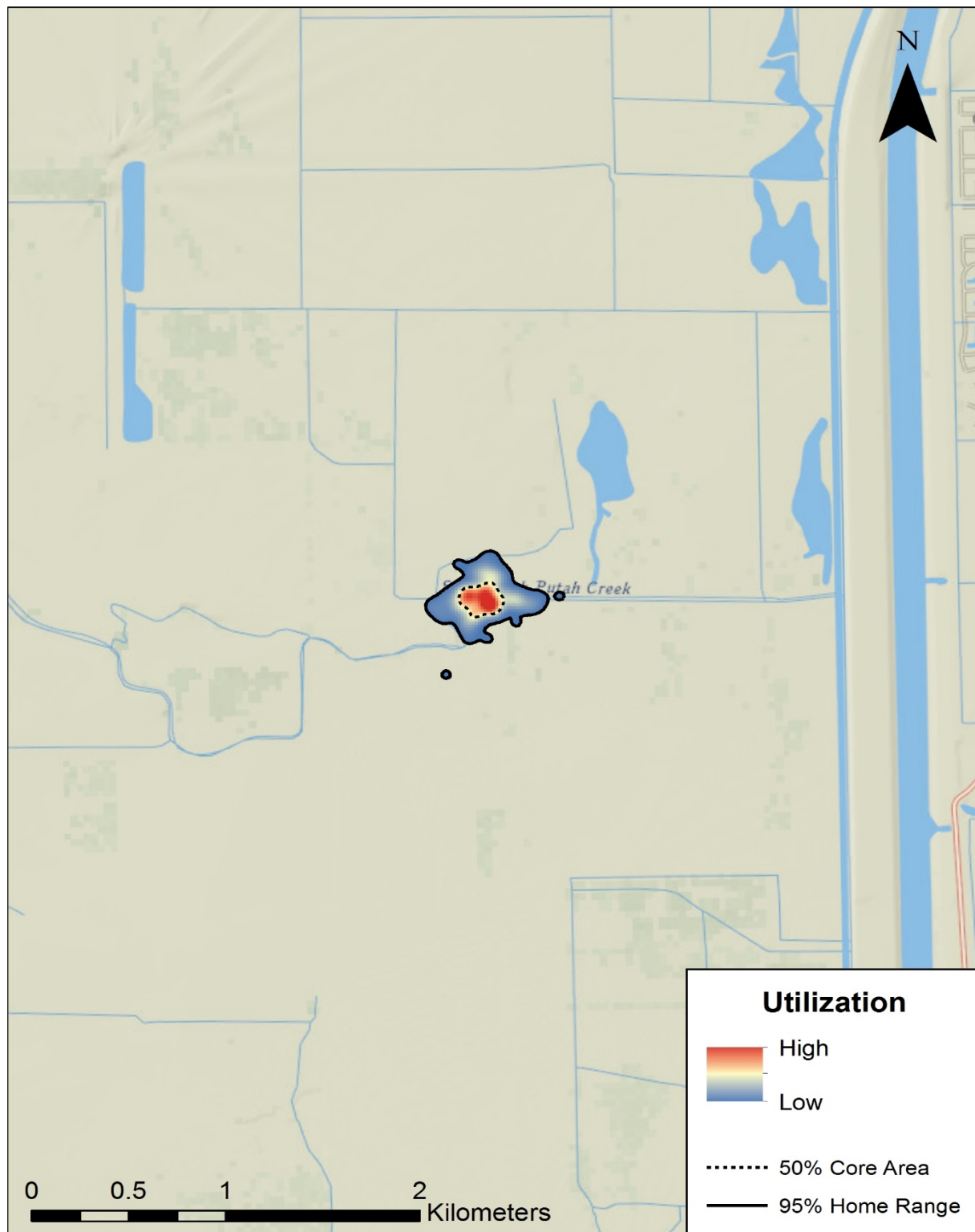


Figure 17. Map showing cumulative utilization distribution of Global Positioning System-marked ring-necked pheasant ($n = 2$, *Phasianus colchicus*), Yolo Bypass Wildlife Area, northern California, spring and summer (March–September) 2015. Utilization distribution was approximated by using kernel density estimators.

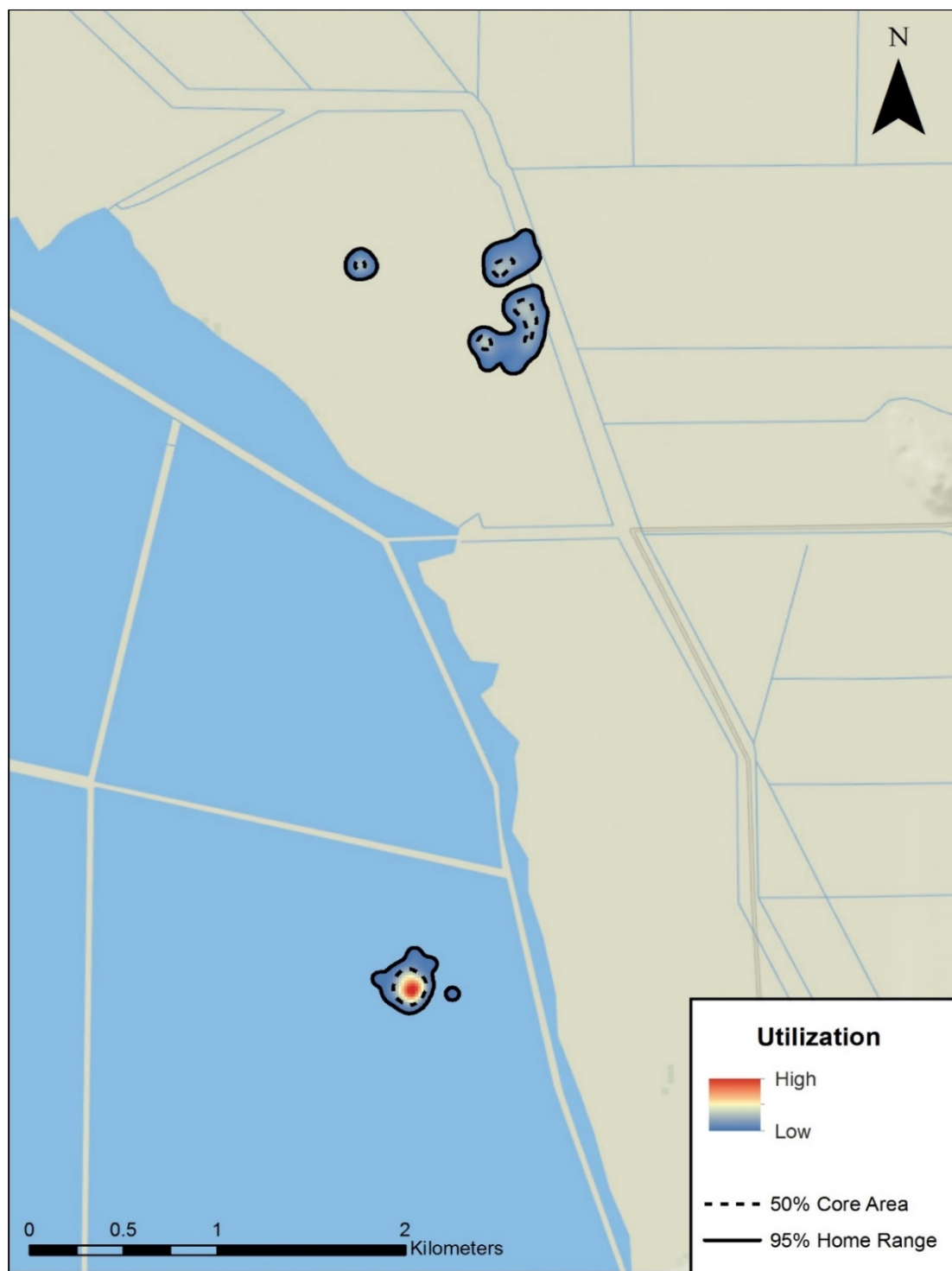


Figure 18. Map showing cumulative utilization distribution of Global Positioning System-marked ring-necked pheasant ($n = 3$, *Phasianus colchicus*), Lower Klamath National Wildlife Refuge, northern California, spring (March–May) 2016. Utilization distribution was approximated by using kernel density estimators.

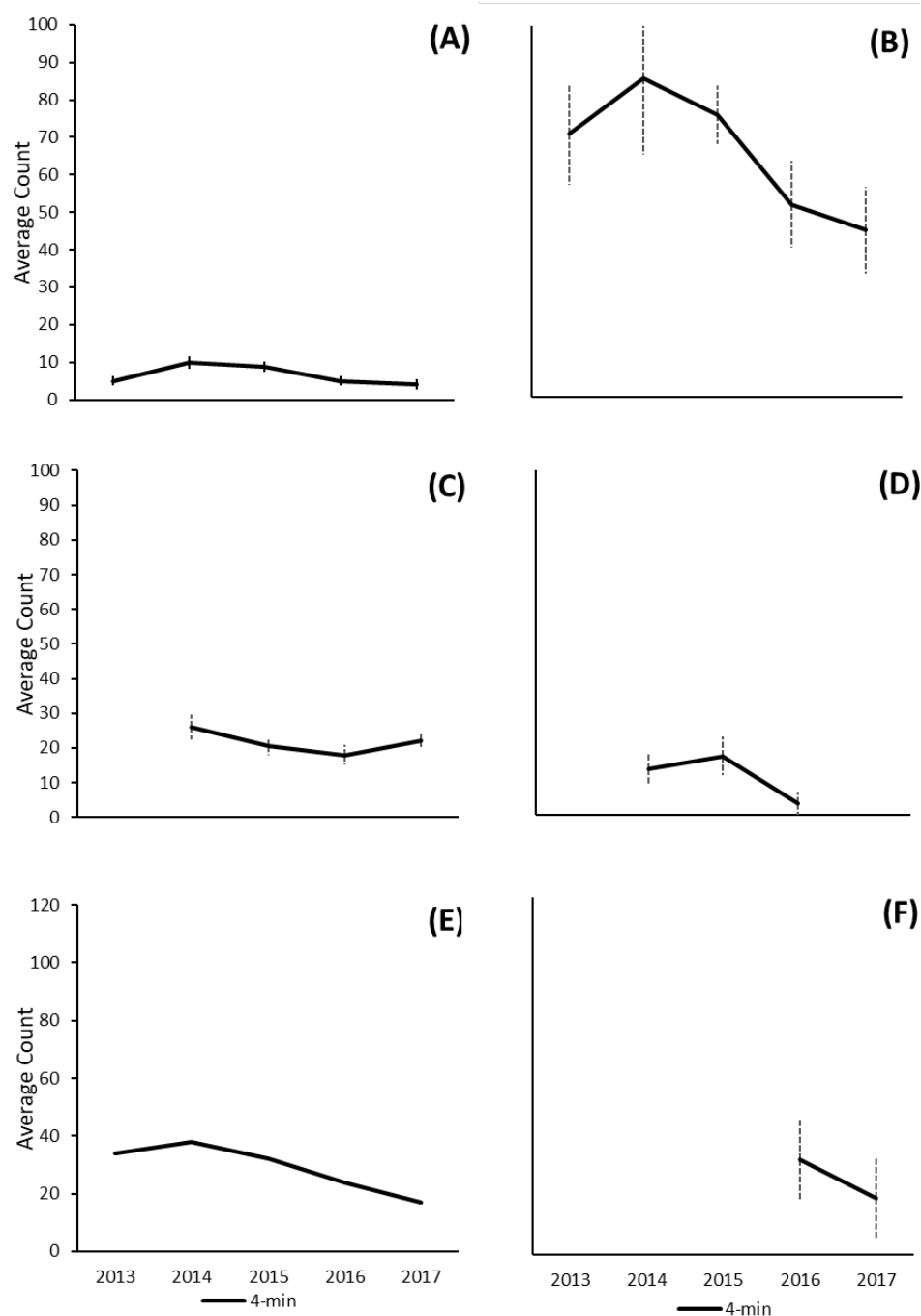


Figure 19. Graphs showing mean ring-necked pheasant (*Phasianus colchicus*) rooster crow counts per station for 4-minute intervals for (A) Gray Lodge Wildlife Area, (B) Mandeville Island Duck Club, (C) Roosevelt Ranch Duck Club, (D) Yolo Bypass Wildlife Area, (E) Little Dry Creek Unit of Upper Butte Basin Wildlife Area, and (F) Lower Klamath National Wildlife Refuge, northern California, 2013–17. Dashed lines represent 95-percent confidence intervals. Means for 4-minute crow counts in 2015 at Mandeville Island Duck Club, Roosevelt Ranch Duck Club, and Yolo Bypass Wildlife Area were estimated from the transformation of 2-minute crow count data.

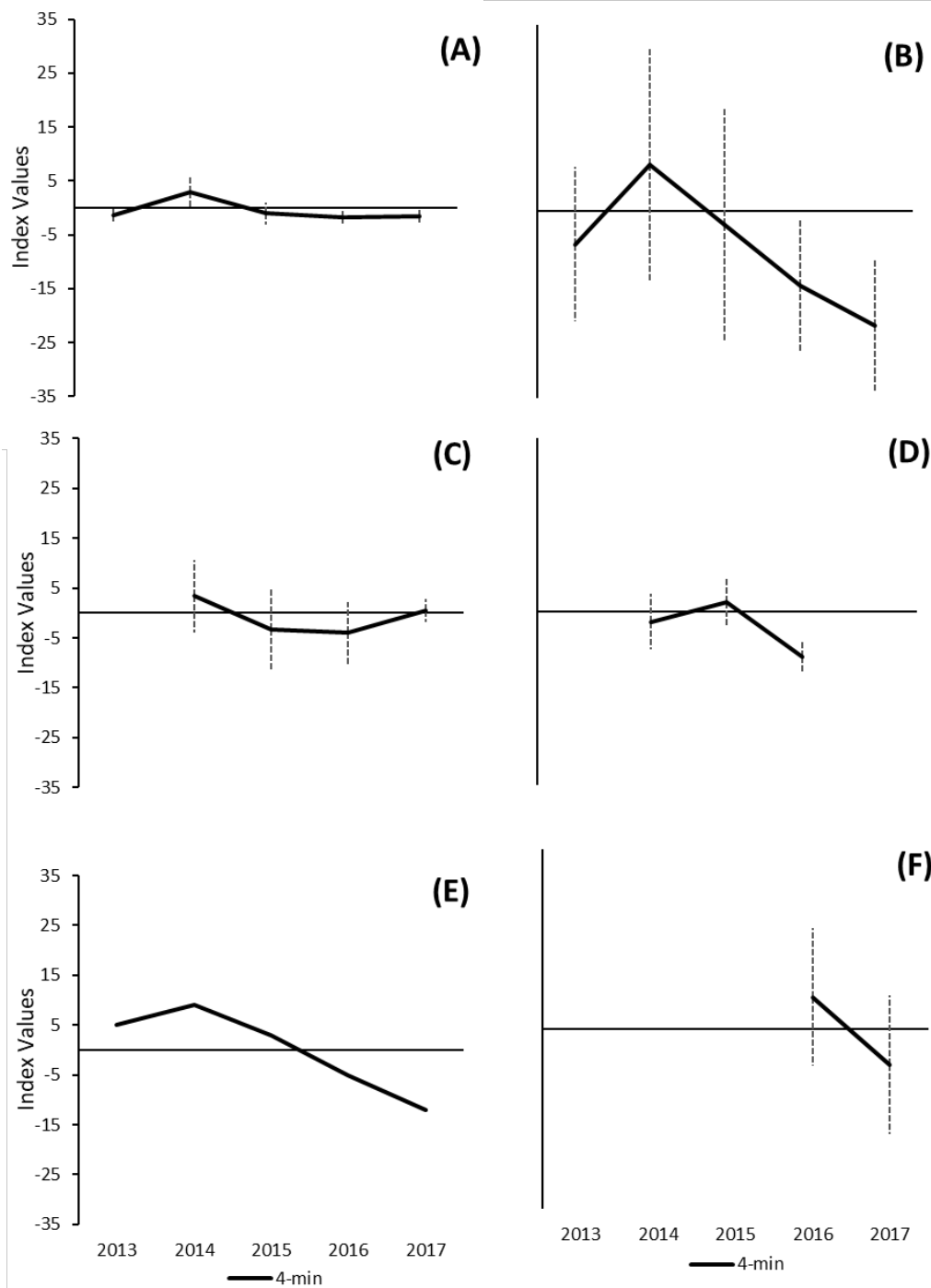


Figure 20. Graphs showing index of mean ring-necked pheasant (*Phasianus colchicus*) rooster crow counts per station for 4-minute intervals for (A) Gray Lodge Wildlife Area, (B) Mandeville Island Duck Club, (C) Roosevelt Ranch Duck Club, (D) Yolo Bypass Wildlife Area, (E) Little Dry Creek Unit of Upper Butte Basin Wildlife Area, and (F) Lower Klamath National Wildlife Refuge, northern California, 2013–17. Dashed lines represent 95-percent confidence intervals. Means for 4-minute crow counts in 2015 at Mandeville Island Duck Club, Roosevelt Ranch Duck Club, and Yolo Bypass Wildlife Area were estimated from the transformation of 2-minute crow count data.

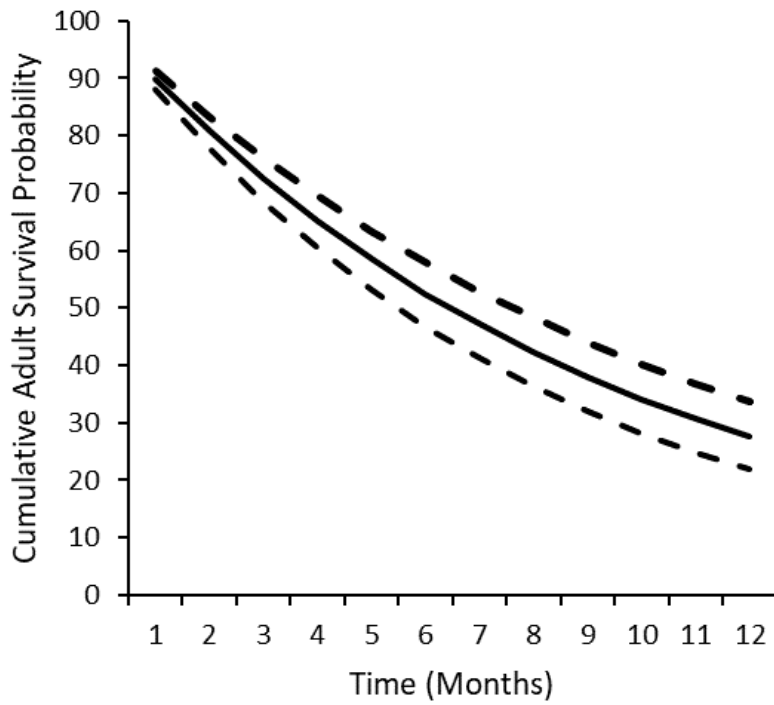


Figure 21. Graph showing cumulative annual adult survival probabilities (in percent) for ring-necked pheasant (*Phasianus colchicus*) averaged across all field sites in the Sacramento-San Joaquin River Delta, Sacramento Valley, and Klamath Basin, northern California, 2013–17. Solid line represents survival estimate; dashed lines represent 95-percent confidence intervals.

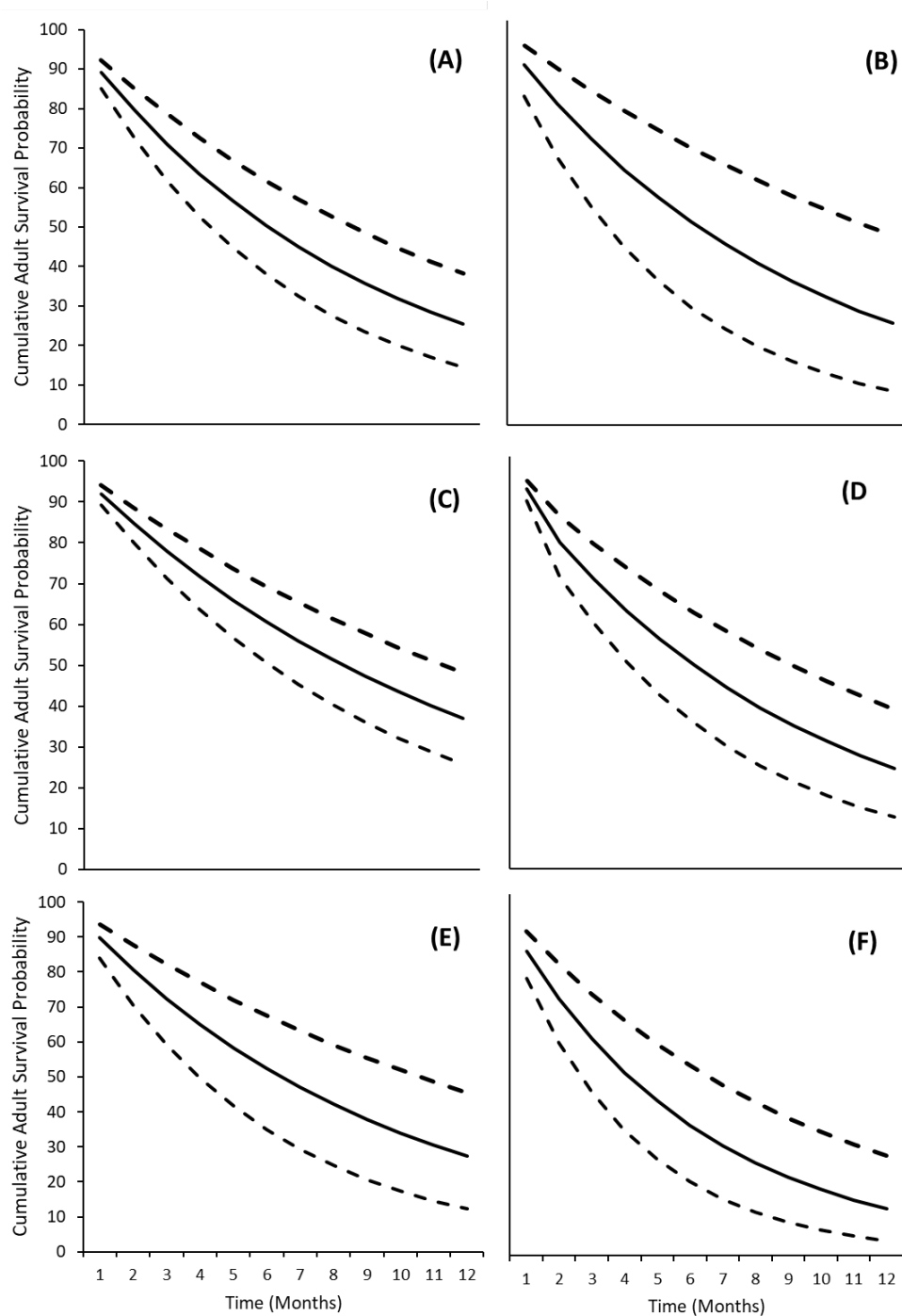


Figure 22. Graphs showing cumulative annual adult survival probabilities (in percent) for ring-necked pheasant (*Phasianus colchicus*) at (A) Gray Lodge Wildlife Area, (B) Mandeville Island Duck Club, (C) Roosevelt Ranch Duck Club, (D) Yolo Bypass Wildlife Area, (E) Little Dry Creek Unit of Upper Butte Basin Wildlife Area, and (F) Lower Klamath National Wildlife Refuge, northern California 2013–17. Solid lines represent survival estimate; dashed lines represent 95-percent confidence intervals.

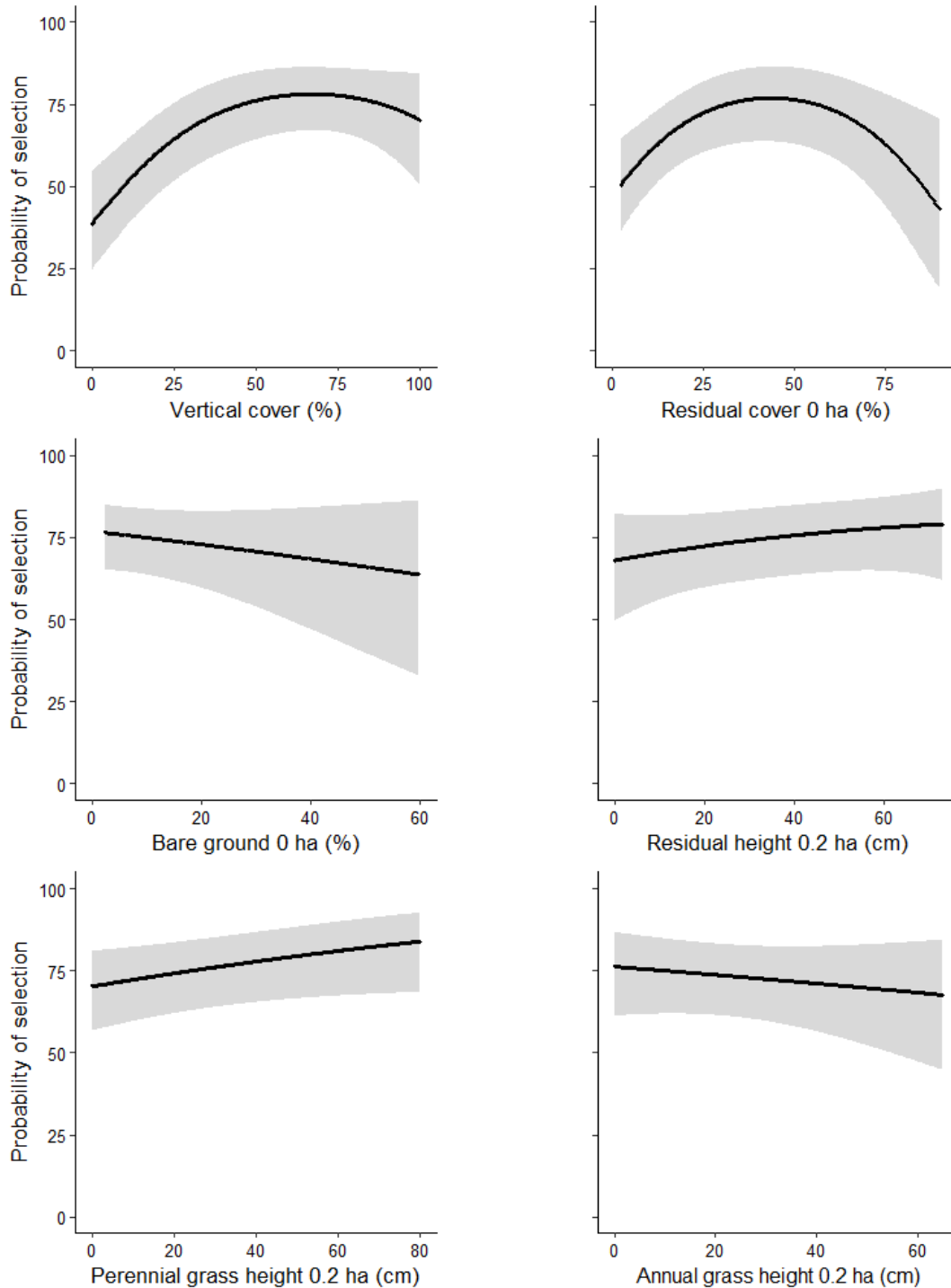


Figure 23. Graphs showing probabilities of selection (in percent) for variables within the top global model (Global 21; see table 8) significant to selection for ring-necked pheasant (*Phasianus colchicus*) nests in the Sacramento-San Joaquin River Delta and Sacramento Valley, northern California, 2014–17. Solid lines represent parameter estimates for the effect of variables on selection; shaded areas represent prediction interval for each parameter estimate. cm, centimeter; ha, hectare; %, percentage.

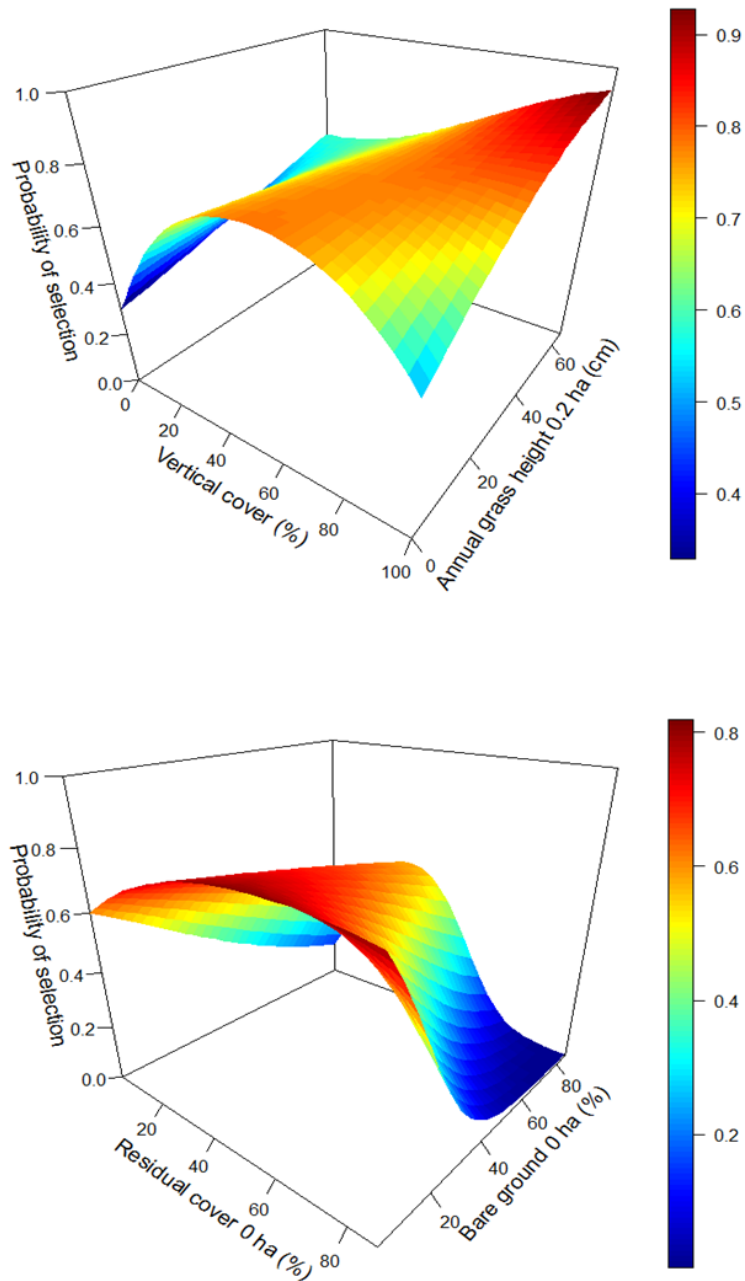


Figure 24. Graphs showing multiplicative interactions of significant variables relative to selection within the top global model (Global 21; see table 8) for ring-necked pheasant (*Phasianus colchicus*) nests in the Sacramento-San Joaquin River Delta and Sacramento Valley, northern California, 2014–17. cm, centimeter; ha, hectare; %, percentage.

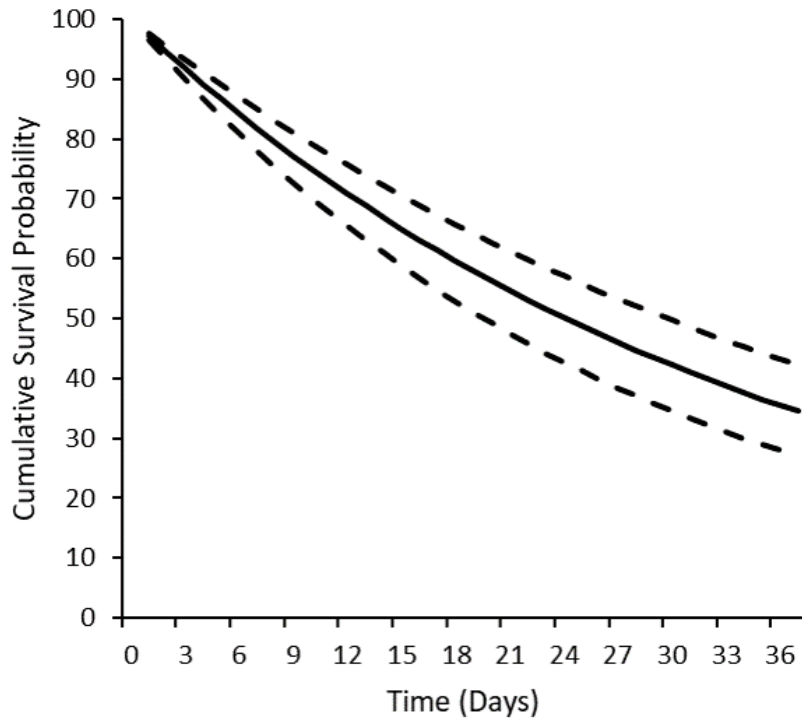


Figure 25. Graph showing cumulative nest survival probabilities (in percent) for ring-necked pheasant (*Phasianus colchicus*) in the Sacramento-San River Delta, Sacramento Valley, and Klamath Basin, northern California, over the 37-day laying and incubation period, 2014–17. Solid line represents survival estimate; dashed lines represent 95-percent confidence intervals.

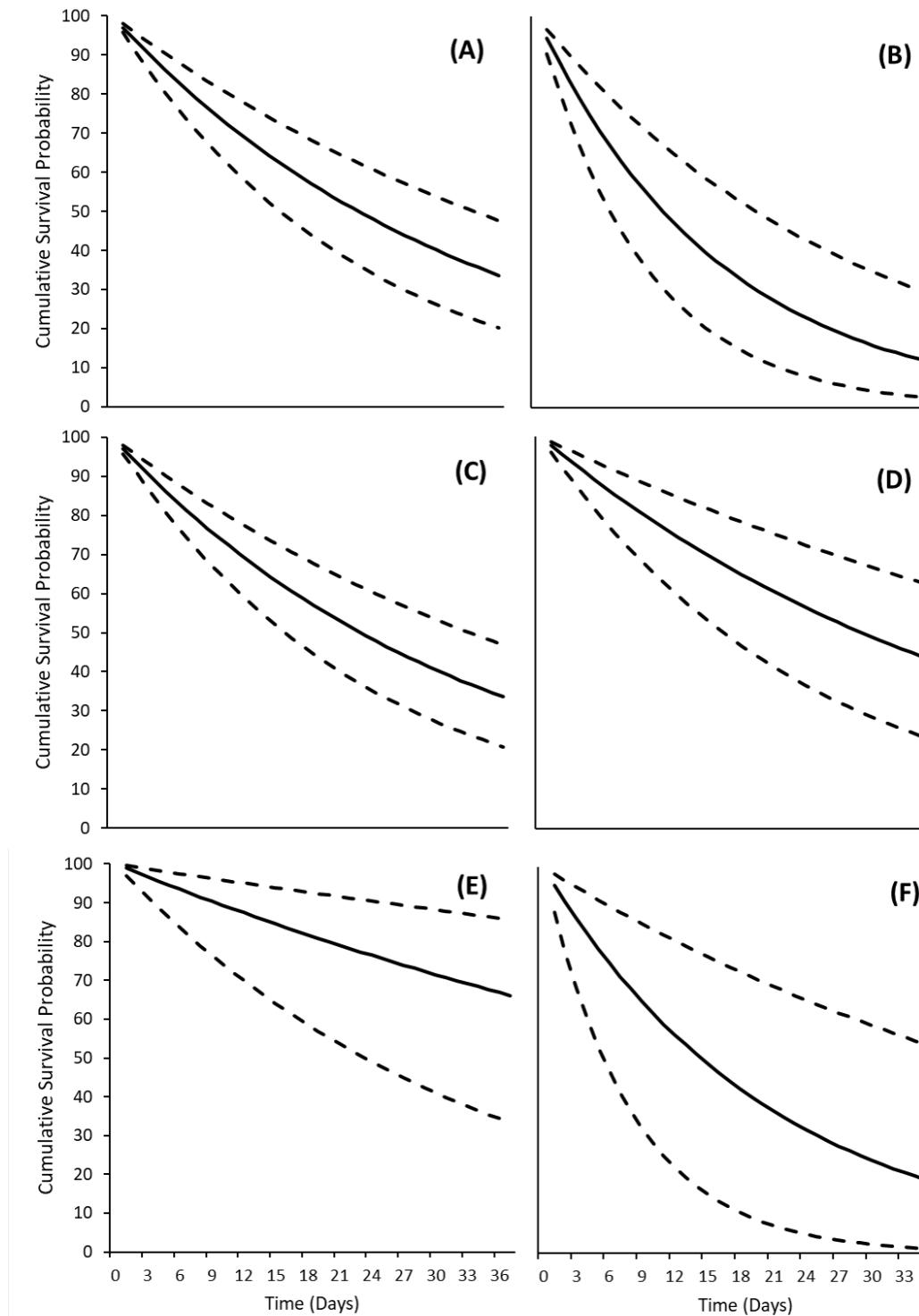


Figure 26. Graphs showing cumulative nest survival probabilities (in percent) for ring-necked pheasant (*Phasianus colchicus*) at (A) Gray Lodge Wildlife Area, (B) Mandeville Island Duck Club, (C) Roosevelt Ranch Duck Club, (D) Yolo Bypass Wildlife Area, (E) Little Dry Creek Unit of Upper Butte Basin Wildlife Area, and (F) Lower Klamath National Wildlife Refuge, northern California, over the 37-day laying and incubation period, 2014–17. Solid lines represent the survival estimate; dashed lines represent 95-percent confidence intervals.

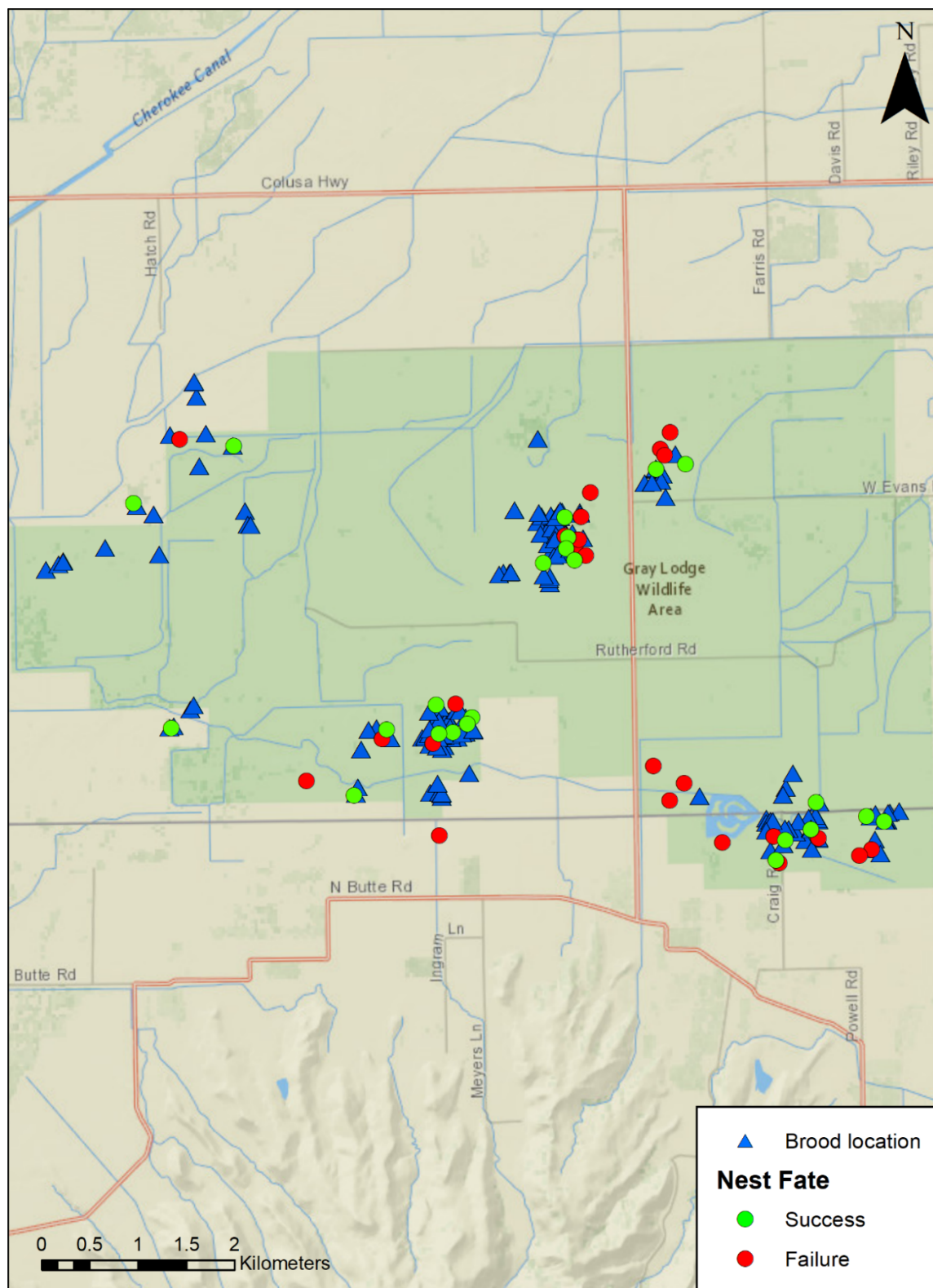


Figure 27. Map showing successful ($n = 24$) and unsuccessful ($n = 25$) nest and brood telemetry locations of Very High Frequency-marked ring-necked pheasant (*Phasianus colchicus*) at Gray Lodge Wildlife Area, northern California, 2014–16.

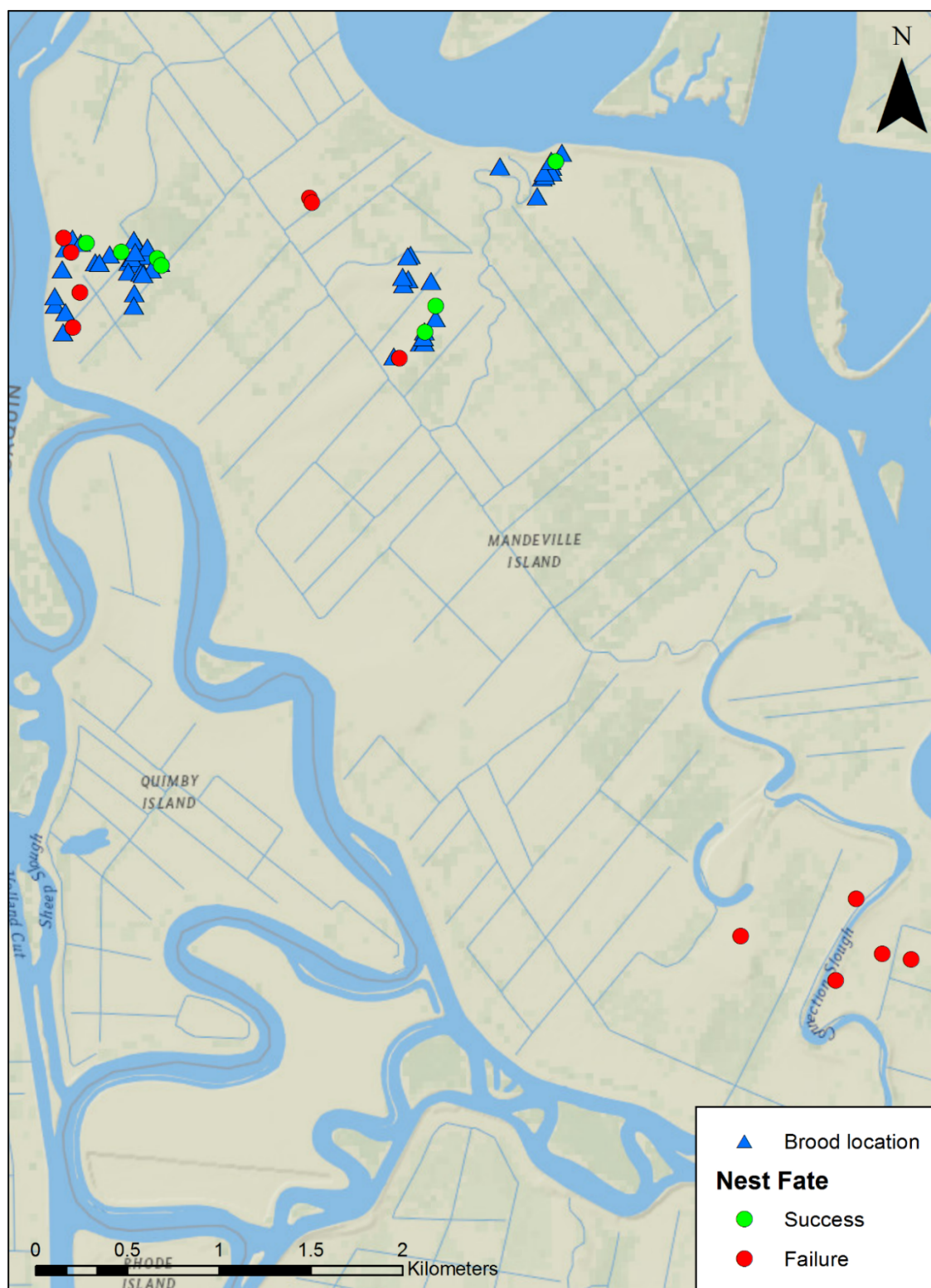


Figure 28. Map showing successful ($n = 7$) and unsuccessful ($n = 12$) nest and brood telemetry locations of Very High Frequency-marked ring-necked pheasant (*Phasianus colchicus*) at Mandeville Island Duck Club, northern California, 2014 and 2016–17.

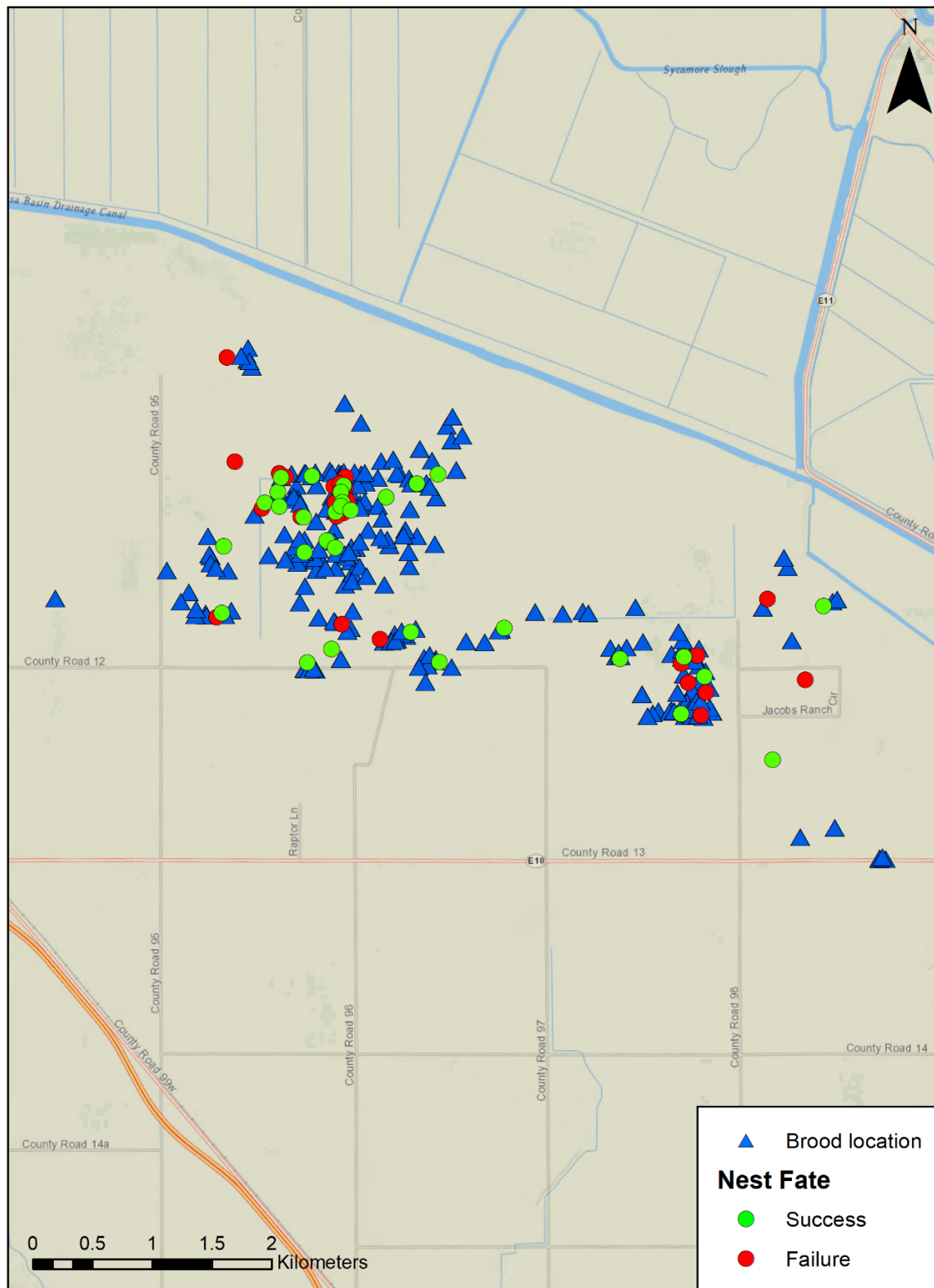


Figure 29. Map showing successful ($n = 32$) and unsuccessful ($n = 29$) nest and brood telemetry locations of Very High Frequency-marked ring-necked pheasant (*Phasianus colchicus*) at Roosevelt Ranch Duck Club, northern California, 2014–17.

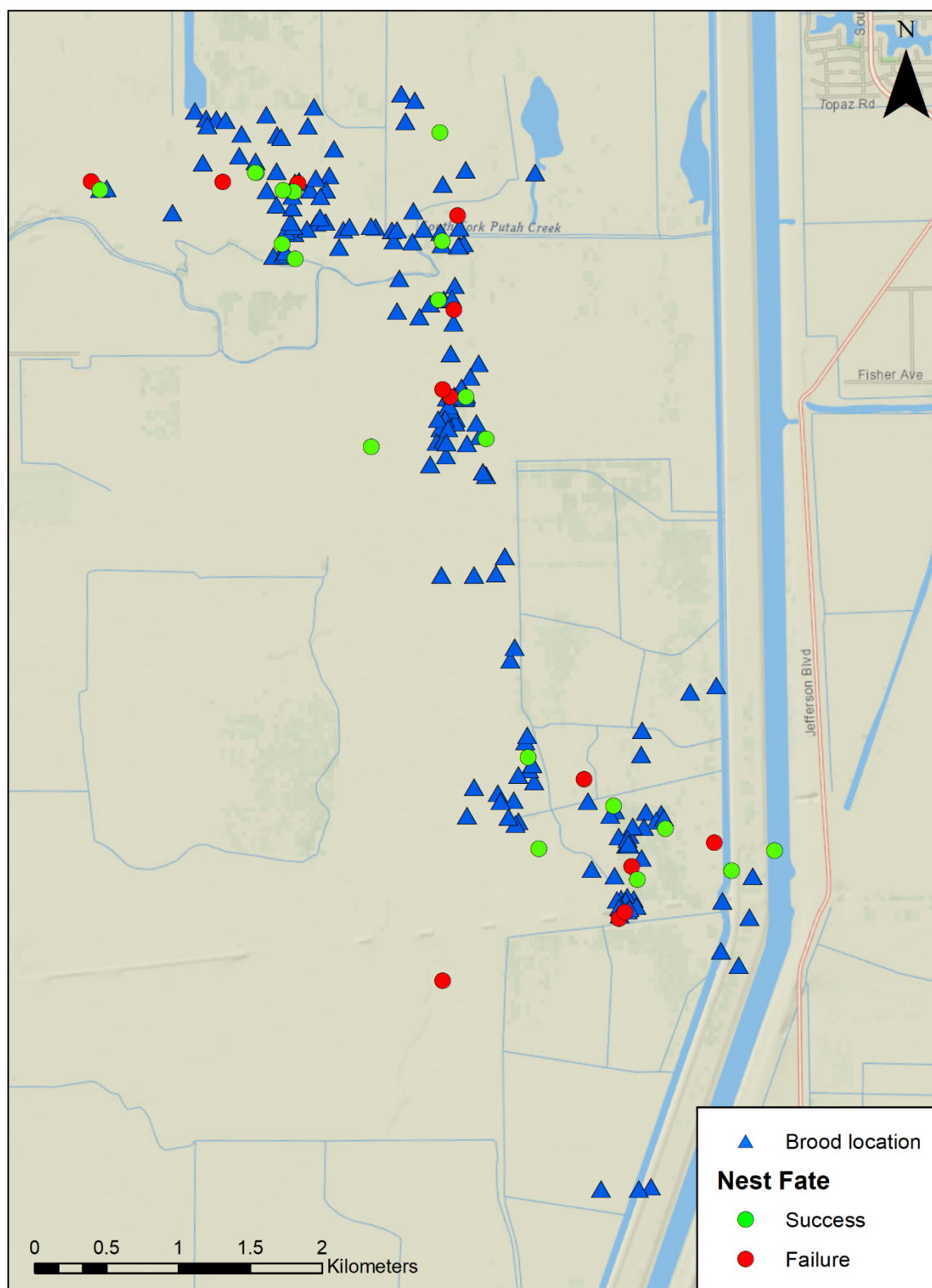


Figure 30. Map showing successful ($n = 20$) and unsuccessful ($n = 13$) nest and brood telemetry locations of Very High Frequency-marked ring-necked pheasant (*Phasianus colchicus*) at Yolo Bypass Wildlife Area, northern California, 2014–16.

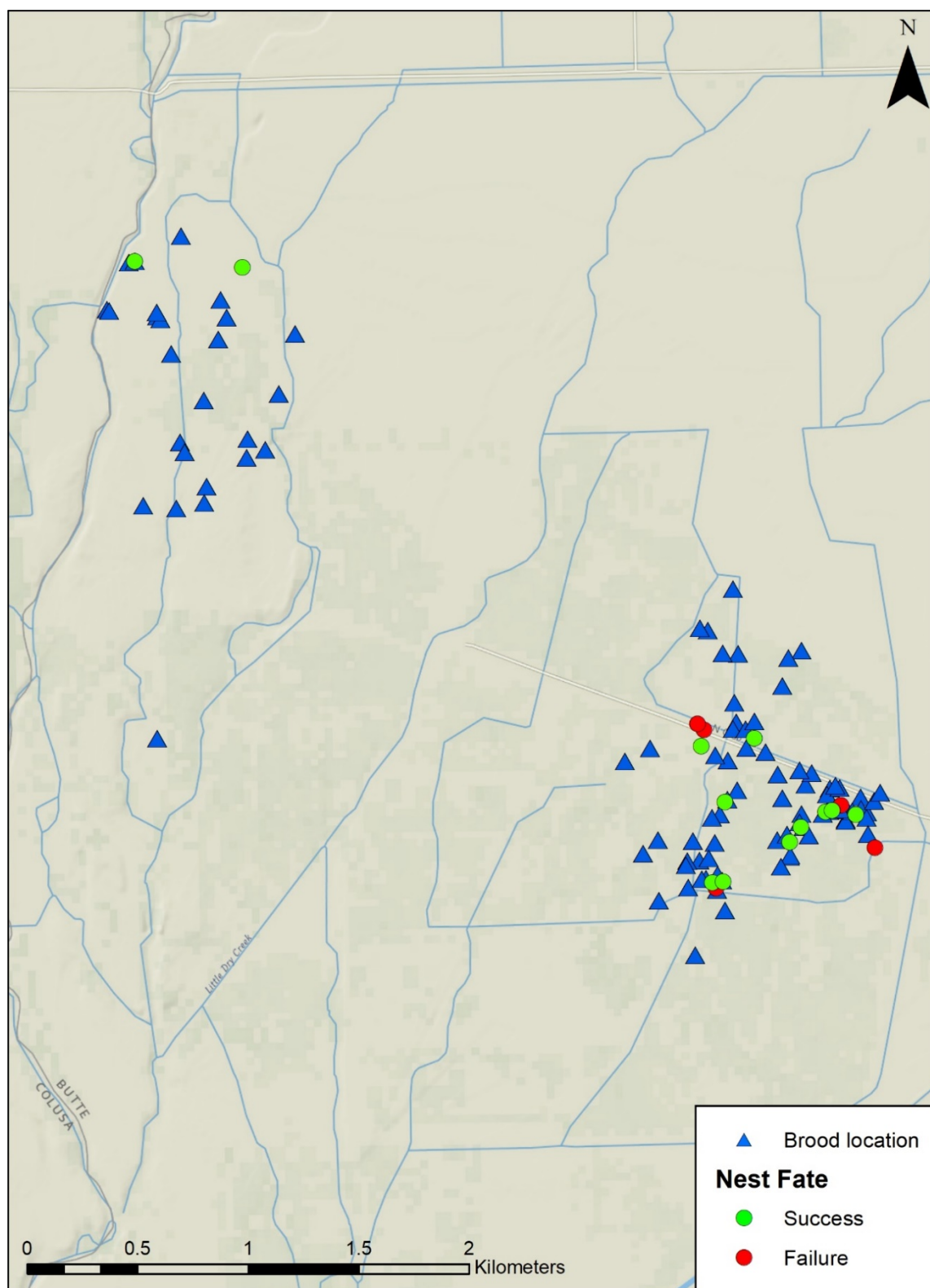


Figure 31. Map showing successful ($n = 12$) and unsuccessful ($n = 5$) nest and brood telemetry locations of Very High Frequency-marked ring-necked pheasant (*Phasianus colchicus*) at Little Dry Creek Unit of Upper Butte Basin Wildlife Area, northern California, 2016–17.

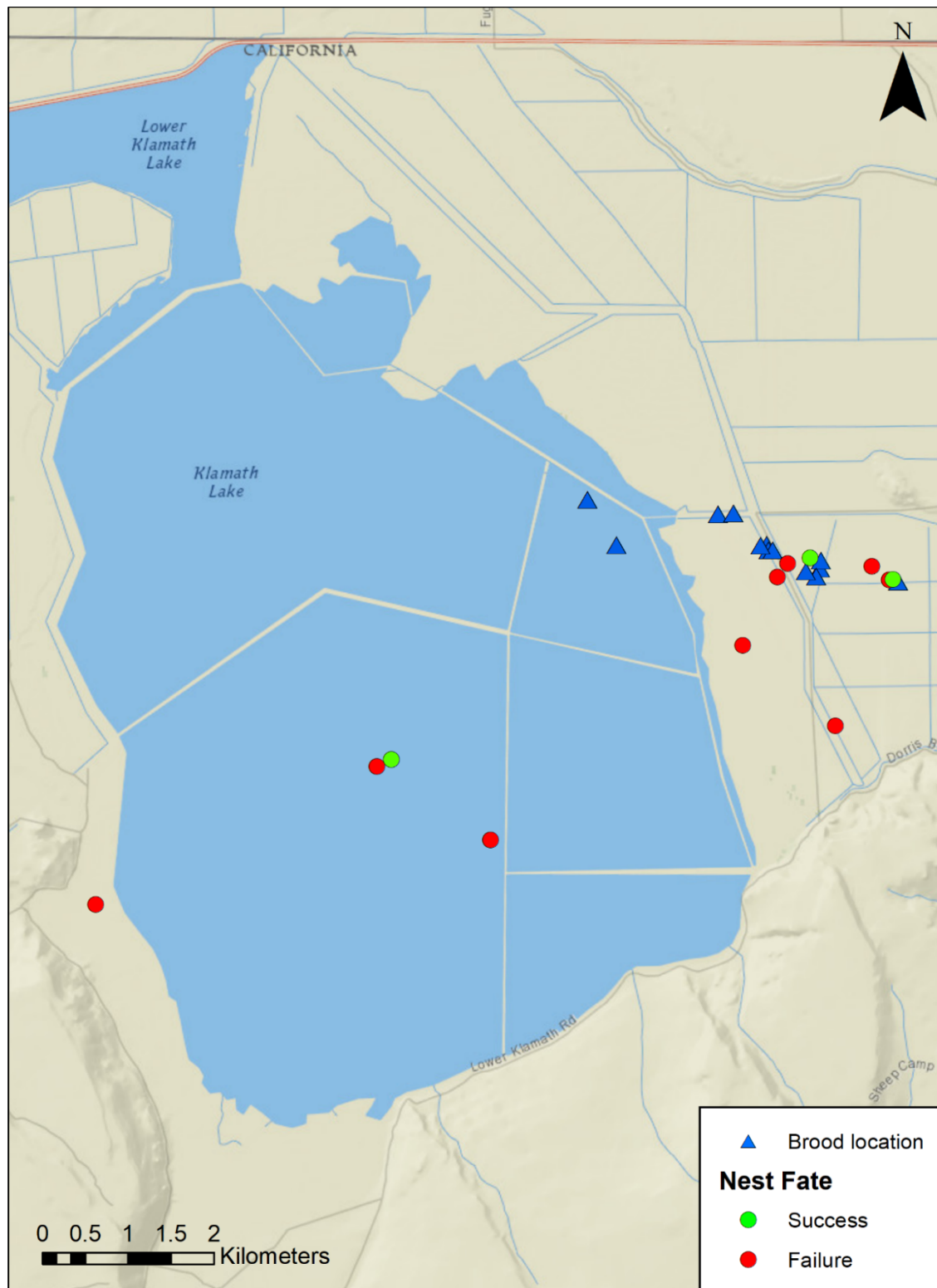


Figure 32. Map showing successful ($n = 3$) and unsuccessful ($n = 9$) nest and brood telemetry locations of Very High Frequency-marked ring-necked pheasant (*Phasianus colchicus*) at Lower Klamath National Wildlife Refuge, northern California, 2016–17.

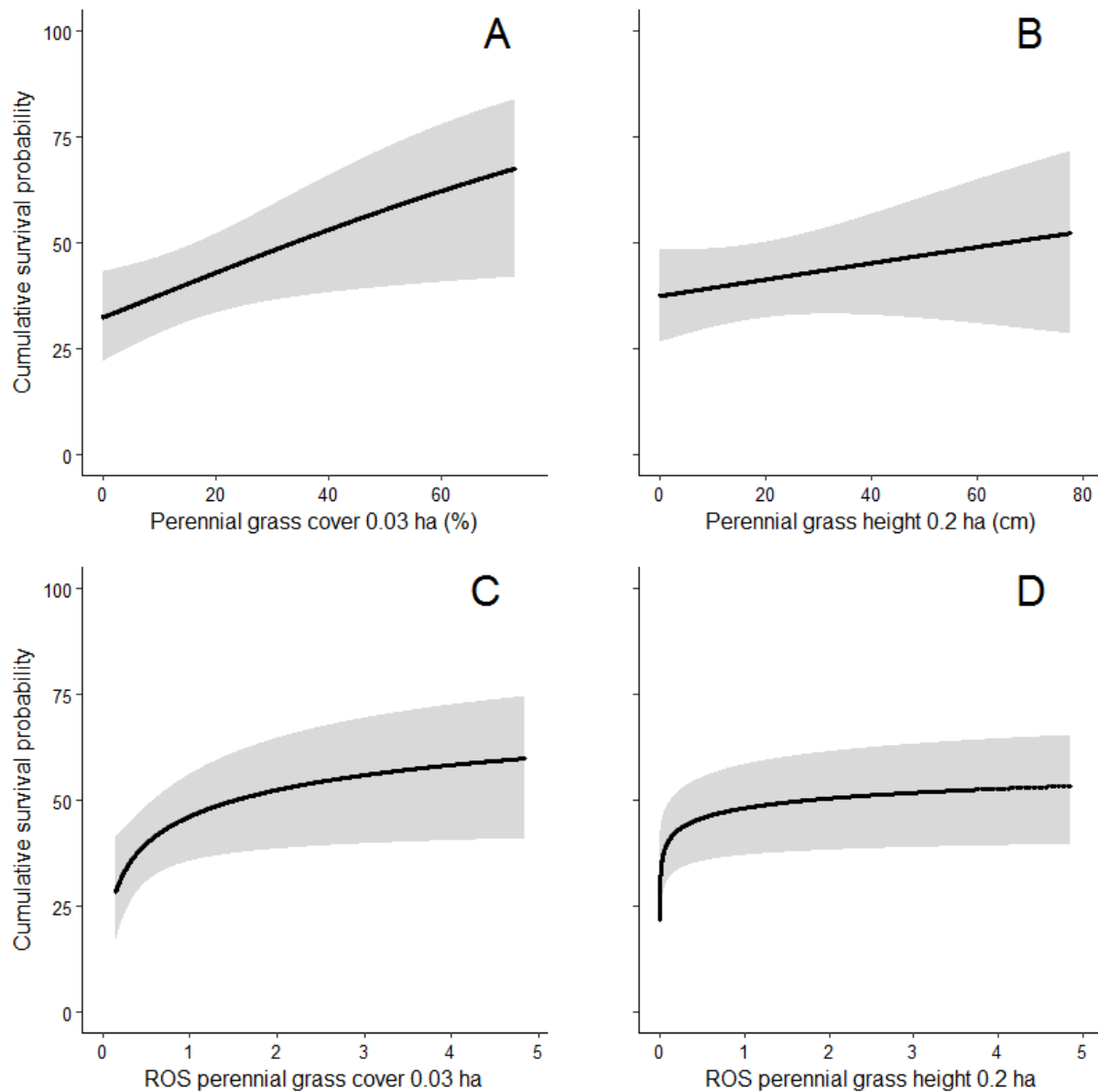


Figure 33. Graphs showing cumulative nest survival probabilities for ring-necked pheasant (*Phasianus colchicus*) nests with (A) increasing perennial grass cover (in percent [%]) at the 0.03-hectare [ha] scale, (B) increasing perennial grass height (in centimeters [cm]) at the 0.2-ha scale, (C) ratio of selection (ROS) for perennial grass cover at the 0.03-ha scale, and (D) ROS for perennial grass height at the 0.2-ha scale in the Sacramento-San Joaquin River Delta and Sacramento Valley, northern California, 2014–17. Solid lines represent parameter estimates for the effect of perennial grass cover; height on survival and shaded areas represent the prediction interval for each parameter estimate.

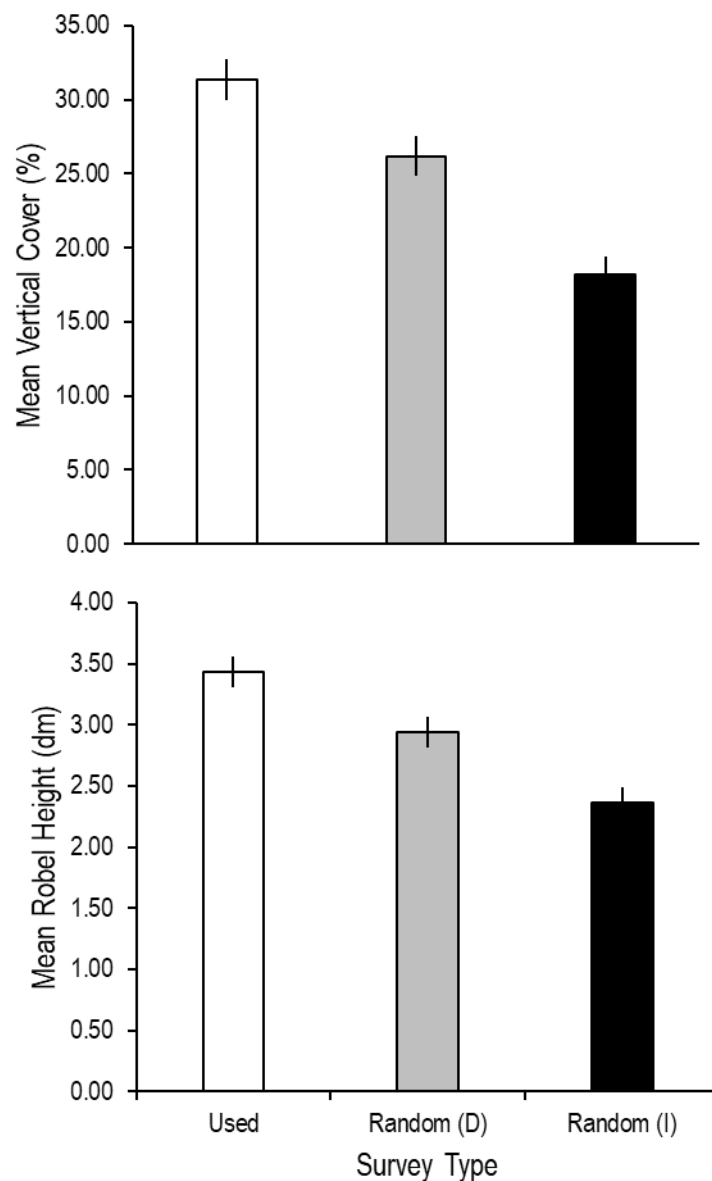


Figure 34. Graphs showing mean percentages (%) of vertical cover and mean Robel pole height (in decimeters [dm]) from ring-necked pheasant (*Phasianus colchicus*) brood locations and at random locations (dependent and independent), averaged across all study sites in the Sacramento-San Joaquin River Delta, Sacramento Valley, and Klamath Basin, northern California, 2014–17. Spatial scale of 0 represents habitat at the center of each survey location. Lines represent standard errors.

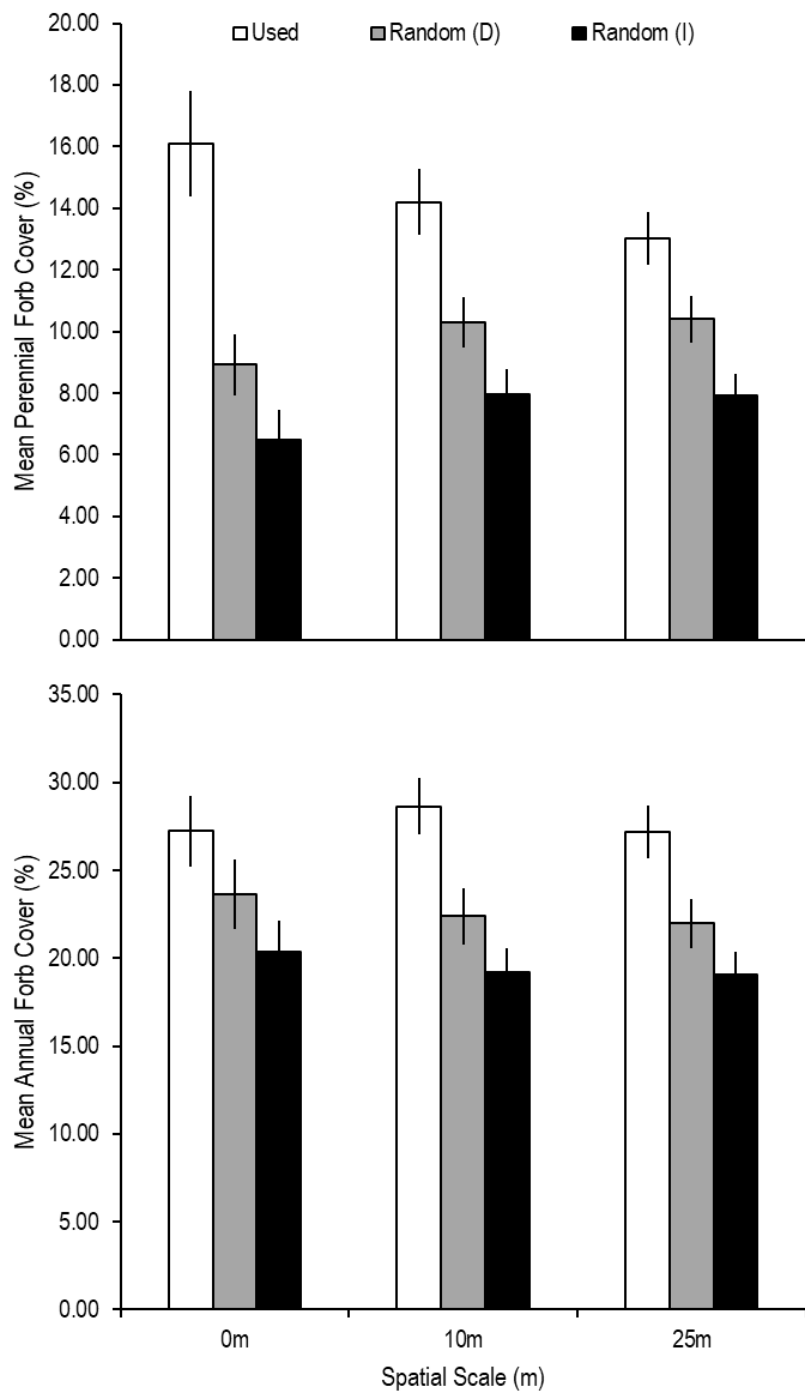


Figure 35. Graphs showing mean percentages (%) of perennial forb cover and annual forb cover from ring-necked pheasant (*Phasianus colchicus*) brood locations and at random locations (dependent [D] and independent [I]) averaged across all study sites in the Sacramento-San Joaquin River Delta, Sacramento Valley, and Klamath Basin, northern California, 2014–17. Spatial scale (in meters [m]) of 0 represents habitat at the center of each survey location. Lines represent standard errors.

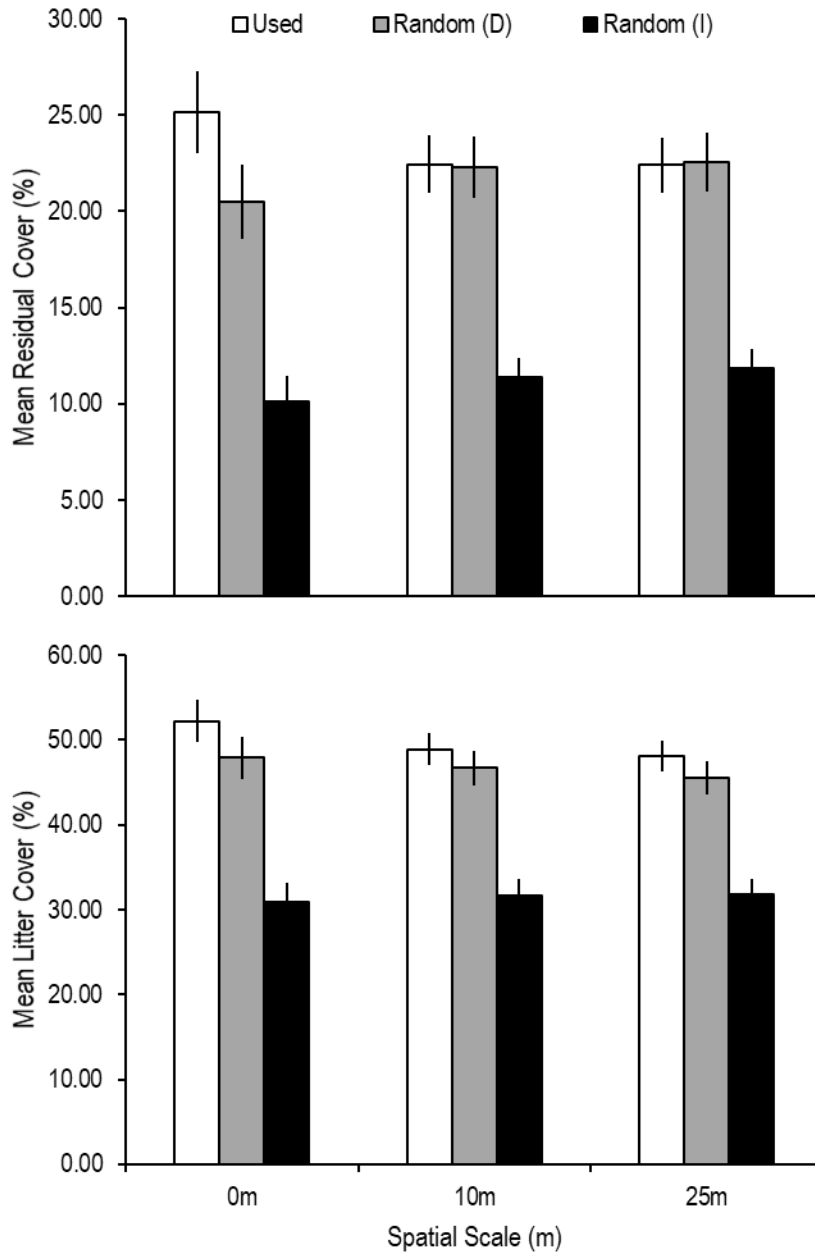


Figure 36. Graphs showing mean percentages (%) of residual cover and litter cover from ring-necked pheasant (*Phasianus colchicus*) brood locations and at random locations (dependent [D] and independent [I]) averaged across all study sites in the Sacramento-San Joaquin River Delta, Sacramento Valley, and Klamath Basin, northern California, 2014–17. Spatial scale (in meters [m]) of 0 represents habitat at the center of each survey location. Lines represent standard errors.

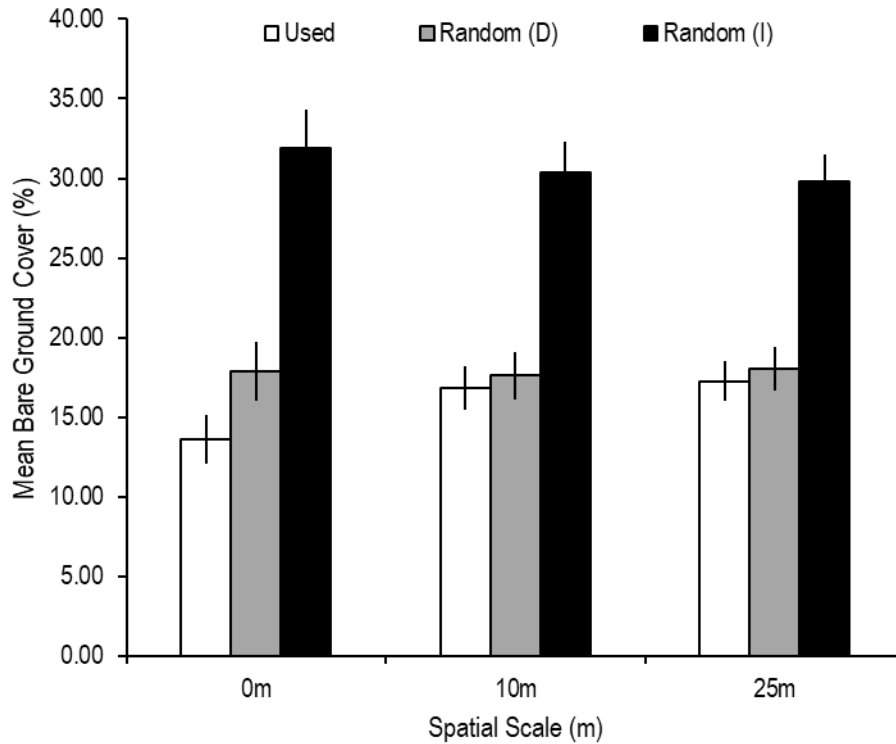


Figure 37. Graph showing mean percentages (%) of bare ground from ring-necked pheasant (*Phasianus colchicus*) brood locations and at random locations (dependent [D] and independent [I]) averaged across all study sites in the Sacramento-San Joaquin River Delta, Sacramento Valley, and Klamath Basin, northern California, 2014–17. Spatial scale (in meters [m]) of 0 represents habitat at the center of each survey location. Lines represent standard errors.

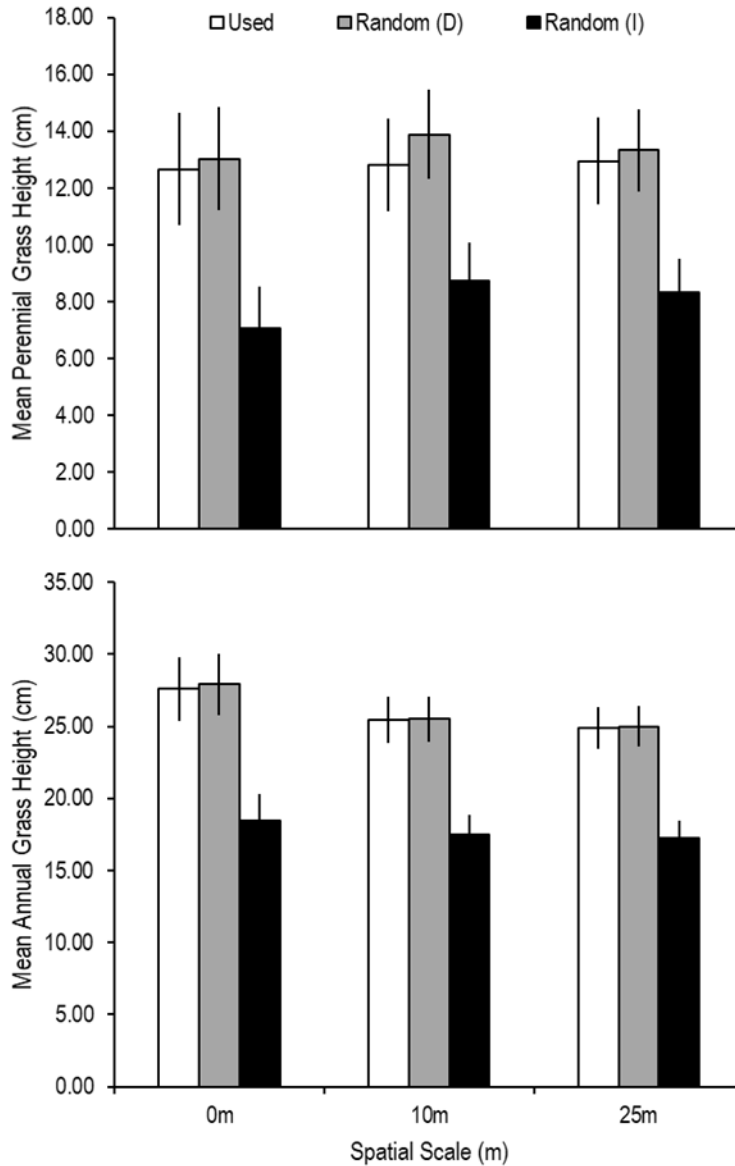


Figure 38. Graphs showing mean perennial and mean annual grass heights (in centimeters [cm]) from ring-necked pheasant (*Phasianus colchicus*) brood locations and at random locations (dependent [D] and independent [I]) averaged across all study sites in the Sacramento-San Joaquin River Delta, Sacramento Valley, and Klamath Basin, northern California, 2014–17. The spatial scale (in meters [m]) of 0 represents habitat at the center of each survey location. Lines represent standard errors.

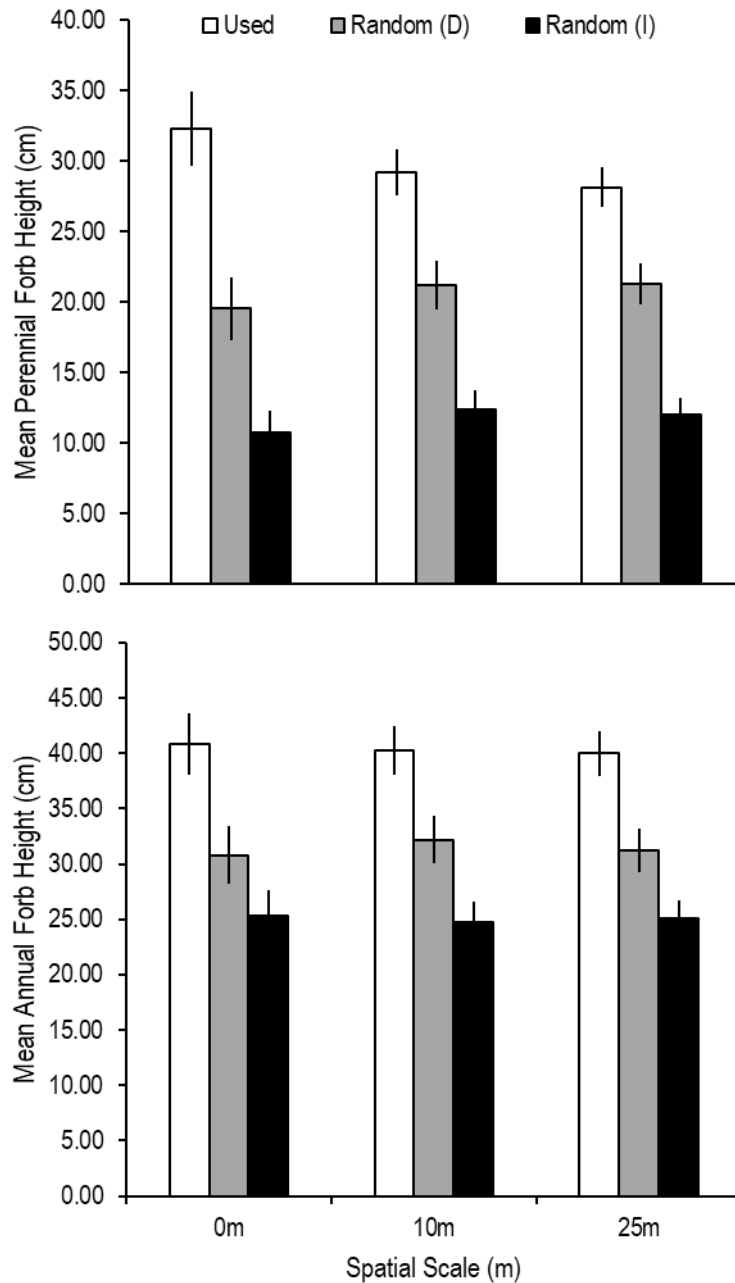


Figure 39. Graphs showing mean perennial and annual forb heights (in centimeters [cm]) from ring-necked pheasant (*Phasianus colchicus*) brood locations and at random locations (dependent [D] and independent [I]) averaged across all study sites in the Sacramento-San Joaquin River Delta, Sacramento Valley, and Klamath Basin, northern California, 2014–17. Spatial scale (in meters [m]) of 0 represents habitat at the center of each survey location. Lines represent standard errors.

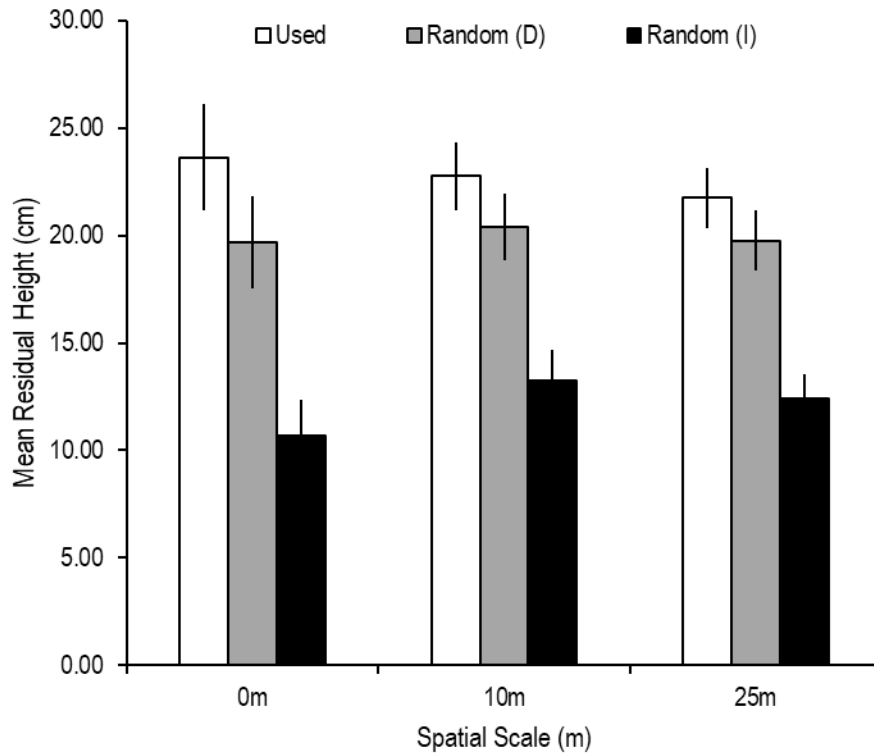


Figure 40. Graph showing mean residual cover height (in centimeters [cm]) from ring-necked pheasant (*Phasianus colchicus*) brood locations and at random locations (dependent [D] and independent [I]) averaged across all study sites in the Sacramento-San Joaquin River Delta, Sacramento Valley, and Klamath Basin, northern California, 2014–17. Spatial scale (in meters [m]) of 0 represents habitat at the center of each survey location. Lines represent standard errors.

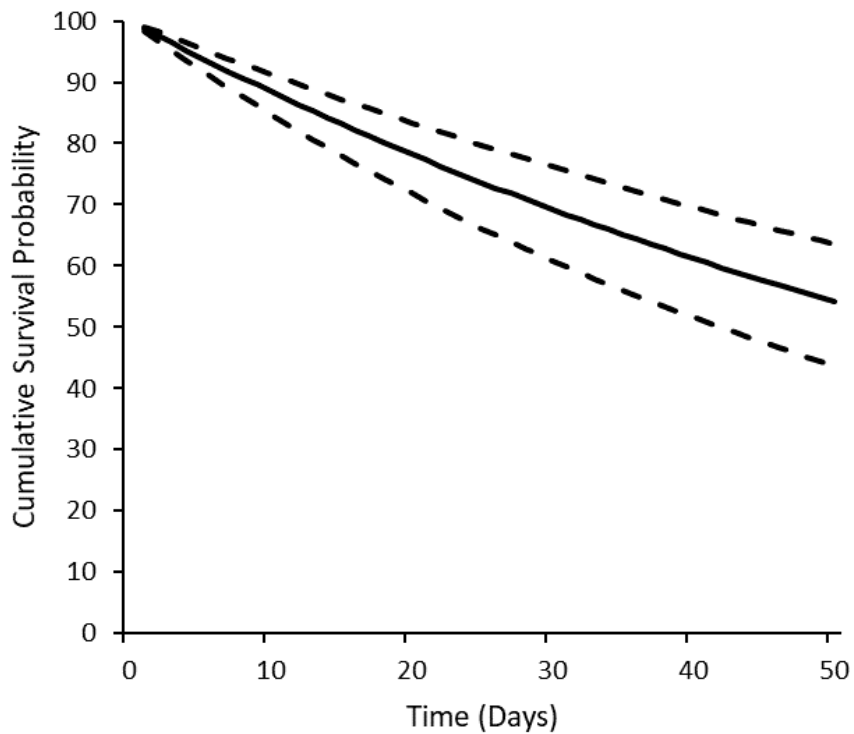


Figure 41. Graph showing cumulative mean survival probabilities (in percent) over the 50-day brood-rearing period for ring-necked pheasant (*Phasianus colchicus*) in the Sacramento-San Joaquin River Delta, Sacramento Valley, and Klamath Basin, northern California, 2014–17. Solid line represents the survival estimate; dashed lines represent 95-percent confidence intervals.

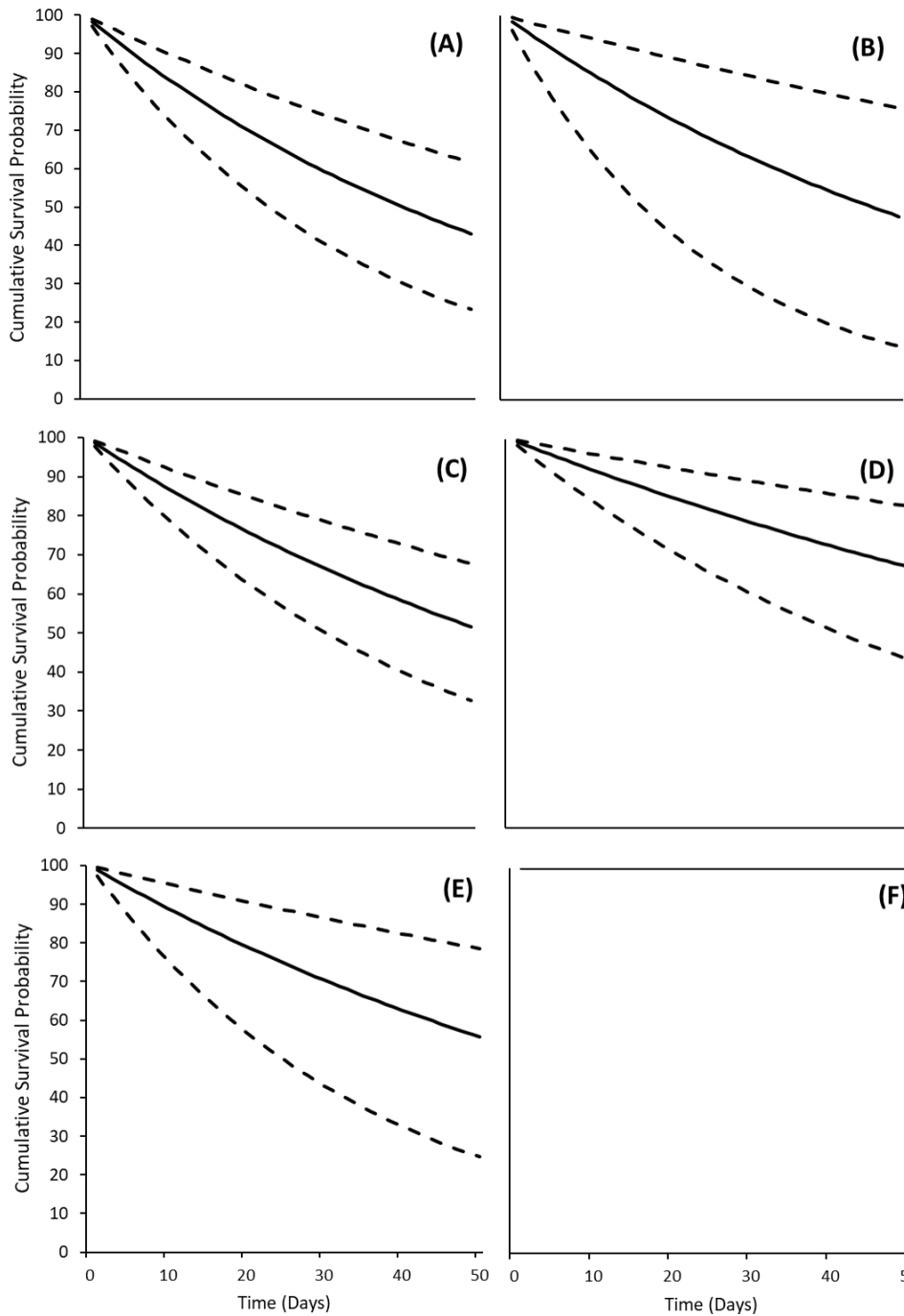


Figure 42. Graphs showing cumulative mean survival probabilities (in percent) for the 50-day brood-rearing phase across age of brood for ring-necked pheasant (*Phasianus colchicus*) broods at (A) Gray Lodge Wildlife Area, (B) Mandeville Island Duck Club, (C) Roosevelt Ranch Duck Club, (D) Yolo Bypass Wildlife Area, (E) Little Dry Creek Unit of Upper Butte Basin Wildlife Area, and (F) Lower Klamath National Wildlife Refuge, northern California, 2014–17. Solid lines represent survival estimate; dashed lines represent 95-percent confidence intervals.

Tables

Table 1. Number and gender of ring-necked pheasant (*Phasianus colchicus*) outfitted with Very High Frequency (VHF) and Global Positioning System (GPS) transmitters during winter (December–February), spring (March–April), and autumn (September–November) trapping seasons, Sacramento-San Joaquin River Delta, Sacramento Valley, and Klamath Basin, northern California, 2013–17.

Study site	Gender	2013		2014		2015		2016		2017	
		VHF	GPS	VHF	GPS	VHF	GPS	VHF	GPS	VHF	GPS
Gray Lodge Wildlife Area	Female	3	0	14	0	13	0	7	0	2	0
	Male	0	0	0	0	0	0	0	0	0	0
Mandeville Island Duck Club	Female	1	1	7	0	0	0	9	0	8	0
	Male	1	2	0	0	0	0	0	0	0	0
Roosevelt Ranch Duck Club	Female	10	0	13	2	20	0	12	0	4	0
	Male	0	0	0	0	0	0	0	0	0	0
Yolo Bypass Wildlife Area	Female	0	0	11	0	16	1	8	0	0	0
	Male	0	0	0	0	0	1	0	0	0	0
Little Dry Creek Unit of Upper Butte Basin Wildlife Area	Female	0	0	0	0	8	0	15	0	2	0
	Male	0	0	0	0	0	0	0	0	0	0
Lower Klamath National Wildlife Refuge	Female	0	0	0	0	0	0	17	2	21	0
	Male	0	0	0	0	0	0	0	2	0	0
Total	Female	14	1	45	2	57	1	68	2	37	0
	Male	1	2	0	0	0	1	0	2	0	0

Table 2. Biological classifications of invertebrate specimens collected ($n = 217,536$) using pitfall traps deployed in brood-rearing pheasant habitat in the Sacramento-San Joaquin River Delta and Sacramento Valley, northern California, 2013–14.

[**Total dry weight:** N/A, total dry weights were not recorded for some samples because individuals were too small for the scale to recognize. **Abbreviation:** n , sample size]

Order	Individuals detected	Total dry weight (grams)
Acari	603	0.020
Amphipoda	4	0.001
Araneae	5,740	40.780
Blattodea	984	11.860
Chilopoda	4	0.002
Coleoptera	9,075	171.290
Collembola	135,288	N/A
Copepoda	2,116	N/A
Cyclopoida	47	0.001
Dermaptera	198	1.950
Diplopoda	10	0.180
Diptera	3,649	0.430
Embiidina	13	0.030
Gastropoda	10	0.110
Hemiptera	6,453	2.470
Hymenoptera	9,624	4.060
Icro	6	0.020
Isopoda	8,216	91.230
Ixodida	62	0.007
Julida	18	0.410
Lepidoptera	327	0.400
Lithobiomorpha	35	0.120
Mantodea	1	0.003
Megadrilacea	1	0.070
Megaloptera	4	N/A
Mesostigmata	6,376	0.005
Microcoryphia	2,278	5.670
Nematoda	3	0.020
Odonata	1	N/A
Opiliones	146	0.960
Oribatida	5,531	0.002
Orthoptera	4,818	337.080
Parasitiformes	1,714	0.050
Polydesmida	20	0.430
Psocoptera	3,353	N/A
Raphidioptera	1	0.003
Scutigleromorpha	6	0.190

Order	Individuals detected	Total dry weight (grams)
Siphonaptera	10	N/A
Stylommatophora	6	0.070
Thysanoptera	435	N/A
Trombidiformes	10,348	0.200
Unidentified	2	0.030

Table 3. Insecticides applied to study sites containing ring-necked pheasant (*Phasianus colchicus*) habitat in the Sacramento-San Joaquin River Delta and Sacramento Valley, northern California, 2013–14.

Chemical type	Chemical name	Application method	Site sprayed
Adulticide	Trumpet [®] EC	Aerial	Mandeville Island
	Evergreen [®] 60-6	Aerial	Roosevelt Ranch
	Pyrocide [®] 7396	Aerial	Roosevelt Ranch
	Unknown	Fogging	Gray Lodge
	Unknown	Aerial	Gray Lodge
Larvicide	VectoBac [®] 12AS	Aerial	Roosevelt Ranch
	Altosid XR-G [®]	Aerial	Roosevelt Ranch
	Unknown	Fogging	Gray Lodge

Table 4. Number of successful (one or more chicks hatched) and failed ring-necked pheasant (*Phasianus colchicus*) nests in the Sacramento-San Joaquin River Delta, Sacramento Valley, and Klamath Basin, northern California, 2014–17.

Study site	Successful	Failed
Gray Lodge Wildlife Area	24	25
Mandeville Island Duck Club	7	12
Roosevelt Ranch Duck Club	32	29
Yolo Bypass Wildlife Area	20	13
Little Dry Creek Unit of Upper Butte Basin Wildlife Area	12	5
Lower Klamath National Wildlife Refuge	3	9
Total	98	93

Table 5. Means plus or minus standard error of variables included in model analyses of habitat surveys used to evaluate nest site selection ($n = 365$) and microhabitat characteristics of nests used to evaluate nest survival ($n = 146$), for ring-necked pheasant (*Phasianus colchicus*) nests in the Sacramento-San Joaquin River Delta and Sacramento Valley, northern California, 2014–17.

[**Microhabitat variable:** Horizontal cover metric was only used in 2014 and was replaced by the Robel pole height measurement during 2015–17; cm, centimeter; %, percentage. **Scale:** ha, hectare. **Abbreviations:** n, sample size. \pm SE, plus or minus standard error]

Microhabitat variable	Scale (ha)	Available ($n = 162$)		Used ($n = 163$)		Success ($n = 88$)		Failure ($n = 58$)	
		Mean	\pm SE	Mean	\pm SE	Mean	\pm SE	Mean	\pm SE
Vertical cover (%)	0	31.7	2.6	53.2	2.5	54.6	3.2	51.5	3.8
Horizontal cover (%)	0	60.8	4.0	83.9	1.5	85.8	2.1	81.2	2.2
Robel pole height (cm)	0	15.6	2.2	22.2	2.7	24.8	3.8	19.3	3.8
Perennial grass (%)	0	13.4	2.5	23.2	2.6	28.0	3.7	17.5	3.4
	0.03	13.9	2.5	24.0	2.2	29.0	3.1	18.2	2.9
	0.2	13.8	2.2	22.9	1.9	27.6	2.8	17.4	2.5
Annual grass (%)	0	29.9	2.8	30.2	2.7	30.7	3.6	29.5	4.1
	0.03	29.3	2.3	31.1	2.3	30.1	3.1	32.3	3.6
	0.2	29.2	2.1	30.5	2.1	30.8	2.9	30.2	3.1
Perennial forb (%)	0	9.2	1.3	8.3	1.3	9.6	2.0	6.8	1.6
	0.03	10.0	1.0	9.6	1.0	10.9	1.5	8.1	1.4
	0.2	10.5	1.0	9.5	0.8	10.8	1.3	8.0	1.1
Annual forb (%)	0	26.5	2.6	22.0	2.3	18.6	2.9	25.9	3.7
	0.03	26.0	2.2	23.0	1.9	20.5	2.4	26.0	3.0
	0.2	25.2	2.0	23.0	1.8	19.7	2.3	27.0	3.0
Residual cover (%)	0	21.6	2.3	41.4	2.5	41.5	3.2	41.3	4.0
	0.03	20.3	1.7	36.7	2.3	38.4	2.9	34.6	3.5
	0.2	20.4	1.6	33.8	2.2	35.4	2.8	31.8	3.4
Bare ground (%)	0	22.7	2.2	8.5	1.2	7.4	1.4	9.7	2.1
	0.03	24.8	1.9	13.6	1.4	13.1	1.9	14.2	1.9
	0.2	25.5	1.8	14.8	1.8	14.2	1.8	15.4	1.9

Microhabitat variable	Scale (ha)	Available (n = 162)		Used (n = 163)		Success (n = 88)		Failure (n = 58)	
		Mean	±SE	Mean	±SE	Mean	±SE	Mean	±SE
Rock (%)	0	2.5	0.0	2.7	0.2	2.5	0.0	3.0	0.3
	0.03	2.8	0.2	2.8	0.2	2.6	0.1	3.1	0.3
	0.2	3.2	0.2	2.7	0.1	2.6	0.1	2.9	0.2
Shrub (%)	0	2.5	0.0	2.5	0.0	2.5	0.0	2.5	0.0
	0.03	2.7	0.2	2.8	0.2	2.7	0.2	2.8	0.3
	0.2	3.3	0.2	2.8	0.2	3.0	0.3	2.7	0.2
Sedge (%)	0	7.0	0.6	2.5	0.0	2.5	0.0	2.5	0.0
	0.03	3.1	0.3	2.6	0.0	2.5	0.0	2.6	0.1
	0.2	3.0	0.2	2.7	0.1	2.7	0.1	2.8	0.2
Rush (%)	0	5.8	1.2	7.4	1.5	6.7	1.8	8.1	2.4
	0.03	4.9	0.7	5.4	0.7	5.1	0.9	5.7	1.2
	0.2	5.3	0.6	5.9	0.7	5.5	0.8	6.2	1.2
Water (%)	0	3.7	0.8	3.6	0.8	4.5	1.4	2.5	0.0
	0.03	5.4	0.9	3.8	0.6	4.2	1.0	3.4	0.5
	0.2	6.3	1.0	5.0	0.7	5.6	1.2	4.2	0.7
Perennial grass height (cm)	0	13.8	2.4	24.8	2.6	29.6	3.5	19.3	3.9
	0.03	13.2	1.9	24.2	2.2	27.5	3.0	20.3	3.3
	0.2	13.1	1.7	24.2	2.2	27.3	3.0	20.7	3.1
Annual grass height (cm)	0	19.9	2.1	27.8	2.4	29.6	3.6	25.6	3.0
	0.03	19.0	1.7	27.6	2.1	28.5	3.0	26.5	2.9
	0.2	18.1	1.6	27.9	2.0	28.5	2.9	27.2	2.8
Perennial forb height (cm)	0	15.0	2.3	18.0	2.5	21.3	3.7	14.2	3.4
	0.03	16.0	1.5	16.9	1.8	17.0	2.0	16.8	3.2
	0.2	15.6	1.4	16.5	1.7	17.1	2.0	15.8	2.8
Annual forb height (cm)	0	34.3	3.4	29.8	2.9	25.2	3.7	35.1	4.5
	0.03	30.1	2.4	29.6	2.6	27.7	3.4	31.9	3.9
	0.2	29.6	2.2	29.2	2.3	27.0	3.1	31.9	3.6

Microhabitat variable	Scale (ha)	Available (n = 162)		Used (n = 163)		Success (n = 88)		Failure (n = 58)	
		Mean	±SE	Mean	±SE	Mean	±SE	Mean	±SE
Residual height (cm)	0	25.4	3.3	32.6	3.0	34.2	4.0	32.6	3.0
	0.03	24.6	2.3	31.0	2.1	32.6	2.9	31.0	2.1
	0.2	23.1	2.0	31.4	1.9	32.7	2.8	31.4	1.9
Shrub height (cm)	0	0.0	0.0	0.0	0.0	0.0	0.0	0.0	0.0
	0.03	0.8	0.4	1.2	0.6	0.5	0.5	2.0	1.3
	0.2	5.8	2.1	1.1	0.5	1.0	0.6	1.3	0.8
Sedge height (cm)	0	1.4	0.7	0.6	0.6	0.0	0.0	1.2	1.2
	0.03	1.2	0.5	0.6	0.4	0.3	0.3	0.9	0.7
	0.2	1.2	0.4	0.9	0.4	0.9	0.4	1.0	0.6
Rush height (cm)	0	10.1	3.6	9.7	2.8	12.1	4.6	6.9	3.0
	0.03	7.9	1.9	8.2	1.9	10.0	3.0	6.1	2.4
	0.2	8.4	1.7	9.9	1.8	10.8	2.6	8.7	2.5

Table 6. Nest-site selection ($n = 163$), nest survival, and ratio of selection models for ring-necked pheasant (*Phasianus colchicus*) nests ($n = 146$) in the Sacramento-San Joaquin River Delta and Sacramento Valley, northern California, 2013–17.

[**Microhabitat models:** (Q) indicates that both the first order and quadratic term were included in the model; cm, centimeter; %, percentage. **-2 LL:** Deviance. **AIC_c:** Akaike's Information Criterion with second-order bias correction. **ΔAIC_c:** Difference between model of interest and most explanatory model with second-order bias correction. **w:** Model probability]

Group	Microhabitat models	Model number	-2LL	Number of parameters	AIC _c	ΔAIC _c	w
Selection	(Q)Vertical cover (%)	1	405.6	5	415.8	0.0	0.98
	Vertical cover (%)	2	415.6	4	423.7	8.0	0.02
	(Q)Residual cover_0 (%)	3	423.6	5	433.9	18.1	0.00
	(Q)Bare ground_0.2 (%)	4	425.2	5	435.3	19.6	0.00
	Bare ground_0 (%)	5	427.4	4	435.4	19.7	0.00
	(Q)Bare ground_0.03 (%)	6	425.4	5	435.6	19.8	0.00
	(Q)Bare ground_0 (%)	7	425.6	5	435.9	20.1	0.00
	Bare ground_0.03 (%)	8	427.8	4	436.0	20.2	0.00
	Bare ground_0.2 (%)	9	428.8	4	436.9	21.2	0.00
	(Q)Residual height_0.2 (cm)	10	428.4	5	438.6	22.9	0.00
	(Q)Residual height_0 (cm)	11	429.2	5	439.3	23.6	0.00
	Residual cover_0.03 (%)	12	433.4	4	441.5	25.8	0.00
	Residual cover_0.2 (%)	13	434.6	4	442.7	26.9	0.00
	(Q)Residual cover_0.03 (%)	14	433.4	5	443.6	27.8	0.00
	(Q)Residual height_0.03 (cm)	15	433.4	5	443.7	27.9	0.00
	(Q)Residual cover_0.2 (%)	16	434.0	5	444.1	28.4	0.00
	Residual cover_0 (%)	17	437.0	4	445.0	29.3	0.00
	(Q)Perennial grass height_0.03 (cm)	18	439.2	5	449.4	33.6	0.00
	Perennial grass height_0.2 (cm)	19	405.6	4	449.9	34.2	0.00
	(Q)Perennial grass height_0.2 (cm)	20	415.6	5	450.4	34.7	0.00
	Residual height_0.2 (cm)	21	423.6	4	450.6	34.8	0.00
	Perennial grass height_0.03 (cm)	22	425.2	4	451.6	35.8	0.00

Group	Microhabitat models	Model number	-2LL	Number of parameters	AIC _c	ΔAIC _c	w
Selection (continued)	Perennial grass_0.03 (%)	23	441.8	4	451.9	36.2	0.00
	(Q)Perennial grass height_0 (cm)	24	440.2	5	453.0	37.2	0.00
	(Q)Perennial grass_0.2 (%)	25	442.4	5	453.2	37.5	0.00
	(Q)Perennial grass_0.03 (%)	26	443.4	5	453.3	37.6	0.00
	Annual grass height_0.2 (cm)	27	443.8	4	453.5	37.7	0.00
	Residual height_0.03 (cm)	28	442.8	4	453.5	37.8	0.00
	Residual height_0 (cm)	29	443.0	4	454.0	38.2	0.00
	Perennial grass_0.2 (%)	30	443.2	4	454.0	38.3	0.00
	Perennial grass_0 (%)	31	445.4	4	454.7	39.0	0.00
	(Q)Annual grass height_0.2 (cm)	32	445.4	5	455.1	39.4	0.00
	Perennial grass height_0 (cm)	33	445.8	4	455.4	39.6	0.00
	Annual grass height_0.03 (cm)	34	446.0	4	455.6	39.8	0.00
	Perennial forb height_0.2 (cm)	35	446.6	4	456.4	40.6	0.00
	(Q)Perennial grass_0 (%)	36	445.0	5	456.4	40.7	0.00
	Water_0.03 (%)	37	447.2	4	456.6	40.8	0.00
	Intercept-Only	38	447.4	3	456.6	40.9	0.00
Survival	Perennial grass_0.03 (%)	1	423.5	2	427.5	0.0	0.35
	Perennial grass_0 (%)	2	425.3	2	429.3	1.8	0.14
	(Q)Perennial grass_0.03 (%)	3	423.5	3	429.5	2.0	0.13
	Perennial grass_0.2 (%)	4	426.7	2	430.7	3.3	0.07
	Bare ground_0 (%)	5	426.9	2	430.9	3.4	0.06
	(Q)Perennial grass_0 (%)	6	425.3	3	431.3	3.8	0.05
	Perennial grass height_0.03 (cm)	7	427.4	2	431.4	3.9	0.05
	Perennial grass height_0 (cm)	8	427.4	2	431.4	3.9	0.05
	Water_0 (%)	9	427.5	2	431.5	4.0	0.05
	Intercept-Only	10	429.7	1	431.7	4.2	0.04

Group	Microhabitat models	Model number	-2LL	Number of parameters	AIC _c	ΔAIC _c	w
Ratio of selection	Perennial grass height_0.2 (cm)	1	423.5	2	427.5	0.0	0.32
	Perennial grass_0.03 (%)	2	423.7	2	427.7	0.2	0.29
	(Q)Perennial grass height_0.2 (cm)	3	423.5	3	429.5	2.0	0.12
	(Q)Perennial grass_0.03 (%)	4	423.7	3	429.7	2.2	0.12
	Intercept-Only	5	429.7	1	431.7	4.2	0.04
	Annual grass height_0.2 (cm)	6	428.9	2	432.9	5.4	0.02
	Bare ground_0 (%)	7	429.0	2	433.0	5.5	0.02
	Residual height_0.2 (cm)	8	429.3	2	433.3	5.9	0.02
	Residual cover_0 (%)	9	429.5	2	433.5	6.0	0.02
	Vertical cover (%)	10	429.7	2	433.7	6.2	0.01
	(Q)Annual grass height_0.2 (cm)	11	428.9	3	434.9	7.4	0.01
	(Q)Bare ground_0 (%)	12	429.0	3	435.0	7.5	0.01
	(Q)Residual height_0.2 (cm)	13	429.3	3	435.3	7.9	0.01
	(Q)Residual cover_0 (%)	14	429.5	3	435.5	8.0	0.01
	(Q)Vertical cover (%)	15	429.7	3	435.7	8.2	0.01
	(Q)Perennial forb_0.2 (%)	16	429.7	3	435.7	8.2	0.01

Table 7. Descriptions of models with one or more interactive terms used to evaluate nest-site selection for ring-necked pheasant (*Phasianus colchicus*) nests ($n = 163$) in the Sacramento-San Joaquin River Delta and Sacramento Valley, northern California, 2014–17.

[**Parameters:** (Q) indicates the quadratic term for variables with second-order effects; cm, centimeter; %, percentage. **Abbreviation:** n, sample size]

Model name	Parameters
Global 1(Base)	(Q)Vertical cover (%) (Q)Residual cover_0 (%) Bare ground_0 (%) (Q)Residual height_0.2 (cm) Perennial grass height_0.2 (cm) Annual grass height_0.2 (cm)
Global 2	Base (Q)Vertical cover (%):(Q)Residual cover_0 (%)
Global 3	Base (Q)Vertical cover (%):Bare ground_0 (%)
Global 4	Base (Q)Vertical cover (%):(Q)Residual height_0.2 (cm)
Global 5	Base (Q)Vertical cover (%):(Q)Perennial grass height_0.03 (cm)
Global 6	Base (Q)Vertical cover (%):Annual grass height_0.2 (cm)
Global 7	Base (Q)Residual cover_0 (%):Bare ground_0 (%)
Global 8	Base (Q)Residual cover_0 (%):(Q)Residual height_0.2 (cm)
Global 9	Base (Q)Residual cover_0 (%):(Q)Perennial grass height_0.03 (cm)
Global 10	Base (Q)Residual cover_0 (%):Annual grass height_0.2 (cm)
Global 11	Base Bare ground_0 (%):(Q)Residual height_0.2 (cm)
Global 12	Base Bare ground_0 (%):(Q)Perennial grass height_0.03 (cm)
Global 13	Base Bare ground_0 (%):Annual grass height_0.2 (cm)
Global 14	Base (Q)Residual height_0.2 (cm):(Q)Perennial grass height_0.03 (cm)
Global 15	Base (Q)Residual height_0 (cm):Annual grass height_0.2 (cm)
Global 16	Base (Q)Perennial grass height_0.03 (cm):Annual grass height_0.2 (cm)

Model name	Parameters
Global 17	Base Perennial grass height_0.2 (cm):Perennial grass_0.03 (%)
Global 18	Base (Q)Vertical cover (%):Annual grass height_0.2 (cm) Bare ground_0 (%):(Q)Residual height_0.2 (cm)
Global 19	Base (Q)Vertical cover (%):Annual grass height_0.2 (cm) (Q)Residual cover_0 (%):Bare ground_0 (%)
Global 20	Base Bare ground_0 (%):(Q)Residual height_0.2 (cm) (Q)Residual cover_0 (%):Bare ground_0 (%)
Global 21	Base (Q)Vertical cover (%):Annual grass height_0.2 (cm) (Q)Residual cover_0 (%):Bare ground_0 (%) Bare ground_0 (%):(Q)Residual height_0.2 (cm)

Table 8. Comparison of global models with combinations of interaction terms used to evaluate nest-site selection for ring-necked pheasant (*Phasianus colchicus*) nests ($n = 163$) in the Sacramento-San Joaquin River Delta and Sacramento Valley, northern California, 2014–17.

[Models greater than or equal to $2\Delta AIC_c$ units relative to the base model were considered significant in contributing to probabilities of nest selection. **-2LL**: Deviance. **K**: Number of parameters. **AIC_c**: Akaike's Information Criterion with second-order bias correction. **ΔAIC_c** : Difference between model of interest and most explanatory model with second-order bias correction. **w**: Model probability. **Abbreviation**: n , sample size]

Model name	Rank	-2LL	K	AIC _c	ΔAIC_c	w
Global 21	1	359.0	15	390.6	0.0	0.37
Global 19	2	362.4	14	391.8	1.2	0.20
Global 18	3	363.8	14	393.1	2.5	0.11
Global 20	4	364.6	14	393.9	3.2	0.07
Global 6	5	366.8	13	393.9	3.3	0.07
Global 7	6	367.6	13	394.8	4.2	0.05
Global 11	7	368.8	13	396.0	5.4	0.02
Base	8	371.8	12	396.7	6.1	0.02
Global 14	9	367.8	14	397.2	6.5	0.01
Global 4	10	370.2	13	397.5	6.8	0.01
Global 10	11	370.8	13	397.9	7.2	0.01
Global 8	12	371.2	13	398.3	7.7	0.01
Global 13	13	371.2	13	398.4	7.8	0.01
Global 9	14	369.2	14	398.6	8.0	0.01
Global 15	15	371.6	13	398.7	8.1	0.01
Global 2	16	371.6	13	398.7	8.1	0.01
Global 3	17	371.6	13	398.9	8.2	0.01
Global 16	18	369.8	14	399.1	8.5	0.01
Global 12	19	369.8	14	399.2	8.5	0.01
Global 5	20	369.8	14	399.2	8.6	0.01
Global 17	21	371.0	14	400.3	9.7	0.00

Table 9. Model descriptions for parameters included in a global selection model for ring-necked pheasant (*Phasianus colchicus*) nests ($n = 163$) in the Sacramento-San Joaquin River Delta and Sacramento Valley, northern California, 2013–17.

[**Parameters:** (Q) indicates the quadratic term for variables with second order effects; cm, centimeter; %, percentage. **SC:** standardized coefficient. **SE:** standard error. **95% CI:** 95-percent confidence interval. **LCL:** lower confidence limit. **UCL:** upper confidence limit. **Abbreviation:** n, sample size]

Parameters	SC	SE	95% CI	
			LCL	UCL
Residual cover_0 (%)	0.68	0.26	0.17	1.2
(Q)Residual cover_0 (%)	-0.67	0.23	-1.12	-0.22
Vertical cover (%)	0.67	0.14	0.39	0.95
(Q)Vertical cover (%)	-0.46	0.17	-0.78	-0.13
(Q)Residual cover_0 (%):Bare ground_0 (%)	-0.63	0.30	-1.22	-0.04
(Q)Vertical cover (%):Annual grass height_0.3 (cm)	0.37	0.16	0.05	0.69
Bare ground_0 (%):(Q)Residual height_0.3 (cm)	0.35	0.19	-0.03	0.72
Bare ground_0 (%)	-0.26	0.28	-0.80	0.28
Perennial grass height_0.3 (cm)	0.25	0.13	-0.01	0.51
Residual height_0.3 (cm)	0.22	0.19	-0.16	0.59
(Q)Residual height_0.3 (cm)	-0.03	0.13	-0.28	0.22
Annual grass height_0.3 (cm)	-0.14	0.20	-0.53	0.25

Table 10. Nest selection, survival, and ratio of selection models for ring-necked pheasant (*Phasianus colchicus*) nests across five field sites within the Sacramento-San Joaquin River Delta and Sacramento Valley, northern California, 2014–17.

[Only models greater than or equal to $2\Delta AIC_c$ units relative to the null model were considered significant in contributing to probabilities of nest selection.

Model description: cm, centimeter; m, meter; %, percentage. **-2LL:** deviance. **K:** number of parameters. **AIC_c:** Akaike's Information Criterion with second-order bias correction. **ΔAIC_c :** Difference between model of interest and most explanatory model with second-order bias correction. **w:** Model probability]

Group	Site	Model description	Model	-2LL	K	AIC _c	ΔAIC_c	w
Selection	Gray Lodge	Residual cover_0 (%)	1	107.6	3	113.9	0.0	0.98
		Intercept-only	2	117.8	2	122.0	8.1	0.02
	Little Dry Creek	Bare ground_0.2 (%)	1	36.4	3	43.1	0.0	0.95
		Annual grass height_0.2 (cm)	2	42.6	3	49.5	6.4	0.04
		Intercept-only	3	47.2	2	51.5	8.4	0.01
	Yolo	Vertical cover (%)	1	78.4	3	84.9	0.0	0.40
		Annual forb_0.2 (%)	2	78.6	3	85.1	0.2	0.37
		Residual cover_0.03 (%)	3	80.2	3	86.6	1.7	0.17
		Intercept-only	4	84.6	2	88.8	3.8	0.06
	Roosevelt Ranch	Vertical cover (%)	1	131.4	3	137.6	0.0	1.00
		Bare ground_0 (%)	2	142.6	3	148.9	11.3	0.00
		Perennial grass height_0.2 (cm)	3	146.0	3	152.3	14.7	0.00
		Residual cover_0.03 (%)	4	146.2	3	152.4	14.8	0.00
		Intercept-only	5	158.0	2	162.1	24.5	0.00
	Mandeville Island	Perennial forb height_0 (cm)	1	35.6	3	42.5	0.0	0.38
		Vertical cover (%)	2	35.8	3	42.6	0.1	0.36
		Bare ground_0.03 (%)	3	36.6	3	43.6	1.0	0.22
		Intercept-only	4	42.6	2	47.1	4.6	0.04

Group	Site	Model description	Model	-2LL	K	AIC _c	ΔAIC _c	w
Survival ¹	Gray Lodge	Perennial grass height 10 m	1	148.6	2	152.6	0.0	0.47
		Rush height 10 m	2	149.6	2	153.6	1.0	0.28
		Intercept-only	3	151.8	1	153.8	1.3	0.25
	Little Dry Creek	Annual grass height_0.03 (cm)	1	29.9	2	34.0	0.0	0.27
		Annual forb height_0 (cm)	2	30.4	2	34.4	0.5	0.21
		Perennial forb height_0 (cm)	3	31.0	2	35.0	1.1	0.16
		Perennial grass_0 (%)	4	31.0	2	35.1	1.1	0.15
		Rush height_0.2 (cm)	5	31.6	2	35.7	1.7	0.11
		Intercept-only	6	34.0	1	36.0	2.1	0.10
	Yolo	Vertical cover (%)	1	59.9	2	63.9	0.0	0.38
		Annual forb height_0.03 (cm)	2	61.5	2	65.5	1.1	0.22
		Intercept-only	3	63.9	1	65.9	2.0	0.14
	Roosevelt Ranch	Perennial forb_0 (%)	1	111.7	5	121.8	0.0	0.38
		Perennial grass height_0.03 (cm)	2	112.5	5	122.5	0.7	0.26
		Rush height_0 (cm)	3	112.8	5	122.9	1.1	0.22
		Year	4	115.8	4	123.8	2.0	0.14
	Mandeville Island	Perennial grass_0 (%)	1	41.7	2	45.8	0.0	0.31
		Residual height_0.03 (cm)	2	42.6	2	46.9	1.1	0.18
		Rush_0 (%)	3	42.8	2	46.9	1.1	0.18
		Intercept-only	4	45.3	1	47.4	1.6	0.14

Group	Site	Model description	Model	-2LL	K	AIC _c	ΔAIC _c	w
Ratio of Selection	Gray Lodge	Intercept-only	1	151.8	1	153.8	0.0	0.51
		Residual cover_0 (%)	2	151.2	2	155.2	1.3	0.26
	Little Dry Creek	Intercept-only	1	34.0	1	36.0	0.0	0.48
		Bare ground_0.2 (%)	2	32.7	2	36.7	0.7	0.34
		Annual grass height_0 (cm)	3	34.0	2	38.0	2.0	0.18
	Yolo	Vertical cover (%)	1	61.2	2	65.2	0.0	0.41
		Intercept-only	2	63.9	1	65.9	0.7	0.29
		Annual forb cover_0.2 (%)	3	63.2	2	67.2	2.0	0.15
		Residual cover_0.03 (%)	4	63.3	2	67.3	2.1	0.15
	Roosevelt Ranch	Year-only	1	120.6	4	123.8	0.0	0.38
		Residual cover_0.03 (%)	2	124.8	5	125.3	1.4	0.18
		Vertical cover (%)	3	124.1	5	125.5	1.7	0.16
		Perennial grass height_0.03 (cm)	4	124.6	5	125.8	2.0	0.14
		Bare ground_0 (%)	5	124.7	5	125.9	2.0	0.14
	Mandeville Island	Intercept-only	1	45.3	1	47.4	0.0	0.40
		Vertical cover (%)	2	43.9	2	47.9	0.6	0.30
		Perennial forb height_0 (cm)	3	45.2	2	49.3	1.9	0.15
		Bare ground_0 (%)	4	45.3	2	49.3	2.0	0.15

¹All models for survival and ratio of selection group were compared to an intercept-only model except for Roosevelt Ranch. Year was shown to have a significant effect on survival at Roosevelt Ranch; thus, a year-only model was used in place of an intercept-only model and year was added as a fixed effect in the models for Roosevelt Ranch.

Table 11. Number of successful, failed, and censored ring-necked pheasant (*Phasianus colchicus*) broods in the Sacramento-San Joaquin River Delta, Sacramento Valley, and Klamath Basin, northern California, 2014–17

[A brood was considered successful if one or more chicks survived to 50-days post-hatch]

	Successful	Failed	Censored
Gray Lodge	8	15	1
Mandeville Island	3	4	0
Roosevelt Ranch	11	18	3
Yolo	14	6	0
Little Dry Creek	7	5	0
Lower Klamath	2	0	1
Total	45	48	5

Publishing support provided by the U.S. Geological Survey
Science Publishing Network, Tacoma Publishing Service Center

For more information concerning the research in this report, contact the
Director, Western Ecological Research Center
U.S. Geological Survey
3020 State University Drive
Modoc Hall, Room 4004
Sacramento, California 95819
<https://www.werc.usgs.gov/>

